

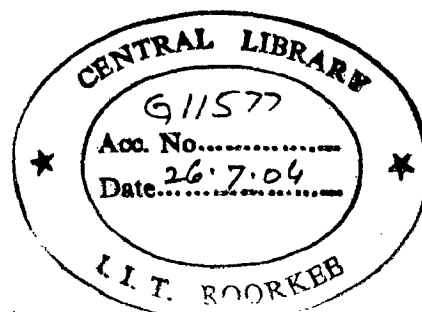
# STUDY OF RIVER BANK EROSION CONTROL BY SOIL NAILING AND GEOSYNTHETICS

A DISSERTATION

Submitted in partial fulfillment of the  
requirements for the award of the degree  
of  
**MASTER OF TECHNOLOGY**  
in  
**WATER RESOURCES DEVELOPMENT**

By

**AKHIL KUMAR BISWAS**



**WATER RESOURCES DEVELOPMENT TRAINING CENTRE  
INDIAN INSTITUTE OF TECHNOLOGY ROORKEE  
ROORKEE-247 667 (INDIA)  
JUNE, 2004**

## **CANDIDATE'S DECLARATION**

---

I hereby certify that the dissertation entitled “**STUDY OF RIVER BANK EROSION CONTROL BY SOIL NAILING AND GEOSYNTHETICS**” being submitted by me in partial fulfillment of requirement for the award of degree of “**Master of Technology in Water Resources Development**” at the Water Resources Development Training Centre, IITR is an authentic record of my own work carried out during the period from July 1, 2003 to June 29, 2004 under the supervision of **Dr. Nayan Sharma**, Professor, WRDTC and **Dr. S. Mittal**, Assistant Professor, Civil Engineering Department, IITR.

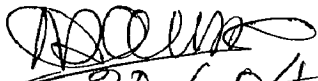
The matter embodied in the dissertation has not been submitted by me for the award of other degree or diploma.

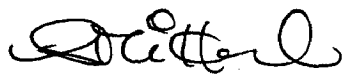
**Dated: 29<sup>th</sup> June, 2004**

  
**(Akhil Kumar Biswas)**

---

This is to certify that above statement made by the candidate is correct to the best of my knowledge.

  
30.6.04  
**(Dr. Nayan Sharma)**  
Professor, WRDTC  
IITR, Uttaranchal, India

  
**(Dr. S. Mittal)**  
Assistant Professor  
Civil Engineering Department  
IITR, Uttaranchal, India

## **ACKNOWLEDGEMENT**

---

I wish to record my sincere thanks with a profound sense of gratitude to **Dr. NAYAN SHARMA**, Professor, WRDTC and **Dr. S. MITTAL**, Assistant Professor, Civil Engineering Department for their valuable guidance, advice and encouragement in preparation and presentation of this dissertation.

I am grateful to **Dr.U.C. Chaube**, Professor & Head, **Professor G.C. Mishra**, Chairman, DRC and all faculty members of WRDTC for providing valuable knowledge during the last two years, which helped me a lot to finish the dissertation. I am thankful to staff of WRDTC who extended possible help whenever required. I am also grateful to all the staff of computer lab for providing me computer facilities.

At this golden moment of submission of my dissertation paper, I should not forget some of my friend's names like **Mr. P.K. Prasad**, **Mr. Gir Bahadur K.C**, **Mr. Rama Nand Yadav** and **Mr. P.N. Zaminder** for their sincere cooperation. I am also grateful to **Mrs. Meenal Gosavi**, research scholar, CED and **Mr. R.N. Sankhua**, research scholar, WRDTC, IITR for helping me a lot.

I am grateful to **M/S Garware-Wall Rope Ltd.** Company for their support in supplying material to conduct performance study of flexible polymer rope in erosion control work in boulder stage river like the **Beas** in Himachal Pradesh of India.


I like to thank **Mr. Dinesh Kumar Upadhyay**, senior executive of the same company, for his technical support and continuous help during installation of the gabion boxes in the riverbed.

I like to thank **MES officers and staff** for their keen interest in field experiment and for supplying labour in the work.

I am thankful to **Almighty God** and greatly indebted to my mother and late father because I believe that without their blessings this work would not be completed.

I wish to record my love and affection to my wife and my two children **Ankon** and **Likhon** who extended their full moral support and encouraged me throughout the course of my study.

Financial assistance provided by **Govt. of India** under **Colombo Plan** during the **M.Tech Course** in WRDTC at IITR is highly acknowledged

  
**(Akhil Kumar Biswas)**  
Trainee officer 47<sup>th</sup> batch  
WRD (Civil), WRDTC  
IIT, ROORKEE

## ABSTRACT

---

The dissertation aims at using the nailing technology and geosynthetics in river bank protection work. With a view to suggest the technique, analytical work and field experiment with flexible polymer ropes in controlling river bed erosion have been carried out and presented in different chapters of this report.

An effort has been made in Chapter-I of this report to describe advantages, application, construction sequences, component of nailing, limitation etc. for easy understanding regarding the nailing technology. In Table -1.2 of the same chapter some investigated information have been presented with a view to justify how confidently soil nailing technique can be used to solve different types of geotechnical related problem.

In Chapter-II, chronological developments of soil nailing technology made by different researchers are presented.

Several methods are available for stability analysis of nailed structure, namely the limit equilibrium method, limit analysis method and the finite element method. Among all these, the limit equilibrium method has attracted the attention of the researchers because of its simplicity, reasonable accuracy and popularity among the practicing engineers. Although these are not correct from the viewpoint of mathematical theory of plasticity for their incorrectly oriented slip surfaces, these have acquitted themselves quiet well for their reasonable accuracy and predictions. These are not very much off from the solutions obtained through more rigorous applications. No universally accepted standard method for design of such structures without any controversy could yet be developed. Chapter-III represents the summary of design methods available.

Chapter -IV deals with how to analyze a soil nailed wall considering circular type wedge failure. In this analysis friction circle method for  $c-\phi$  soil has been adopted. Soil nail interface friction angle has been considered as  $2/3$  of angle internal friction. Since this angle has to be measured from pullout test under in-situ field condition, it does not guarantee accurate analysis. The analysis includes the role of bending stiffness in factor of safety. This chapter results in an equation for computing factor of safety. With the help of computer program, the effect of variation of design parameters such as nail length, nail diameter, nail inclination, wall inclination, wall height, angle of internal friction as well



as cohesion of soil in factor of safety can be determined. At the end of this chapter some graphs are plotted to have a look at the variation of factor of safety with the variation of different design parameters.

The dissertation aims at how to use the technology in river training works. It can be concluded that this technology can be used in riverbank protection work above HFL i.e. in free board zone successfully. It can also be used in rainfall erosion control. In hilly region where riverbank level is too high and it has a tendency to slide, this technology may be more suitable. It can also be mentioned here that due to turbulence, velocity and ground water effect the technology may not be suitable under water.

Uses of geosynthetics in water resources projects are increasing day by day. Due to wide range of uses of this material, some basic properties as well as selection criteria are presented in Chapter-VI in order to make it more popular among the water resources engineers. Emphasis has been given only on the use of the material. Additional attention has been put on the use of geo-jute and it can be added that it may be a suitable alternative of geo-synthetics in riverbank erosion control as a filter material.

Theoretical background of different approaches for designing the bank protection work is presented in Chapter-VII. This may be treated as an over view of design procedure so far available in literature. Some formulae for determination of roughness of bed material especially in gravel stage river and the same for scour depth are also presented here.

One 'Case Study' of Beas river regarding bank protection work has been presented in Chapter-VIII. Different alternative methods are designed and finally best suitable method has been recommended for implementation depending upon many factors.

Field experiment for performance study of flexible polymer rope in gabion boxes in riverbank protection work is conducted in the river Beas located in Himachal Pradesh. Behavior of polymer rope was observed. Since observational time period was limited, preliminary assessments that were observed in the field are presented here.

# CONTENTS

---

	Page no
CANDIDATE'S DECLARATION	i
ACKNOWLEDGEMENT	ii
ABSTRACT	iii
CONTENTS	v
LIST OF FIGURES	ix
LIST OF TABLES	xii
LIST OF SYMBOLS	xiii
<b>CHAPTER-I INTRODUCTION</b>	
1.1 Concept of soil nailing	1
1.2 History of soil nailing	1
1.3 Soil nailing advantages	1
1.4 Soil nailing construction sequences	2
1.5 Soil nailing components	3
1.5.1 The insitu ground	3
1.5.2 Tension resisting nails	4
1.5.3 Facing on the structural retaining element	8
1.5.4 Wall connector	9
1.5.5 Drainage	9
1.6 Soil nailing interaction	10
1.7 Applications	11
1.8 Limitation of the existing soil nailing technology and proposed new enhancement	15
1.9 Comparison of soil nailing with reinforced soil	17
1.10 Objective of study	18
<b>CHAPTER-II REVIEW OF LITERATURE</b>	19
2.1 Studies on full scale model tests	19
2.2 Studies on large scale model tests	22

2.3 Studies on small scale model tests	24
--	----

### **CHAPTER-III DESIGN METHODS OF SOILED NAILED STRUCTURE**

	27
3.1 Design principle	27
3.2 Failure curves for reinforced and unreinforced soil	30
3.3 Theoretical models for evaluating the role of bending stiffness	31
3.4 Distribution of shear stress along the failure surfaces	36
3.5 Data required for soil nailing design	38
3.6 Steps for the design of nailed –soil structure	39
3.7 Comparative analysis of various design methods	42

### **CHAPTER-IV ANALYSIS OF SOIL NAILING WALL WITH FRICTION CIRCLE METHOD**

46

### **CHAPTER-V SOIL NAILING IN EROSION CONTROL**

74

5.1 Soil nailing technique in rainfall erosion control	74
5.2 Soil nailing in river bank erosion control	75

### **CHAPTER-VI GEOSYNTHETICS IN EROSION CONTROL**

76

6.1 Introduction	76
6.2 Historical development of geosynthetics	76
6.3 Function of geotextile	76
6.4 Geotextile specifications	76
6.5 Geotextile in filtration and erosion control	78
6.6 Erosion control on slopes of canals, river banks drains /water ways	79
6.6.1 Riprap protection	80
6.6.2 Concrete block/articulated concrete mattresses	80
6.6.3 Gabion protection	81
6.6.4 Geojute	82
6.6.5 Synthetic gunny bag/jute bag	83

6.6.6 Gabion mattresses protection	84
<b>CHAPTER-VII    RIVER TRAINING TECHNIQUE</b>	<b>86</b>
7.1 General	86
7.2 River regulator	86
7.3 Estimation of scour	87
7.3.1 Local scours around bridge piers	87
7.3.2 Local scour around embankments	91
7.3.3 Scour due to long constriction	91
7.3.4 Local scour at groynes	92
7.3.5 Estimation of scour depth in alluvial channel according to Lacey	93
7.3.6 Armoring in river bed	94
7.4 Flow resistance in river	95
7.5 Design of cover layer	97
7.5.1 Selection criteria of thickness and stone size of riprap	106
7.6 Design criteria of filter layer in river training work	112
7.6.1 Soil tightness	112
7.6.2 Permeability	112
7.6.3 Selection criteria of granular filter	114
7.6.4 Thickness of filter layer	114
7.7 Design of apron in bank protection work	115
<b>CHAPTER-VIII    CASE STUDY</b>	<b>117</b>
8.1 Problem of present case study	117
8.2 Estimation of design flood	118
8.3 Hydraulics of Beas River	122
8.4 Design of embankment along the left bank	124
8.5 Design of protective measures in slopes and in river bed	125
8.5.1 Design of riprap cover layer in Beas river	125
8.5.2 Design of riprap apron	128
8.5.3 Design of cover layer with gabion	131

8.5.4 Design of launching apron with gabion	132
8.5.5 Design of cover layer with concrete block	133
8.5.6 design of launching apron with concrete block	134
8.6 Design of filter under cover layer	135
8.6.1 Design of granular filter under cover layer	135
8.6.2 Design of fabric filter	137

## **CHAPTER-IX PERFORMANCE STUDY OF FLEXIBLE POLYMER**

### **ROPE GABION IN GRAVEL BED RIVER** 141

9.1 General	141
9.2 Probable type of damage	141
9.3 Location of field experiments	142
9.4 Material Specification	142
9.5 Objective of field study	143
9.6 Installation procedure	143
9.7 Preliminary assessment and findings	144

## **CHAPTER-X DISCUSSION S, CONCLUSIONS AND RECOMMENDATIONS**

	152
10.1 Discussions on soil nailing	152
10.2 Discussions on geosynsthetics	153
10.3 Conclusions and recommendations	154
10.4 Scope of further study	155

## **REFERENCES** 156

Appendix-A Computer Programming (FORTRAN)	162
Appendix-B Result file	168
Appendix-C Input file	171

## LIST OF FIGURES

Figure No	Title	Page No
Fig-1.1	Construction steps in a typical soil nailing methods (Pokharel and Ochiani, 1997)	3
Fig-1.2 (a)	A typical permanent nail used in Germany (Gassler, 1990)	4
Fig-1.2 (b)	Corrosion protection for permanent nails used in Germany (Gassler, 1990)	5
Fig-1.3 (a)	Connection of nails and facing by bending the nails	5
Fig-1.3 (b)	Connection of nail and facing by using steel plate	6
Fig-1.4 (a,b,c,d)	Applications of soil nailing (Juran and Elias, 1992)	12
Fig-1.5	Qualitative comparison between a conventional and the proposed axial forces	17
Fig-2.1	Measured nail force distribution in a full scale nailed test wall (Plumelle et al.1990)	20
Fig-2.2 (a)	Variation of measured maximum nail force with depth	21
Fig-2.2 (b)	Measured horizontal displacement in a full scale nailed test wall (Plumelle et al.1990)	21
Fig-2.3	Typical large scale test cross-section (Stocker et al.1979)	24
Fig-2.4	Observed slope failure lines and axial forces in the reinforcement (Teramoto et al.1992)	26
Fig-3.1	Failure modes	28
Fig-3.2	Modes of failure (internal failure)	29
Fig-3.3	Failure curves of reinforcement and unreinforced soil	31
Fig-3.4	Elastic analysis for nail bending stiffness ( Schlosser, 1992)	33
Fig-3.5	Plastic analysis for nail bending stiffness (Jewell and Pedley, 1992)	34
Fig-3.6	Effect of the transfer length on the displacement necessary to mobilize	37
Fig-3.7	Soil nailed wall showing active and passive zone	41
Fig-4.1	Principle of friction circle	46

Fig-4.2 (a)	Resultant cohesive forces	48
Fig-4.2 (b)	Force polygon	48
Fig-4.3	Circular wedge failure showing all the forces	54
Fig-4.4	Circular wedge to find out the center of gravity	55
Fig-4.5	Calculation of normal stress on inclined nail face	60
Fig-4.6 (a)	FOS VS Angle of internal friction curve ( $c=0$ )	67
Fig-4.6 (b)	FOS VS Cohesion curve ( $k =0$ )	67
Fig-4.7 (a)	FOS VS nail diameter curve	68
Fig-4.7 (b)	FOS VS nail inclination curve	68
Fig-4.8 (a)	FOS VS nail inclination curve (wall vertical))	69
Fig-4.8 (b)	FOS VS nail inclination curve (wall inclination 10 degree)	69
Fig-4.9 (a)	FOS VS wall inclination curve (nail inclination 10 degree)	70
Fig-4.9 (b)	FOS VS wall inclination curve (nail horizontal)	70
Fig-4.10 (a)	FOS Vs wall inclination curve	71
Fig-4.10 (b)	FOS VS L/H curve (driven and grouted nail)	71
Fig-4.11 (a)	FOS VS Yield Stress of nail material curve (for diff. L/H)	72
Fig-4.11 (b)	FOS VS Yield Stress curve (for different spacing of nails)	72
Fig-4.12 (a)	FOS VS L/H ratio curve	73
Fig-4.12 (b)	FOS VS L/H ratio curve (for diff.yield stress)	73
Fig-6.1	Geotextile in erosion control at Farakka (Char et al.1989)	79
Fig-6.2	Bank protection with articulated concrete mattress, Lower Mississippi river	81
Fig-6.3	Gabion boxes in erosion control	82
Fig-6.4	Cross-sectional view of bank protection work using geojute at Hoogly Estuary	83
Fig-6.5 (a)	Placement of riprap over geojute	83
Fig-6.5 (b)	Construction of toe of the slope for using geojute	83
Fig-6.6	Sand cement bag revetment (after U.S Army Corps of Engineers, 1981)	84
Fig-6.7	Gabion mattress in erosion control	85
Fig-6.8	Rock and wire mattress revetment	85

Fig-7.1	Critical water velocity for Quartz sediment as function of mean grain size (after ASCE Task Committee, 1967)	89
Fig-7.2	Shields Diagram for incipient motion	90
Fig-7.3	Correction factor in Logarithmic velocity distribution (Einstein, 1950)	90
Fig-7.4	Comparison of nominal stone diameter	104
Fig-7.5	Significant wave height ( $H_s$ ) as a function of fetch and wind speed with a mean water depth of 10m	105
Fig-7.6	Significant wave height ( $H_s$ ) as a function of fetch and wind speed with a mean water depth of 20m	105
Fig-7.7	Suggested riprap gradation curve	106
Fig-7.8	Particle stability diagram	108
Fig-7.9	Gabion stone size and mattress thickness related to velocity	109
Fig-7.10	Neill's curve for size of riprap stone	110
Fig-7.11	Maximum stone size for riprap according to USBR	110
Fig-7.12	Reduction factor ( $\eta$ ) with geotextile permeability ( after Veldhuijzen Van Zanten et al.1986)	114
Fig-8.1	Grain size distribution curve of bed material	124
Fig-8.2	Grain size distribution of filter material	137
Fig-8.3	Cross-section of river bank protection work with gabion along with granular filter under it	138
Fig-8.4	Cross-section of river bank protection work with gabion along with geotextile filter	138
Fig-8.5	Cross-section of river bank protection work with P.C.C Concrete block along with granular filter	139
Fig-8.6	Cross-section of river bank protection work with P.C.C Concrete block along with geotextile filter	139
Fig-8.7	Cross-section of river bank protection work with riprap along with granular filter	140
Fig-8.8	Cross-section of river bank protection work with riprap	140
Fig-9.1	Site selection to conduct field trial with polymer gabion	145



Fig-9.2	GI wire gabioni affected by corrosion	145
Fig-9.3	Due to rigidity GI wire gabions do not adhere to undulation	146
Fig-9.4	Stones are coming out due to mesh opening	146
Fig-9.5	Polymer tope gabion box carried to the river bed	147
Fig-9.6	Polymer rope gabion box is anchored	147
Fig-9.7	Polymer rope gabion is being filled with stones	148
Fig-9.8	Geotextile is being placed on the river bed	148
Fig-9.9	Top surface is being leveled with required size of stones	149
Fig-9.10	Gabion box is ready for covering	149
Fig-9.11	After filling gabion box is covered	150
Fig-9.12	After covering, gabion box is anchored with laces	150
Fig-9.13	Gabion box filling, covering and anchoring complete	151
Fig-9.14	After completion top levels are taken	151
Fig-A1	Longitudinal profile of Beas River	
Fig-A2	Location map of the project of Beas River	

## **LIST OF TABLES**

---

<b>Table No</b>	<b>Title</b>	<b>Page No</b>
TABLE- 1.1	Summary of Estimated Ultimate Interface Shear Stress	10
TABLE- 1.2	Application of Soil Nailing Technique	13
TABLE -3.1	Comparison of Design Methods	44
TABLE -6.1	Some Physical Properties of Jute Geotextile	82
TABLE- 7.1	Lacey's Factor in Scour Depth Calculation	94
TABLE- 7.2	Values of 'C' for Use in Escarameia and May's Equation	111
TABLE -9.1	Frequency Analysis	118

- $F_\phi$  = Factor of safety with respect to angle of internal friction  
 $F_p$  = Factor of safety with respect to material  
 $D$  = Diameter of nail  
 $F_N$  = Friction resistance of nail  
FOS = Factor of safety  
 $C_m$  = Mobilized cohesive forces  
 $\alpha$  = Arc angle of failure wedge  
 $q$  = Intensity of surcharge load acting on the wall  
 $S$  = Length on which surcharge load is acting  
 $P$  = Inter-granular forces  
 $T_i$  = Axial force /pullout resistance  
 $f_i$  = Limit bond stress  
 $\sigma_{ni}$  = Normal stress at mid depth of nail in the length  $l_{ei}$   
 $p_i$  = Perimeter of nail  
 $l_{ei}$  = Length of nail beyond the failure surface  
 $i$  = Number of nail rows/hydraulic gradient  
 $l_{si}$  = Shear width of nail  
 $T$  = Axial force in the nail at mid point of maximum bending moment/return period  
 $T_p$  = Fully plastic axial force  
 $D$  = Grout hole diameter/scour depth  
 $M_p$  = Fully plastic moment capacity of nail  
 $\sigma_b$  = Bearing stress of nail

- $T_{ci}$  = Shear force in the nail at mid point of intersection of failure surface
- $\theta$  = Inclination of nail with horizontal
- $\psi$  = Inclination of wall with vertical
- $k_g$  = Co-efficient of permeability of flow across the geotextile
- $k_s$  = Co-efficient of soil permeability
- $b$  = Width of bridge pier normal to flow/ stability factor incorporating turbulence
- $D_s$  = Depth of scour below mean bed elevation
- $D_0$  = Mean depth of flow upstream of pier
- $U_b$  = Mean upstream velocity
- $F_c$  = Critical Froude number
- $\xi$  = laminar sub-layer factor
- $X$  = Correction factor
- $U_c$  = Critical flow velocity
- $f$  = Silt factor
- $d_{50}$  = Average grain diameter
- $U_*$  = Dimensionless velocity factor
- $B$  = Channel width
- $A$  = Embankment length normal to the wall of flumes
- $q$  = Discharge per unit run
- $d$  = Grain diameter
- $\Delta Z$  = Relative scour depth
- $d_{sc}$  = Minimum grain diameter
- $S$  = Longitudinal slope of river

- $\Delta p_c$  = Fraction of material
- $S_f$  = Friction slope
- $d_a$  = Average channel flow depth
- $\Phi_c$  = Stability factor
- $D_n$  = Nominal thickness of protection unit
- $k_T$  = Turbulence factor
- $K_h$  = Depth and velocity distribution factor
- $\Delta m$  = Relative density of protection unit
- $K_s$  = Slope factor
- $\rho_s$  = Density of riprap material
- $\rho$  = Density of water
- $\alpha$  = Slope angle with horizontal
- $K_r$  = Mean equivalent roughness factor
- $n$  = Porosity of soil
- $N$  = Total number of rows of nail/SPT value
- $U_b$  = Bottom velocity or maximum return current velocity
- $U_b$  = Screw-race velocity
- $S_f$  = Safety factor
- $C_v$  = Velocity distribution co-efficient
- $R$  = Center line radius of bends/Scour depth from top of water surface
- $W$  = Water surface width at upstream end of bend
- $C_T$  = Blanket thickness co-efficient
- $K_1$  = Side slope correction factor

## **LIST OF TABLES**

---

<b>Table No</b>	<b>Title</b>	<b>Page No</b>
TABLE- 1.1	Summary of Estimated Ultimate Interface Shear Stress	10
TABLE- 1.2	Application of Soil Nailing Technique	13
TABLE -3.1	Comparison of Design Methods	44
TABLE -6.1	Some Physical Properties of Jute Geotextile	82
TABLE- 7.1	Lacey's Factor in Scour Depth Calculation	94
TABLE- 7.2	Values of 'C' for Use in Escarameia and May's Equation	111
TABLE -9.1	Frequency Analysis	118

## LIST OF SYMBOLS

---

$K_a$	= Coefficient of active earth pressure
$K_0$	= Co-efficient of earth pressure at rest.
$\gamma$	= Unit weight of soil mass
$\phi^*$	= Angle of internal friction for nailed soil
$\phi'$	= Angle of internal friction for unreinforced soil
$C^*_0$	= Apparent cohesion due to nail shear
$\tau^0$	= Shear forces
$\tau_s$	= Shear stresses
$\nabla\tau$	= Variation of shear stresses
$\sigma$	= Normal stresses
$l_0$	= Transfer length
$E$	= Young's modulus of the nail
$I$	= Moment of inertia of nailed cross-section/Longitudinal slope of river
$K$	= Modulus of soil reaction
$\delta$	= Displacement/soil-nail interface friction angle
$T_{max}$	= maximum tensile force
$T_d$	= Design tension
$H$	= Total height of wall/open cut
$S_h$	= Horizontal spacing of nails
$S_v$	= vertical spacing of nails
$F_c$	= Factor of safety with respect to soil cohesion.

- $F_\phi$  = Factor of safety with respect to angle of internal friction
- $F_p$  = Factor of safety with respect to material
- $D$  = Diameter of nail
- $F_N$  = Friction resistance of nail
- FOS = Factor of safety
- $C_m$  = Mobilized cohesive forces
- $\alpha$  = Arc angle of failure wedge
- $q$  = Intensity of surcharge load acting on the wall
- $S$  = Length on which surcharge load is acting
- $P$  = Inter-granular forces
- $T_i$  = Axial force /pullout resistance
- $f_i$  = Limit bond stress
- $\sigma_{ni}$  = Normal stress at mid depth of nail in the length  $l_{ei}$
- $p_i$  = Perimeter of nail
- $l_{ei}$  = Length of nail beyond the failure surface
- $i$  = Number of nail rows/hydraulic gradient
- $l_{si}$  = Shear width of nail
- $T$  = Axial force in the nail at mid point of maximum bending moment/return period
- $T_p$  = Fully plastic axial force
- $D$  = Grout hole diameter/scour depth
- $M_p$  = Fully plastic moment capacity of nail
- $\sigma_b$  = Bearing stress of nail



- $T_{ci}$  = Shear force in the nail at mid point of intersection of failure surface  
 $\theta$  = Inclination of nail with horizontal  
 $\psi$  = Inclination of wall with vertical  
 $k_g$  = Co-efficient of permeability of flow across the geotextile  
 $k_s$  = Co-efficient of soil permeability  
 $b$  = Width of bridge pier normal to flow/ stability factor incorporating turbulence  
 $D_s$  = Depth of scour below mean bed elevation  
 $D_0$  = Mean depth of flow upstream of pier  
 $U_b$  = Mean upstream velocity  
 $F_c$  = Critical Froude number  
 $\delta$  = laminar sub-layer factor  
 $X$  = Correction factor  
 $U_c$  = Critical flow velocity  
 $f$  = Silt factor  
 $d_{50}$  = Average grain diameter  
 $U_*$  = Dimensionless velocity factor  
 $B$  = Channel width  
 $A$  = Embankment length normal to the wall of flumes  
 $q$  = Discharge per unit run  
 $d$  = Grain diameter  
 $\Delta Z$  = Relative scour depth  
 $d_{sc}$  = Minimum grain diameter  
 $S$  = Longitudinal slope of river

- $\Delta p_c$  = Fraction of material
- $S_f$  = Friction slope
- $d_a$  = Average channel flow depth
- $\Phi_c$  = Stability factor
- $D_n$  = Nominal thickness of protection unit
- $k_T$  = Turbulence factor
- $K_h$  = Depth and velocity distribution factor
- $\Delta m$  = Relative density of protection unit
- $K_s$  = Slope factor
- $\rho_s$  = Density of riprap material
- $\rho$  = Density of water
- $\alpha$  = Slope angle with horizontal
- $K_r$  = Mean equivalent roughness factor
- $n$  = Porosity of soil
- $N$  = Total number of rows of nail/SPT value
- $U_b$  = Bottom velocity or maximum return current velocity
- $U_b$  = Screw-race velocity
- $S_f$  = Safety factor
- $C_v$  = Velocity distribution co-efficient
- $R$  = Center line radius of bends/Scour depth from top of water surface
- $W$  = Water surface width at upstream end of bend
- $C_T$  = Blanket thickness co-efficient
- $K_1$  = Side slope correction factor

$\Delta$	= Relative density of rock
$Z_{\max}$	= Total height of transversal stern wave
$H_i$	= Height of interference peak of wave
$H$	= Wave height
$T$	= Wave Period
$H_s$	= Significant wave height
$T_p$	= Wave peak period
$B$	= Exponent related to the interaction between waves and revetment
$\Phi_u$	= System determined stability factor
$Z_{*c}$	= Critical value of Shields number
$d_m$	= Effective grain size
$\tau_o$	= Applied shear stress
$TI$	= Turbulence intensity
$U_d$	= Depth averaged velocity
$C_u$	= Coefficient of uniformity
$T_g$	= Thickness of geotextile
$\eta$	= Reduction factor of permeability of geotextile
$L_a$	= Apron length
$D$	= Mean diameter of stone
$d_s$	= Anticipated depth of scour
$S_y$	= Standard deviation
$C_s$	= Co-efficient of Skewness
$P$	= Probability of occurrence

$Q$  = Discharge  
 $HFL$  = Highest water level  
 $n$  = Roughness co-efficient  
 $\Lambda$  = Area of flow  
 $EL$  = Energy level  
 $B_T$  = Top width of river / channel  
 $R_n$  = Hydraulic mean depth  
 $F, Fr, F_0$  = Froude Number  
 $V$  = Velocity of flow

## INTRODUCTION

---

### 1.1 CONCEPT OF SOIL NAILING

The basic concept of soil nailing is to reinforce and strengthen the existing ground by installing closely spaced steel bars called 'nails' into a slope or excavation as construction proceeds from 'top to down'. This process creates a reinforced section that is itself stable and able to retain the ground behind it. The reinforcements are passive and develop their reinforcing section through nail ground interactions as the ground deforms both during and following construction. Nails work predominantly in tension but are considered by some to also work in bending, shear under certain circumstances. Generally the soil nails significantly increase apparent cohesion of the nail through their ability to carry tensile loads. A construction facing is also usually required and is typically shotcrete reinforced by welded wire mesh. For permanent walls, the shotcrete construction facing is typically covered in cast- in- place concrete facing.

### 1.2 HISTORY OF SOIL NAILING

Soil nailing technology was first used in France to build a permanent retaining wall cut in soft rock. Project undertaken in 1961, was the first where steel nails were used to reinforce a retaining wall. The first soil nail wall to use modern soil nailing techniques was built near Versailles in 1972. The technique included installing high- density grouted soil nails into a 18.3m high wall and facing it with reinforced concrete. Europe, particularly France and Germany continues to lead the world in soil nailing technology. Soil nail construction is fairly new to North America. The first soil nail techniques are believed to have been applied to temporary retaining wall in Vancouver in the late 1960s. The first documented construction project to use soil nailing was in Poland in 1976.

### 1.3 SOIL NAILING ADVANTAGES

- Requires less space and manpower
- Can be used to follow grade curves.
- Equipment is portable and fits in small spaces.
- The process is flexible and modifications are easy to do.
- Construction creates less noise and traffic obstructions.

- Has less impact on nearby properties

It may be mentioned here that soil nailing is possible in clay, sandy soils, weathered rock, stratified soils and soil nailing is not possible in soft plastic clay, organic/peat, loose ( $N < 10$ ) low density and or saturated soil.

#### 1.4 SOIL NAILING CONSTRUCTION SEQUENCE

Standard construction steps for a typical soil nailing method can be broadly divided into four steps and three steps are repeated in cycle as outlined below.

- Excavation of slopes (Fig-1.1a): Soil is excavated in lifts to accommodate at least a single row of facing panels. Besides this, each height of such lift should secure the overall stability of the uncovered soil until before soil nail is ready to transfer the load to soil mass under the critical slip surface.
- Positioning of facing material (Fig-1.1b): Facing material e.g. Facing panels are positioned or laid down in rows as shown in Fig-1.1b.
- Drilling, Nailing & Grouting (Fig-1.1c): Nail holes are then drilled to designed nail length and inclination. Then design nails are inserted into the hole and grouted to develop a strong bond between the nail and the soil. To confirm the perfect contact between the back of the facing panel and soil surface, the gap behind the facing material is filled by injecting a cement slurry or mortar. In the case of full-length cast in-situ facing material, this work is part of the works under step no-2.
- Reinforcement tightening (Fig-1.1d): Nails are tightened by nut-bolt connection so that tensile bar force near the facing can be mobilized to the design level. It is usually necessary to ensure the stability of soil slope close to the slope face especially in the case of sandy soil. Once the tightening of reinforcement for a particular row is over, the aforementioned steps (steps 1 to 3) are repeated for the successive row of soil nails i.e. next row.

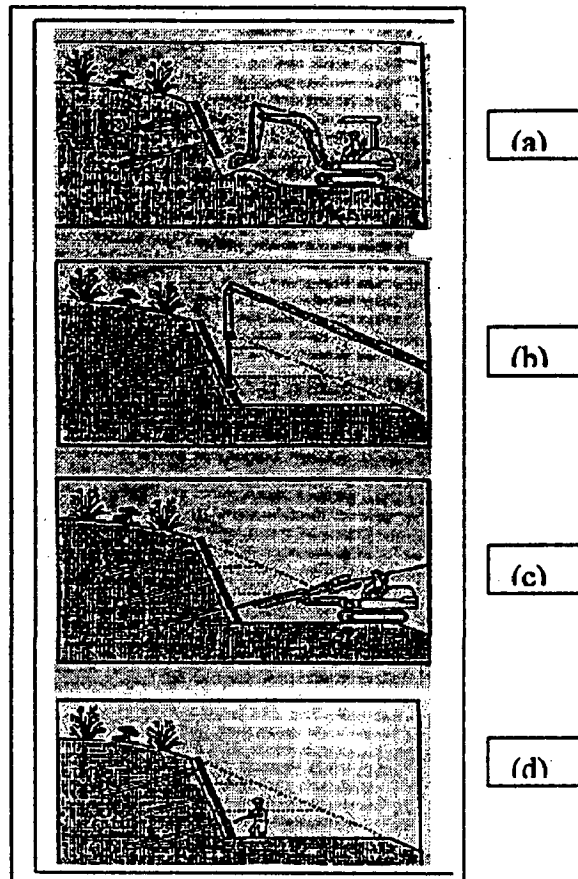


**Fig-1.1 Construction Steps in a Typical Soil Nailing Method (Pokharel and Ochiai, 1997)**

## **1.5 SOIL NAILING COMPONENTS**

### **1.5.1 The In-Situ Ground**

The excavation is generally carried out using conventional earthwork equipment, starting at the ground surface and progressing downwards. Seepage of ground water towards the excavated face must be avoided by drainage. The total allowable excavation depth depends on the global stability of the excavation. The maximum incremental excavation depth is determined by the stability of the soil to stand unsupported for several hours. In granular soils the short- term capillary cohesion may be sufficient to ensure local stability of each excavated depth (Gassler, 1990). In silt and clay the natural cementation and cohesive strength of the soils give the necessary short-term stability of the cut depth. In any case the excavation depth is limited to 1.5m.

### 1.5.2 Tension Resisting Nails

Conventionally the steel reinforcing elements used for soil nailing can be classified as (a) driven nail and (b) grouted nails. However, especially designed corrosion-protected nails have been used in permanent structures, specifically in aggressive environment. During the past decade the most significant technological innovations have been the development and use of the jet-grouted nails (Louis, 1986) and the launched soil nails (Ingold and Miles, 1996). A brief description of the available nailing system is outlined below.

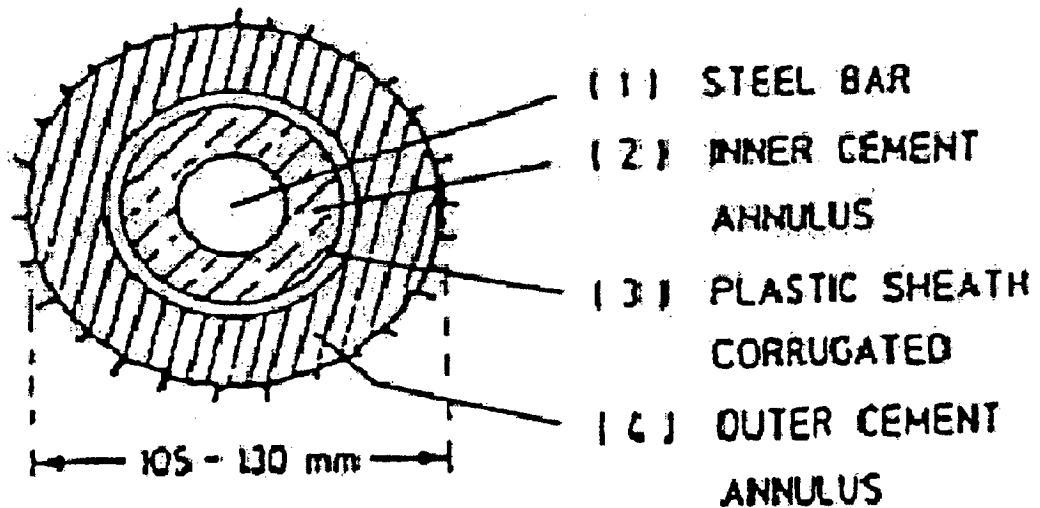


Fig-1.2a A Typical Permanent Nail used in Germany ( Gassler, 1990 )



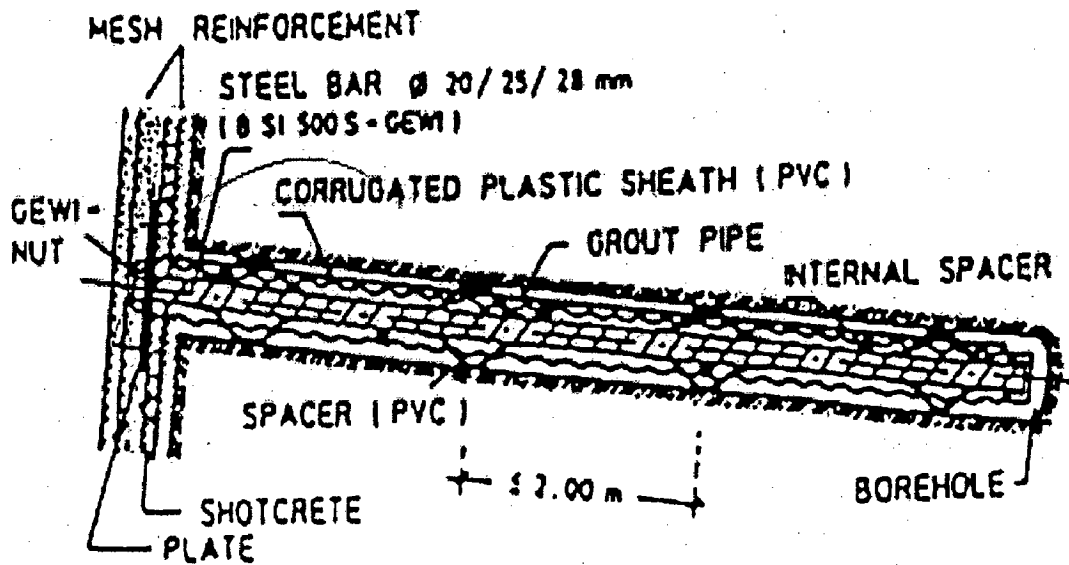


Fig-1.2b Corrosion Protection for Permanent Nails used in Germany (Gassler, 1990)

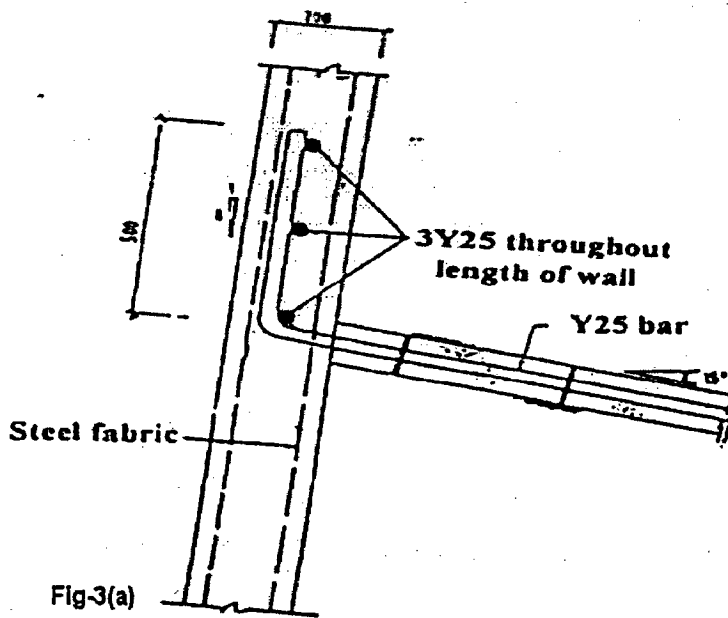
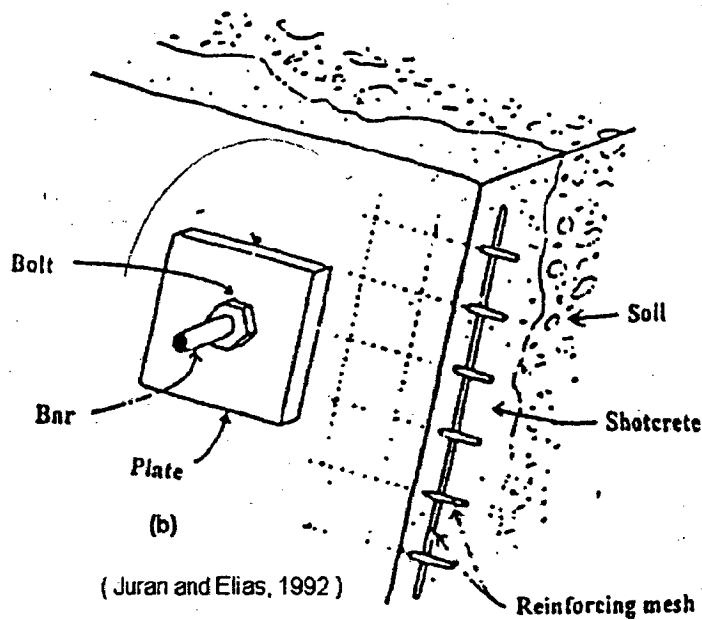


Fig-1.3 (a) Connection of Nails and Facing by Bending the Nails



**Fig-1.3 (b) Connection of Nail and Facing by using Steel Plate and Nut.**

Driven nails commonly used in France and Germany are small-diameter (15mm to 46mm) rods or bars or metallic section made of mild steel with yield strength of 350 Mpa. They are closely spaced (2 to 4 bar per square meter) and create a rather homogenous composite reinforced soil mass. The nails driven into the ground at the designed inclination using a vibro percussion pneumatic or hydraulic hammer with no preliminary drilling. Special nails with an axial channel can be used to allow for grout sealing of the nail to the surrounding soil after its complete penetration. This installation technique is rapid and economical (4 to 6 per hour). However it is limited by the length of the bars (maximum length about 20m) and by the heterogeneity of the ground (e.g., presence of boulders).

Grouted nails are generally steel bars (15mm to 46 mm in diameter) with yield strength of 420Mpa. They are placed in borehole (10 to 15 cm) in diameter with a vertical and horizontal spacing varying typically from 1 to 3 m depending on the type of the in-situ soil. The nails are usually cement grouted by gravity or under low pressure. Ribbed bar can be used to improve the nail grout- adherence and especially perforated tubes have been developed to allow injection of the grout through the inclusion.

Corrosion protected nails generally used double protection schemes similar to those commonly use in ground anchor practice. Proprietary nails have recently been developed by

specialty French contractors (Intrafor-Cofor, Solrenfor) to be used in permanent structures. For permanent applications of soil nailing, based on current experience, it is recommended that a minimum grout cover of 3.8cm be achieved along the total length of the nail (Elias and Juran, 1991). Secondary protection should be provided by electro statically applied resin- bonded epoxy on the bars with a minimum thickness of about 14mm. In aggressive environment, full encapsulation is recommended. It may be achieved as for anchors by encapsulating the nail in corrugated plastic or steel tube grouted into the ground. For driven nails, a preassembled encapsulated nail has been developed by the French contractor Solrenfor (Louis, 1986)" as found on Internet"

Jet-grouted nails are composite inclusions made of a grouted soil with a central steel rod which can be as thick as 30 to 40cm. A technique that combines the vibro percussion driving and high pressure (greater than 20Mpa) jet grouting has been developed recently by Louis (1986). The nails are installed using a high frequency (up to 70Hz) vibro percussion hammer and cement grouting is performed during installation. The grout is injected through a small-diameter (few millimeters) longitudinal channel in the reinforcing rod under a pressure that is sufficiently high to cause hydraulic fracturing of the surrounding ground. However nailing with a significant lower grouting pressure (about 4Mpa) has been used successfully particularly in granular soils. The inner nail is protected against corrosion using a steel tube. The jet grouting installation technique provides recompaction and improvement of the surrounding ground and increases significantly pull-out resistance of the composite inclusion

The nail launching technology (Bridle and Myles, 1991; Ingold and Myles, 1996) consists of firing directly into the ground using a compressed air launcher, nails of 25mm and 38mm in diameter made from bright bar (EN3B to BS982) with nail lengths of 6 meters or more. This installation technique enables an optimization of nail installation with a minimum of the disruption. During penetration the ground around the nail is displaced and compressed. The annulus of compression developed reduces the surface friction and minimizes damage to protective coatings such as galvanized and epoxy. The technology is presently used primarily for slope stabilization although successful applications have also been recorded for retrofitting of retaining system. However, a rigorous evaluation of the pullout resistance of launched nails is required prior to their use in retaining structures.

### **1.5.3 Facing on the Structural Retaining Elements**

In soil nailed structures the facing is found to play only a minor mechanical role (Juran and Elias, 1992). The function of facing is to ensure local stability of the soil between the nails and to limit the decompression of the soil. The facing protects the soil from erosion and weathering effects. It also gives an aesthetic appearance and prevents moisture loss. Shotcrete facing is most commonly used, depending upon the site condition and the ultimate wall batter or slope. Shotcrete is defined as concrete or mortar that is projected at high velocity into a surface. Shotcrete is comprised of cement, water and aggregate typically less than 12.7mm sieve size with the majority of the aggregate classified as sand size particles. Wet-mix shotcrete is normally used since it is usually less expensive and easier to install. The properties of the shotcrete that are critical during installation are its ability to be pumped and its adhesion. These are controlled by the mix-design, cement water ratio, air entrainment, the pumping system used and other variables. The required strength of the shotcrete will be determined as part of the design process. However as a minimum to provide adequate strength and durability the shotcrete will need to have a minimum 28-day compressive strength of 27.58 Mpa and a water cement ratio of less than 0.5. There are other options that may be desirable. Each of these is discussed below:

#### **❖ Temporary facing**

This includes shotcrete and welded wire mesh, welded wire mesh, steel channels and geotextiles and timber shoring. The most effective is shotcrete since it creates a bond with the soil and fills in voids, which may develop due to sloughing of soil at the wall face. For projects involving nearly vertical walls where minimal wall movement is required, this is the best option. Typically 7.5cm or 10cm layer of shotcrete is applied. The shotcrete is lightly reinforced with welded wire mesh. Drainage can be provided if needed between soil nails at less than 50% area coverage to allow for bond of the shotcrete with the soil. For sloping walls or for sites where vertical cuts are not required to install soil nails (cut and fill situations) use of a welded wire mesh facing may be effective. In these situation where soils have an apparent cohesion and are cut on a slope and soil sloughing is not a problem, the facing can be designed to contain the fill rather than provide a structural face to span nails in flexure.

#### ❖ **Permanent facing**

These include reinforced shotcrete, cast in place and precast concrete panels, concrete masonry segment wall units and gabions. These facings must be designed to structurally support the soil loading applied between soil nails and be attached with a connector that is strong enough to resist punching failure of the nail at the wall face. For soil nailed slopes where the slope facing is stable without reinforcements, a facing consisting of an erosion mat and vegetation consistent with the area can be utilized.

#### **1.5.4 Wall Connector**

Connection to the shotcrete facing can be designed and constructed in several ways. The cost of the connector is a function of the performance desired and the design life. For temporary soil nail wall, the connection needs to be of sufficient durability to last until the end of the project. Stress transfer to the face occurs over an extended period of time in a soil-nailing wall, depending on the shear strength of the reinforced soil. Connectors utilizing a 1.9cm thick plate and #4 rebar are typically sufficient. The shotcrete thickness will vary 7.5cm to 10cm and should completely cover the connector. For permanent walls, the ability to positively tension the connector is desired. The use of threaded connector facilitates tensioning the anchor by torqueing the nut, thus reducing the potential for localized movement of the face.

#### **1.5.5 Drainage**

Drainage is a critical element in planning and construction. Most commonly, face drainage is used; a drainage element is placed behind the shotcrete wall covering the nailed structure. The drainage elements are installed from top to down as construction proceeds. Typically synthetic strips or perforated pipes (20-30cm) are installed, usually spaced about 1.5-2m apart. The water is collected at the wall base and channeled away. Alternatively weep holes can be made through face of the wall used with or without perforated drainpipe.

## 1.6 SOIL NAIL INTERACTION

In a soil nailing, similar to ground anchors, the transfer mechanism and ultimate pull-out resistance of the nails depend primarily on soil type and strength characteristics, installation technique, drilling method size and shape of the drilled hole as well as grouting method and pressure used. To date estimates of the pullout resistance of nails are mainly based upon empirical formulae (or ultimate interface shear stress values) derived from field experience. These formulae are useful for feasibility evaluation and preliminary design. Table -1.1 (Elias and Juran, 1991) provides a summary of estimated ultimate interface shear stress values for soil nails as function of soil type and installation technique.

**TABLE-1.1 (Summary of estimated ultimate interface shear stress)**

<b>Grouted nails</b>	<b>Soil type</b>	<b>Soil nailing (Elias and Juran, 1991)</b>
<b>Construction method</b>		<b>Ultimate lateral shear force, KN/m</b>
Rotary drilled	silty sand	29.24 to 58.48
	Silt	17.54 to 23.39
	Piedmont residual	21.93 to 36.55
Driven casing	Sand	87.72
	Dense sand/gravel	116.96
	Dense moraine	116.96 to 175.44
	Sandy colluvium	14.62 to 29.24
	Clayey colluvium	14.62 to 29.24
Jet grouted	Sand	116.96
	Sand/gravel	292.40
Augered	soft Clay	5.85 to 8.77
	Stiff to hard clay	11.69 to 17.54
	Clayey silt	14.62 to 29.24
	Calcareous sandy clay	58.48 to 87.72
	Silty sand fill	5.85 to 8.77

## **1.7 APPLICATIONS**

### **A. New construction**

- **Stabilization of railroad and highway cut slopes**
- **Excavation retaining structures in urban areas for high rise building and underground facilities**
- **Construction and retrofitting of bridge abutments with complex boundaries involving wall support under pile foundation**

### **B. Remedial works**

- **Repair of unstable old gravity retaining walls.**
- **Stabilization of failed soil slopes**
- **Repair of anchored wall that failed due to overloading or corrosion of tendon.**
- **Repair of reinforced soil wall**

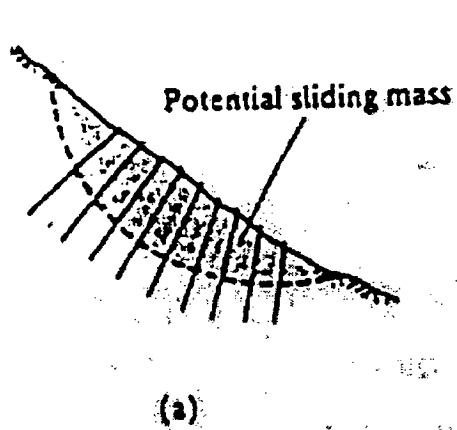


Fig-1.4 (a) Landslide Stabilization

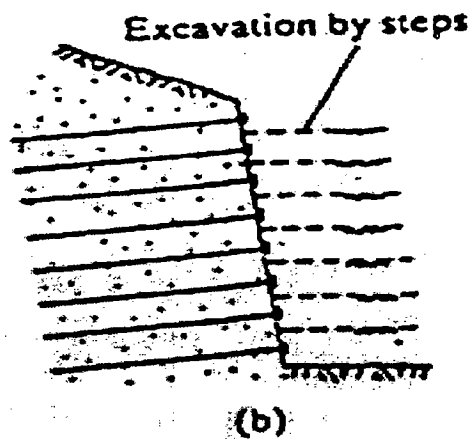


Fig-1.4 (b) Retaining Structures

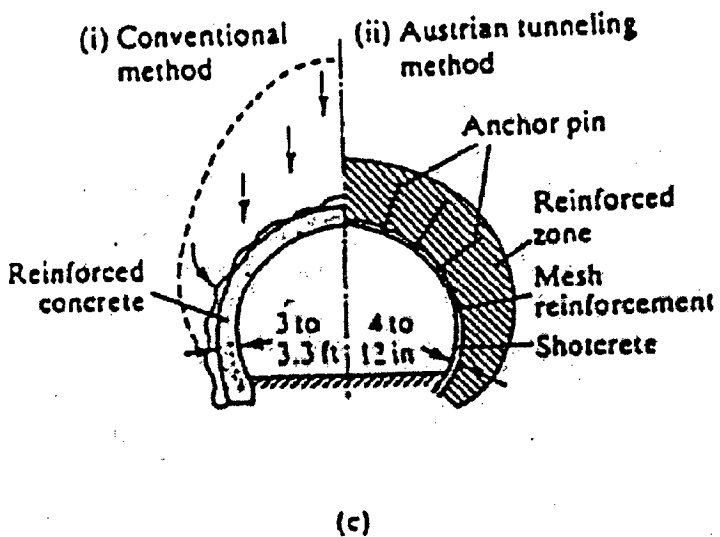


Fig-1.4 (c) Tunnel Portal

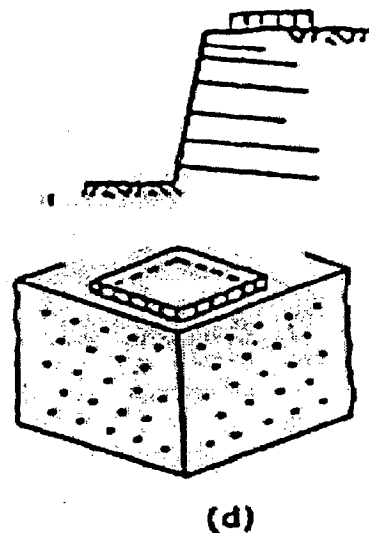


Fig-1.4 (d) Abutments

Fig-1.4 (a, b, c, d) Applications of Soil Nailing (Juran and Elias, 1992)

An overview of experimental and theoretical studies leading to the development of various methods of analysis of soil nailed structures is presented below:



**TABLE-1.2(An overview of experimental and theoretical studies)**

Site	Objective	Construction	Investigators
At Lor.Terigu Bukit Timah diversion Canal phase-1, Singapore	To stabilize a failed slope (about 24m high and 100m in length) along the canal by nailing	First stabilized by sheet piles then by nailing	Tan et al. (1988)
Near Singapore General Hospital	To stabilize a steep slope near Singapore General hospital	The slope has been reinforced with 8m long nails at 2mc/c	Tan et al. (1988)
Pennsylvania, USA	Stabilization of road cut into steep hillside along the bench of a river	Inserts placed to provide maximum width at top	Schnabel (1991)
Cumberland land gap, Border of Kentucky and Tennessee, USA	Replacing the steep grades and present road resulting in 12m high nailed wall	Excavating in lifts of 1.5m with sequential installation of shotcrete and nails	Schnabel (1991)
Easton, PA, USA	Construction of 14.4m high permanent nailed wall	Construction began with excavation of a shallow cut	Schnabel (1991)
Phoenix, Arizona	Construction of a deck by soil nailing which allows for the protection of adjacent property	A cut was required to be made adjacent to a row of bushes and palm trees	Schnabel (1991)
San Francisco, CA, USA	To underpin heavily loaded structures by soil nailing	Concrete piers, soil nail and shotcrete were adopted	Schnabel (1991)
Phoenix, Arizona	Stabilize a cut required to install a 2.5m pipe 19.8mbelow grade	No sufficient room to slope the cut by retaining wall	Schnabel (1991)

Monroeville, Pennsylvania, USA	For the construction of parking lot for commercial development in hillside	In-situ nailing adopted as an alternative to costly cantilevered retaining wall	Schnabel (1991)
Bypass channel, Walnut Creek, California, USA	For the excavation of a 15.25m wide by 6.1m deep drainage within a few feet of existing building, for the bank protection	Buildings were under pinned by drilling through the footing. Reinforced horizontally with soil nailing.	David (1991)
Phoenix, Arizona	Protection of street and utilities nearby an excavation to install a drainage tunnel junction and avoid high cost of drilling soldier beam	Soil nailing was installed in 1.5m lift by placing wire mesh and shotcrete to exposed surface	David (1991)
Fredericksburg, Virginia, USA	Stabilization of a 9.6m cut action of tiebacks with soil nails called TEN wall (Tieback element nailed wall)	Seven rows of nails and one row of tie backs were installed by pressure-injected grout method	David (1991)
Marine Training Facility, Near Coleville, California, USA	To retain the slope above a bench cut 6.1m high for a water storage tank; nailing was adopted to avoid aesthetically undesirable over excavation required for a conventional retaining wall.	Wire mesh was welded to bars and nails were installed in 10cm diameter drilled holes	David (1991)
Pullman, Washington	Building a soil nailing support system needed to excavate a 12.2 m cut for a new chemistry building of Washington State University	The system could be constructed rapidly short steel tendon and shotcrete that are	Schnabel (1991)

		readily available	
Pullman, Washington, University, Washington, USA	For building an extension to the chemistry building at Washington State University the protection to the excavation on four sides (7.6m to 13.7m deep) soil nailing was adopted because of the quick start up time and construction duration	Soil nailing was installed with a hollow-stem auger to prevent the drill hole from collapsing. Vertical drains, wire mesh and shotcrete were applied to each lift while excavating in a spiral fashion	David (1991)
St.Peter Port, Guemsey, U.K	For the construction of a new office and residual development, where an existing 20m high 53 degree slope was to be re-graded to 70 degree over the lower 10m and below the base of slope a basement was constructed	Nails installed at 20 degree below horizontal. Corrosion protection was provided by a corrugated P.V.C sheath .A geogrid was rolled over the surface of the slope.	Pedley (1992)

## 1.8 LIMITATION OF THE EXISTING SOIL NAILING TECHNOLOGY AND PROPOSED NEW ENHANCEMENT

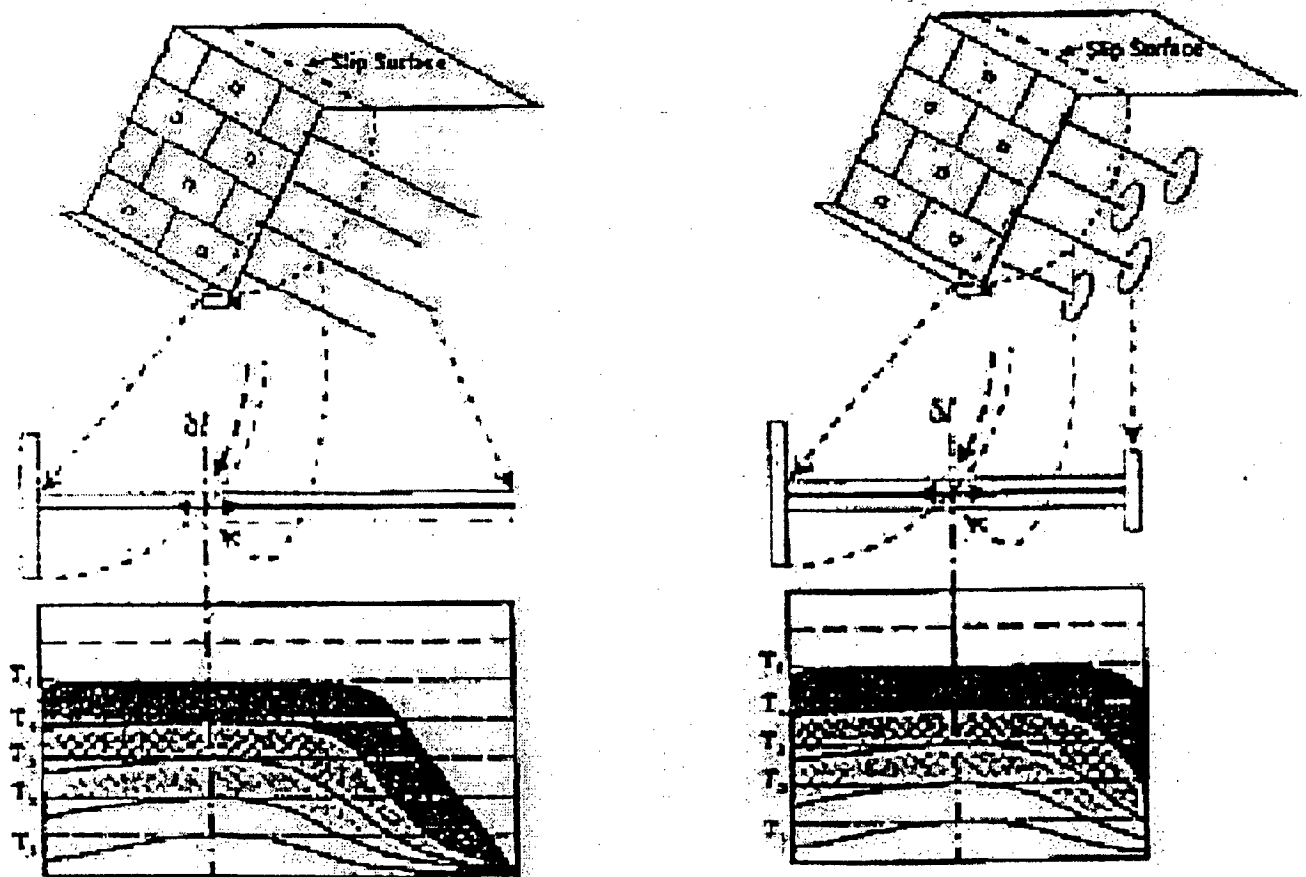
- The technique of the soil nailing requires cuts, which can stand unsupported for depths of about 1 to 2m at least for a few hours prior to shotcreting and nailing. This requires some cohesion and apparent cohesion in natural soil. Otherwise a pretreatment such as grouting may be necessary to stabilize the face (Gassler 1990). This pretreatment will add both complication and cost.

Also it is desirable to have a dewatered face in excavation for soil nailing .If ground water percolates through the face, the unreinforced soil will slip locally on initial excavation.

- Mobilization of tension in the nail requires relative displacement of soil and reinforcement. Hence in urban sites where ground movement must be avoided, the technique may not be feasible.
- In corrosive ground, durability considerations rule out the use of soil nails as permanent support.

The pull out test conducted by Pokharel et.al (1997) showed that the conventional soil nailing requires a minimum length to mobilize the design axial force shown in Fig-1.6 and it controls overall length and size of the soil grout interface. The cumulative deformation of a long soil nail at slip surface or slope face might exceed the allowable deformation limit and the serviceability of the structure becomes questionable when it is close to sensitive structure e.g. the railway track, building etc. This requires either an enlarged grouted zone or closely spaced nails (increase in the number of nails). This might result nailing system expensive and obsolete with respect to other alternatives. It requires an efficient solution. Considering the limitations of the existing soil nailing method, the soil slope that passes low or negligible angle of internal friction has to be treated differently and the conventional soil nailing method has to be either redesigned or enhanced to such site conditions. The most important solution considering economic factor could be reduction in the mandrel length (soil-grout interface sleeve and its diameter). The second criteria i.e. excessive cumulative deformation of nail at slip surface and slope faces, requires a widening of load transfer area by reducing the total length of nails thus avoiding the creep effect too. If anchor plate (Fig-1.5) can be attached at the end of a soil nail or if multiple anchor plates are attached at different lengths of soil-nails in addition to the end, the method could be an economic means of solving the aforementioned problem. The main advantage of the proposed anchor plate attached soil nailing method over the existing methods is the reduction of on the minimum length of reinforcement required to mobilize the peak axial force behind the critical slip surface as

shown in Fig-1.5. This might considerably reduce the over all cost of the soil nailed structure and also reduce the cumulative deformation of soil nail at the slip plane.



(a) Axial force distribution in conventional soil nailing (b) Proposed axial force distribution pattern

Fig- 1.5 Qualitative Comparison between a Conventional and the Proposed Axial Force

## 1.9 COMPARISON OF SOIL NAILING WITH REINFORCED SOIL

Soil nailing and reinforced soil appear similar in friction that is mobilized at the soil /reinforcement interface as a result of which the lateral deformation of the soil are restrained .The two however differ in the following respect.

- Soil nailing is constructed by staged excavation from 'Top to down' while reinforced soil is constructed from 'Bottom to top' layer by layer. This

difference leads to some difference in the stress and the strain pattern particularly during the construction stages

- The reinforcement used in nailed soil structures is generally grouted to effectively bond the reinforcement to the surrounding ground. So the reinforcement is much stiffer compared to reinforced soil.
- Since soil nailing is an in-situ reinforcing technique the soil properties cannot be pre-selected. In contrast, the soil in reinforced soil is a new fill, which can be selected and controlled.

### **1.10 OBJECTIVE OF THE STUDY**

1. To analyze the soil nailed wall of C-J soil with friction circle method
2. To determine the factor of safety at different conditions
3. To develop a computer programming to compute factor of safety.
4. To use the technique in river bank erosion
5. To conduct a case study of riverbank protection work in Beas River in Himachal Pradesh of India
6. To conduct a field experiment for performance study of flexible polymer rope in river bank erosion control in boulder stage river.

REVIEW OF LITERATURE

---

2.1 STUDIES ON FULL-SCALE MODEL TESTS

Plumelle et al. (1990), Plumelle and Schlosser (1990) tested a full-scale soil nailed wall to failure progressively by saturating the reinforced soil mass (Fig-2.1). The nails, soil and wall were instrumented and pullout tests were performed to determine the soil nail lateral friction. Analysis of the same using both finite element and a computer program (TALREN) gave rise to the following conclusions:

- a) The line of maximum tensile and maximum bending moment generated in the nails coincides with the actual failure zone observed.
- b) The mobilized tensile force develops progressively during excavation and can increase with time especially if the safety factor is low.
- c) Under large deformations, the bending resistances of the nails are mobilized, providing a greater resistance to failure.
- d) The failure surface intersects the ground surface at a distance of 0.33 times the height of cut/wall from the face.
- e) The lateral deformation of the wall is of the order of 0.3% of the wall height.
- f) The finite element analysis predicts lower values for the horizontal displacements developed in the soil mass of nailed structures whereas TALREN method predicts the actual behavior of the same.

Stocker and Riedinger (1990) made the following observations by carrying out long term test (over a period of 10years) on a 15m high nailed-wall in a cohesive soil:

- (a) The top nail does not substantially contribute to the retaining force of the wall system

- (b) The nail force increases for a short duration during construction and remains almost constant thereafter
- (c) The main deformations occur at the top of wall
- (d) The horizontal displacements of nailed wall are larger than that of anchored structure.

Juran (1987), Juran et al. (1988), Juran and Elias (1990) presented field observations during and after construction of instrumented full-scale nailed soil retaining structures. They observed a significant post construction increase in both facing displacement and nail forces.

$\lambda =$  Width of failure wedge at the top of wall

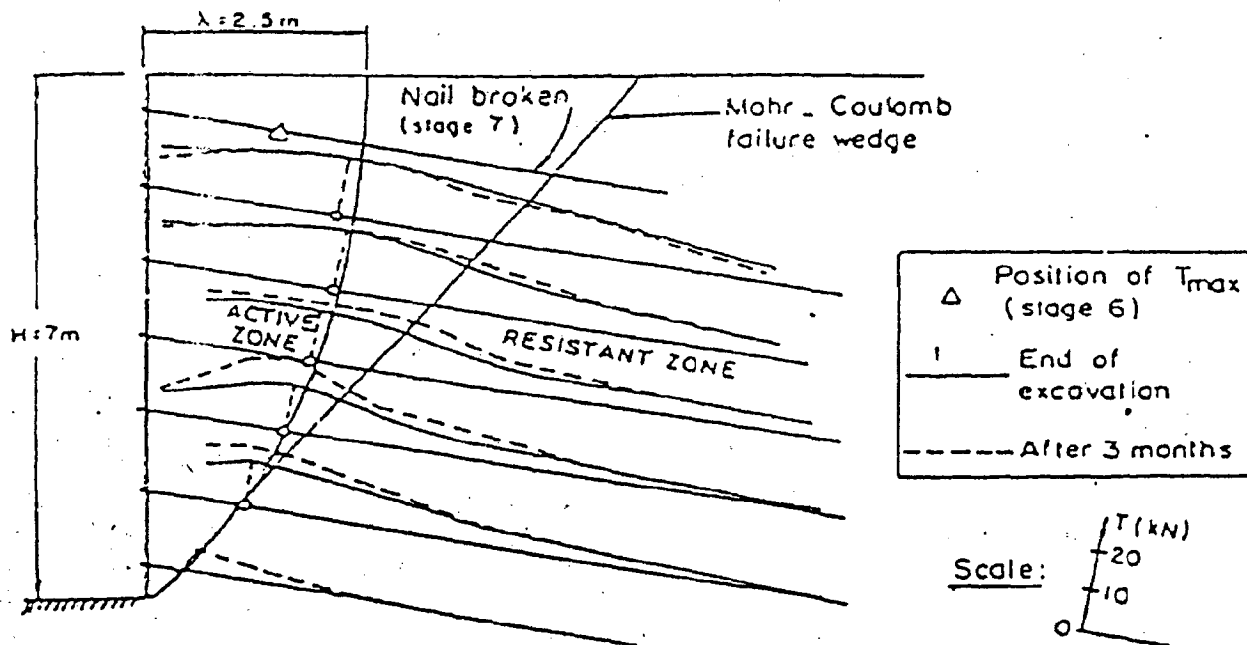
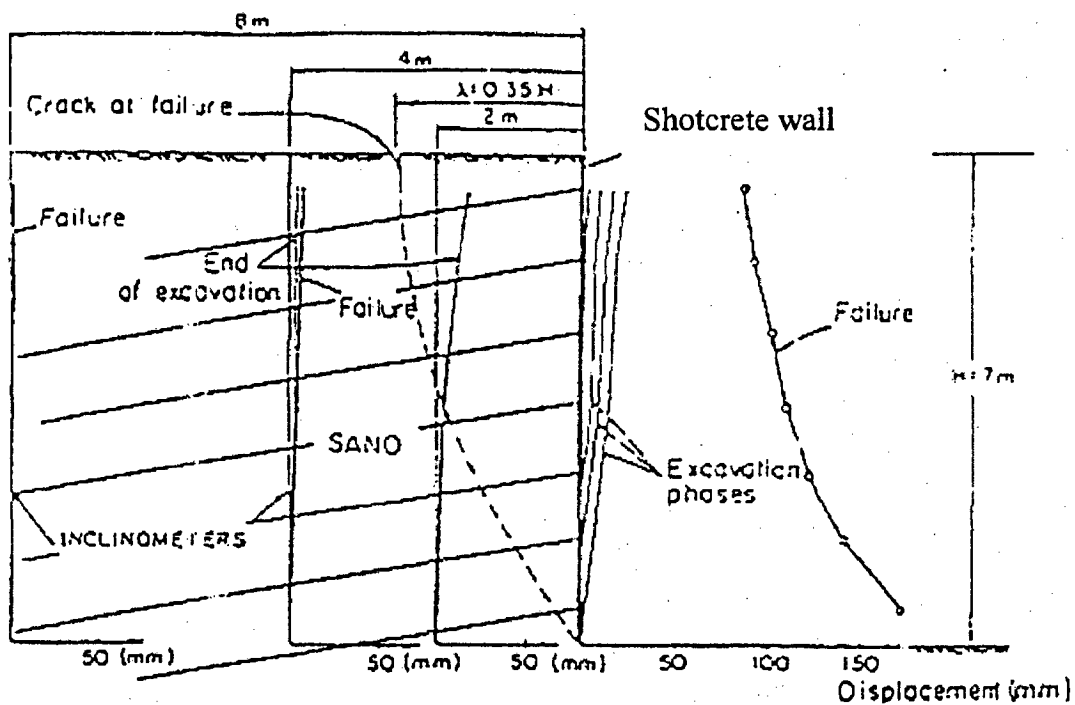
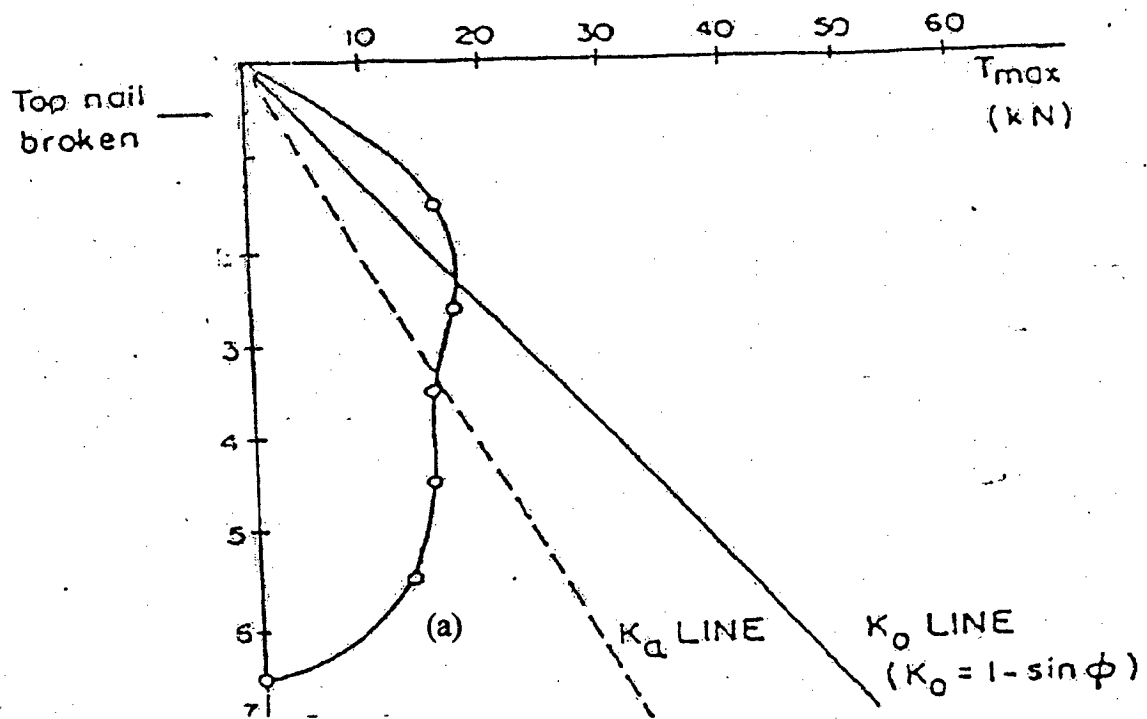


**Fig-2.1 Measured Nail Force Distribution in a Full Scale Nailed Test wall (Plumelle et al.1990)**





(b)

**Fig-2.2 (a) Variation of Measured Maximum Nail Force with Depth (b) Measured Horizontal Displacement in a Full Scale Nailed Test Wall (Plumelle et al.1990)**

## 2.2 STUDIES ON LARGE-SCALE MODEL TESTS

Stocker et al. (1979) carried out model tests and large-scale field tests and measured deformations within the reinforced soil, surface deformation of the nailed ground along with the forces and strains in the nails. They observed two kinds of failure mechanism governed by the location of the loading. Where loads are closer to the edge of the slope, a simple failure mechanism with one slope line has been observed. But when loads are away from the edge of the slope, a composite mechanism of two blocks, consisting of a triangular soil block under the load and trapezoidal nailed soil mass separated from each other by a secondary slip line was observed.

Shen et al. (1981a, 1981b) reported the performance of a lateral earth support (in-situ-earth reinforcement) at two sites. The predictions from finite element analysis agree with the field measurements indicating that the analytical procedure so developed can predict correctly the field behavior.

Cartier and Gigan (1983) studied the behavior of an instrumented experimental soil nailed wall of height 5.5m reinforced with 50x50x5mm driven steel angles in sand. At the end of excavation, the displacements of the wall measured by inclinometers were very low, about 6mm at the top, 0.1% of the height of the wall. No bending of the wall was detected. The measured nail force at the end of excavation was maximum in the nails in the middle half of the wall height. The maximum nail force was measured at some distance away from the facing. Based on these observations and the locus of maximum tensile stresses in the nails, the authors concluded that the behavior of nailed walls is similar to reinforced soil.

Gassler and Gudehus (1981), Gassler (1988) conducted large scale field tests on nearly vertical cuts in cohesionless soils and analyzed various failure mechanisms based on their field and model tests. Only tensile strength of the reinforcement has been taken care of while determining stability of the reinforced soil mass. The authors adopted kinematically admissible failure mechanism of rigid bodies to find minimum factor of safety varying the inclination of slip planes and suggested four failure modes such as translation of a rigid body, translation of two rigid bodies, rotation of one rigid body and rotation of two rigid bodies. The results obtained from the above

failure modes are in good agreement with model and field test results and the translation mechanism of one or two bodies and the simple rotation mechanism are found to be more relevant to practical design.

Nagao et al. (1988) conducted large -scale field loading tests on natural earth slope reinforced with steel bars to study the mechanism of stability of reinforced earth. Loading tests were simulated using two and three-dimensional FEM analysis and opined that two dimensional plane strain FEM analysis is more effective.

Gassler (1992) presented the results of a large scale nailed wall test in clay. The clay was heavily overconsolidated with a mean value of undrained shear strength ( $c_u$ ) of 125Kpa and a dry density of 16.4KN/m<sup>3</sup>. Nailing was achieved by grouting 22 mm diameter Gewi-steel bars in boreholes of 110mm. The wall was loaded to failure using reinforced concrete blocks placed on H-beams and loaded by a hydraulic Jack with a reaction arrangement. Based on the creep displacements of the wall under the surface loads Gassler concluded that:

- (a) The horizontal displacement due to creep follows a logarithmic law
- (b) The creep effect changes the distribution of forces in the nails and

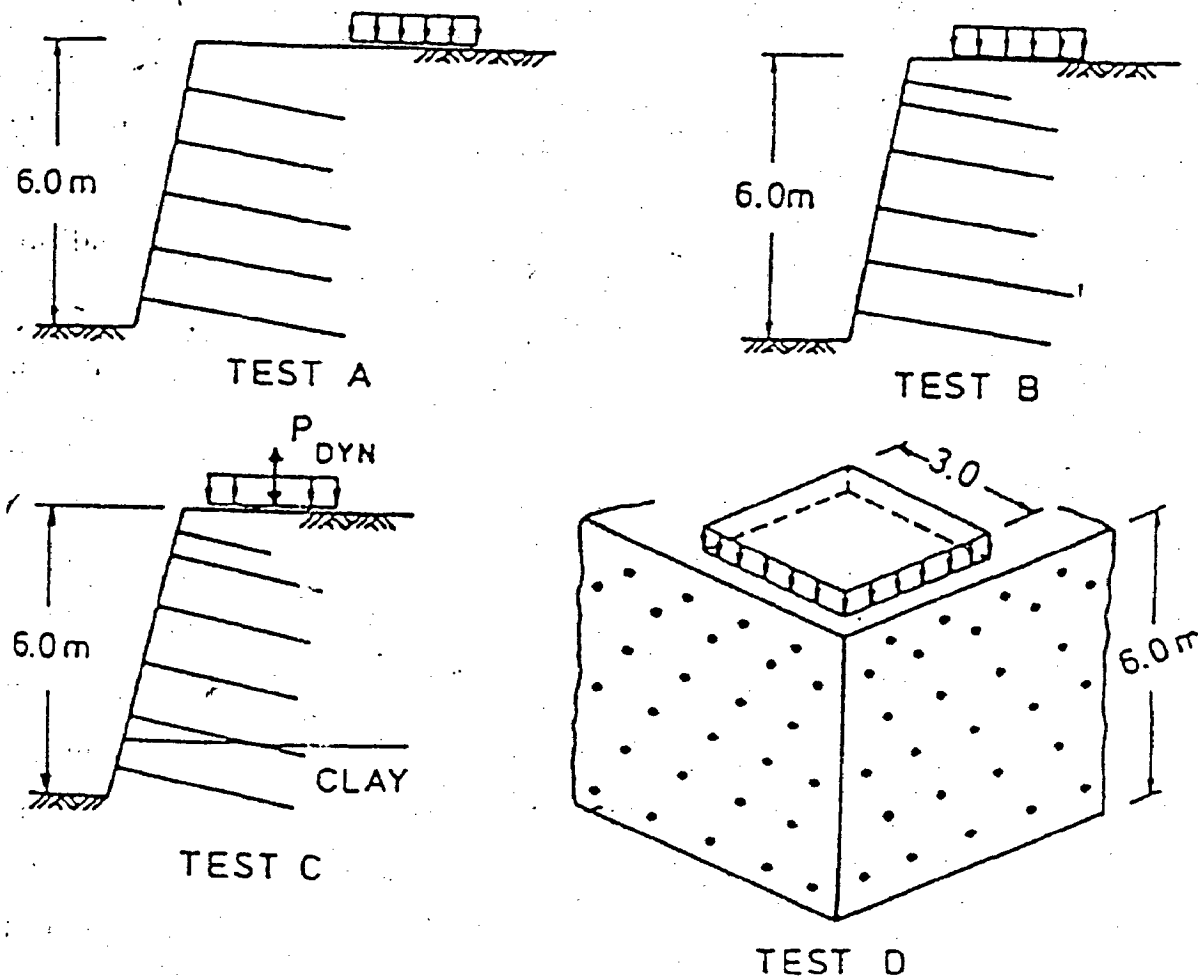


**Fig-2.3 Typical Large Scale Test Cross Sections (Stocker et al.1979)**

### 2.3 STUDIES ON SMALL- SCALE MODEL TEST

Juran et al. (1984) used small-scale models to investigate the effect of construction method on the behavior of reinforced soil and nailed soil structures. The effect of nail inclination and nail bending stiffness on the behavior of nailed soil retaining structures was also investigated. Three types of reinforcements namely: 0.1mm thick flexible aluminium strips were used and 0.2mm thick relatively rigid channel shaped polystyrene strips were used. The excavation led to displacements that were larger at the top of the wall and decrease with depth. The reinforced soil method of construction led to more or less uniform with depth. In both the cases the maximum displacement of the

model walls was about 1.2% of the wall height which is higher than those observed in some full scale structures. (Bruce and Jewell, 1987)

The excavation process led to larger tensile stresses at the top of the nailed soil wall and smaller tensile forces in the lower part of the wall. Increasing the inclinations of the inclusions led too much larger facing displacements and smaller maximum tensile forces in the inclusions. Post failure observations showed that the flexible aluminum and polystyrene strips failed by tension breakage, while the polystyrene strips failed by excessive bending. The model tests also indicated that the higher the bending stiffness of nail, the smaller is the failure height.

Teramoto et al. (1992) investigated the behavior of steel reinforced slopes by conducting a series of model tests in clayey sand. The models were loaded to failure and the failure surfaces were identified by viewing through the sidewalls of the test tank. These studies led to the following conclusions.

- (a) For sandy slopes, longer the reinforcement the more effective is the reinforcement. The reinforcement effect was compared in terms of a ratio defined as

$$\text{Reinforcement ratio} = \frac{\text{Failure load for reinforced soil}}{\text{Failure load for unreinforced soil}}$$

- (b) The failure surface passed through near end of the loading plate

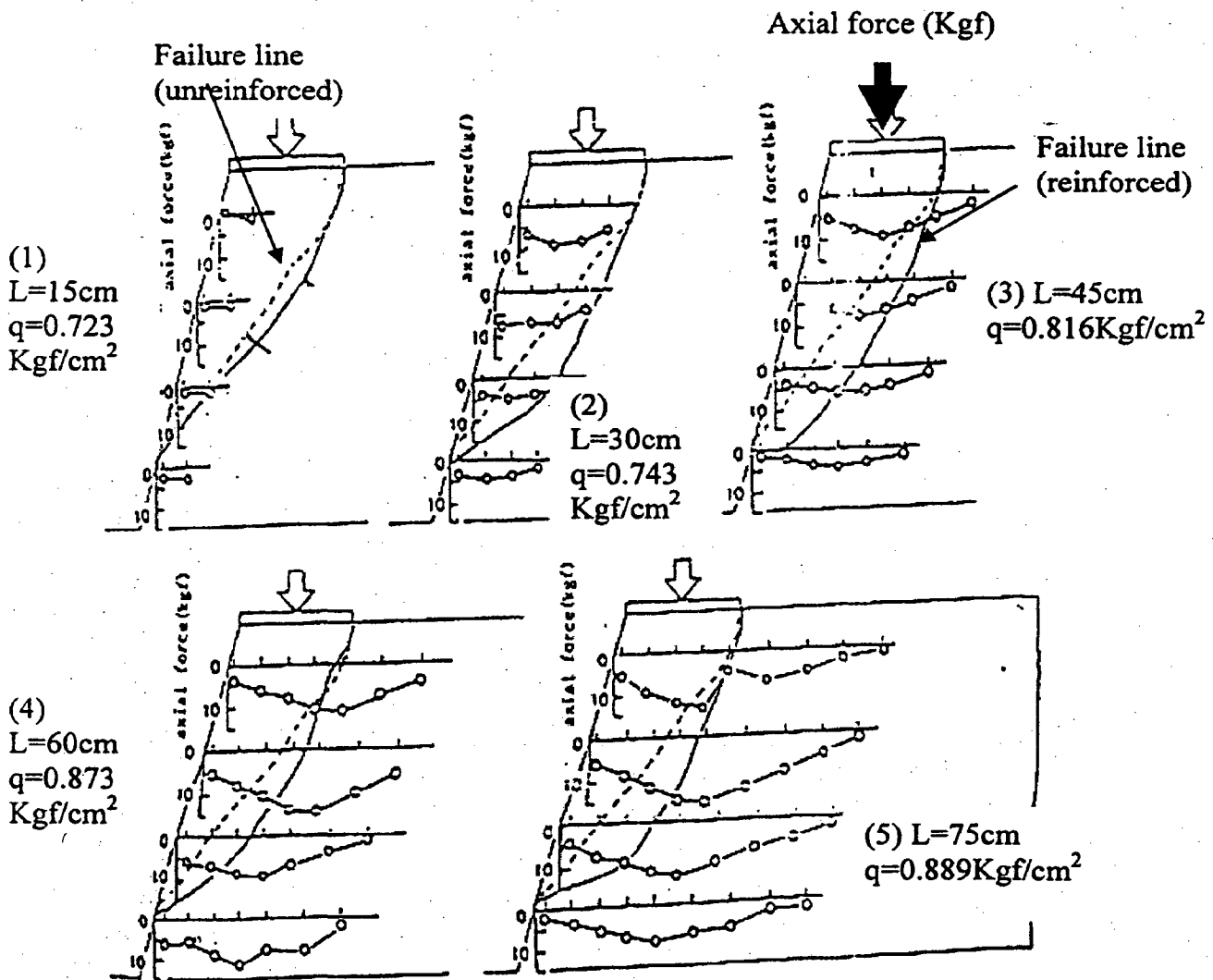


**Fig-2.4 Observed Slope Failure Lines and Axial Forces in the Reinforcement (Teramoto et al.1992)**

**DESIGN METHODS OF SOIL NAILED STRUCTURES**

---

**3.1 DESIGN PRINCIPLE**

Modes of failure in soiled nailed structures:

● **External stability:**

External stability assumes that the reinforced zone acts as a monolithic block of material. This homogeneity of the reinforced zone for modular facing systems is assured by limiting spacing between layers (e.g. not more than 1m according to FHWA, (1989). The composite must be stable against sliding along the base of the structure at the foundation /backfill interface, overturning about the toe, and bearing capacity failure of the supporting foundation soils. Bearing capacity calculations assume that the base of reinforced zone acts as an eccentrically loaded footing with an equivalent footing width of  $L-2e$ . where 'L' is the reinforcement length including the width of the facial and 'e' is the eccentricity of the vertical load acting at the base of reinforced zone. AASHTO, (1990) and FWHA, (1989) guide lines recommend that the reinforced zone be dimensioned to ensure that eccentricity of loading falls within the middle one-third of the base width of the reinforced soil mass. In general, the longer the base reinforcement length, the more is the factor of safety against external modes of failure. Typical ratios of length of reinforcement to height of wall are from 0.5 to 0.7. AASHTO, (1990) recommends that the ratio of reinforcement length be not less than 0.7 or that the reinforcement length be not less than 2.4m, whichever makes the reinforcement length greater. The measure of relative stability against the external modes of failure shown below is defined by the ratio of resisting forces to restraining forces (moments in the case of overturning) as in the conventional gravity wall structures.

### 3.2 FAILURE CURVES FOR REINFORCED AND UN-REINFORCED SOIL

Fig-3.3 shows the Finite Element (F.E) failure curves for reinforced and un-reinforced soils. The failure is defined by a relative displacement of  $X_F = 10\%$ . It can be indicated that a straight line can adequately represent the failure curves. The slope of this line corresponds to the internal friction angle and its coordinate at the origin corresponds to apparent cohesion. As shown in Fig-3.3 reinforcing a non-cohesive soil ( $\phi' = 32.5^\circ$ ) results in the mobilization of an apparent cohesion ( $c^* = 0.08 \text{ Mpa}$ ) and in a decrease of the internal friction angle ( $\phi^* = 28.5^\circ$ ). The F.E results are quite comparable with the experimental results obtained from the reinforcements of  $5\phi 8$  steel bars. Fig -3.3 also shows 3 components of the overall shear resistance of the nailed soil. These components are:

a) The apparent cohesion ( $C^*_0$ ) due to the shear forces ( $\tau_0$ ) mobilized in the bars

$$(C^*_0 = \tau_0/A),$$

Where 'A' is the total area of the potential failure surface.

b) The shear stresses ( $\tau_s$ ) mobilized in the soil along the potential failure surface in the absence of the bars.

c) The variation of the shear stresses in the soil ( $\nabla\tau$ ) due to the effect of reinforcing bars.



**DESIGN METHODS OF SOIL NAILED STRUCTURES**

---

**3.1 DESIGN PRINCIPLE**

Modes of failure in soiled nailed structures:

● **External stability:**

External stability assumes that the reinforced zone acts as a monolithic block of material. This homogeneity of the reinforced zone for modular facing systems is assured by limiting spacing between layers (e.g. not more than 1m according to FHWA, (1989). The composite must be stable against sliding along the base of the structure at the foundation /backfill interface, overturning about the toe, and bearing capacity failure of the supporting foundation soils. Bearing capacity calculations assume that the base of reinforced zone acts as an eccentrically loaded footing with an equivalent footing width of  $L-2e$ . where 'L' is the reinforcement length including the width of the facial and 'e' is the eccentricity of the vertical load acting at the base of reinforced zone. AASHTO, (1990) and FWHA, (1989) guide lines recommend that the reinforced zone be dimensioned to ensure that eccentricity of loading falls within the middle one-third of the base width of the reinforced soil mass. In general, the longer the base reinforcement length, the more is the factor of safety against external modes of failure. Typical ratios of length of reinforcement to height of wall are from 0.5 to 0.7. AASHTO, (1990) recommends that the ratio of reinforcement length be not less than 0.7 or that the reinforcement length be not less than 2.4m, whichever makes the reinforcement length greater. The measure of relative stability against the external modes of failure shown below is defined by the ratio of resisting forces to restraining forces (moments in the case of overturning) as in the conventional gravity wall structures.

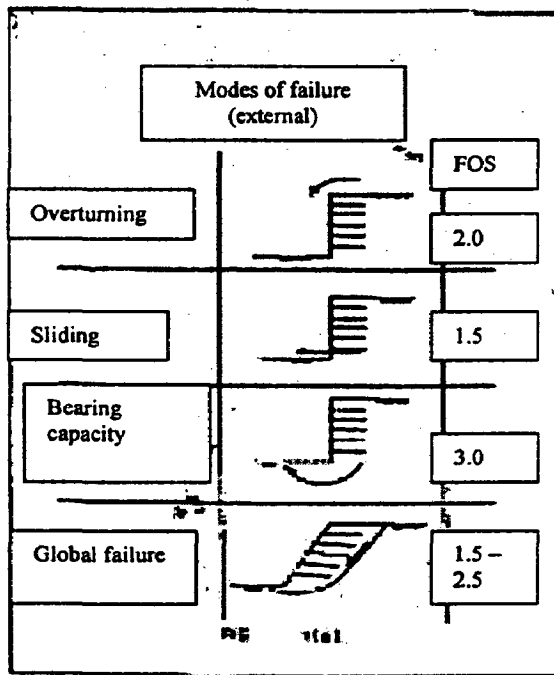


Fig-3.1 Modes of Failure(External)

● **Internal modes of failure mechanisms include:**

- Rupture of the reinforcement due to tensile over-stressing

The design tension  $T_d$  at each level of the reinforcing element is calculated from the design pressure distribution. The design tensile resistance of a reinforcing element which is given by factoring the selected tensile strength of the reinforcing element by  $\gamma_m$  should not be less than  $T_d$ .

- Pullout of the reinforcement within the reinforced soil mass

For checking against pullout failure, the effective bond length of a reinforcing element is taken as that protrudes beyond the potential failure surface under consideration. The potential failure surface corresponding to the maximum design stabilization force may not necessarily be the critical surface in checking against pull out failure. Hence sufficient number of potential failure surface should be checked to ensure that the pull out resistance is adequate in all cases.

- Failure of the facing connection

Where facing elements are provided, the connection between a facing element and a reinforcing element is designed to withstand the design tension  $T_d$ . For bolted

connection, all modes of failure including shear and bearing should be checked. The requirement of relevant local structural standards should be observed in the design. In addition, selected strength of the connection should exceed that of the reinforcing element in order to avoid brittle failure at the connection.

➤ Rupture of facing element

Where facing elements are provided their structural design is based on the design pressure distribution incorporating compaction-induced stress. Adequate measures should be provided to ensure local stability at the face and to protect it from surface erosion.

➤ Rupture through selected fill material and rupture along a reinforcing element surface

Shearing failure of the selected fill material along any plane parallel to the reinforcing element and along the surface of any layer of the reinforcing elements should be checked. Rigorous methods of limit equilibrium stability analysis may be adopted.

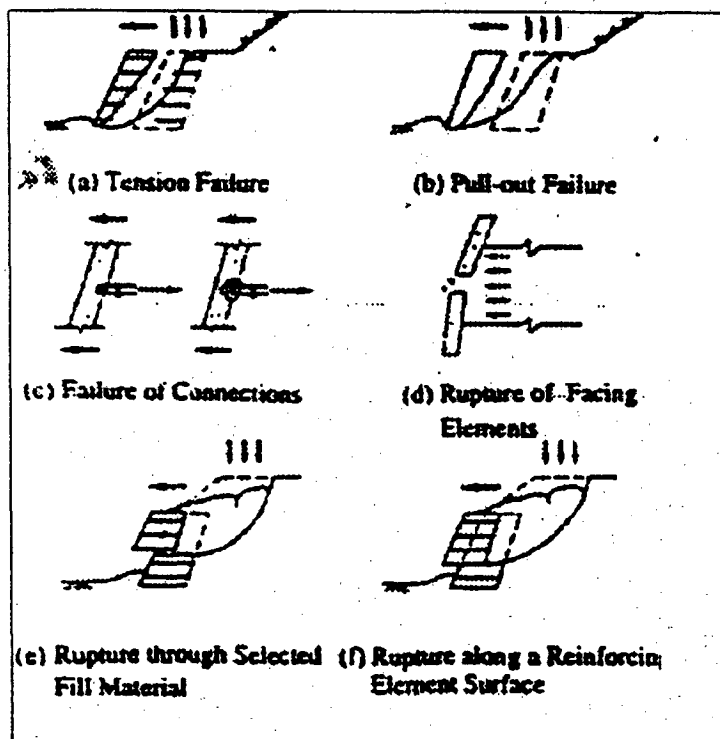


Fig -3.2 Modes of Failure in Nailed Soil (internal failure)

### 3.2 FAILURE CURVES FOR REINFORCED AND UN-REINFORCED SOIL

Fig-3.3 shows the Finite Element (F.E) failure curves for reinforced and un-reinforced soils. The failure is defined by a relative displacement of  $X_F = 10\%$ . It can be indicated that a straight line can adequately represent the failure curves. The slope of this line corresponds to the internal friction angle and its coordinate at the origin corresponds to apparent cohesion. As shown in Fig-3.3 reinforcing a non-cohesive soil ( $\phi' = 32.5^\circ$ ) results in the mobilization of an apparent cohesion ( $c^* = 0.08 \text{ Mpa}$ ) and in a decrease of the internal friction angle ( $\phi^* = 28.5^\circ$ ). The F.E results are quite comparable with the experimental results obtained from the reinforcements of  $5\phi 8$  steel bars. Fig -3.3 also shows 3 components of the overall shear resistance of the nailed soil. These components are:

- a) The apparent cohesion ( $C^*_0$ ) due to the shear forces ( $\tau_0$ ) mobilized in the bars  
( $C^*_0 = \tau_0/A$ ),

Where 'A' is the total area of the potential failure surface.

- b) The shear stresses ( $\tau_s$ ) mobilized in the soil along the potential failure surface in the absence of the bars.

- c) The variation of the shear stresses in the soil ( $\nabla\tau$ ) due to the effect of reinforcing bars.

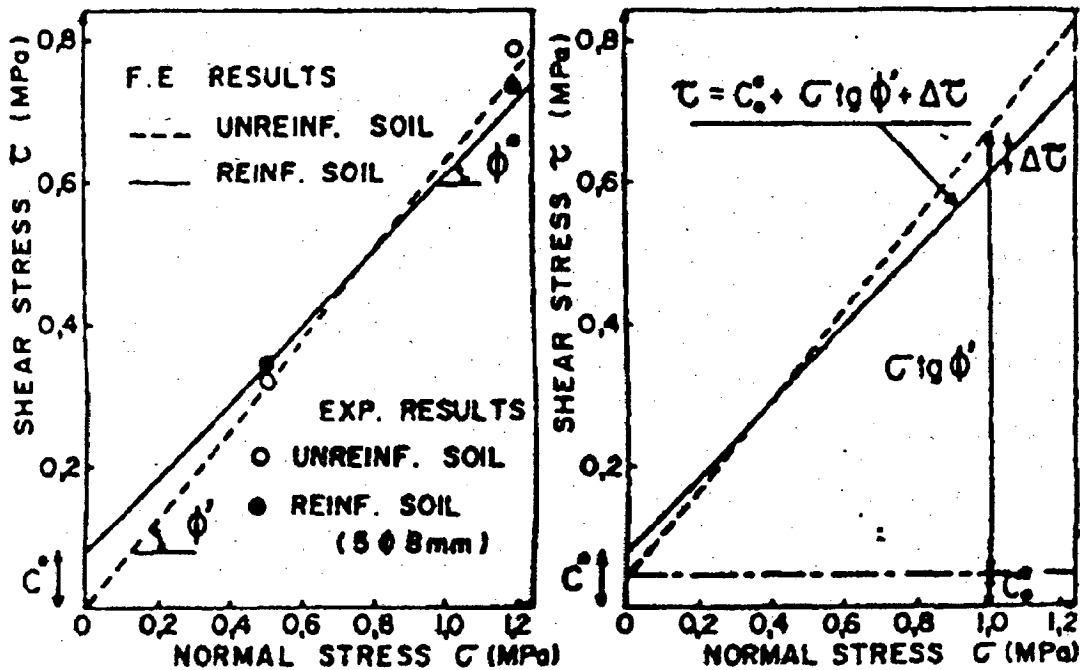


Fig-3.3 Failure Curves of Reinforced and Un-reinforced Soil

Hence the shearing resistance of the nailed soil is equal to

$$\tau = C^*_0 + \sigma' \tan \phi' + \nabla \tau$$

The F.E. results show that the shear forces mobilized in the nails ( $\tau_0$ ) and corresponding apparent cohesion ( $C^*_0$ ) are practically independent of the applied normal stresses ( $\sigma$ ). The effect of the reinforcing bars ( $\nabla \tau$ ) is highly dependent on the applied normal stresses. Moreover it is positive for low normal stresses and negative for high normal stresses. Consequently the total apparent cohesion ( $C^*$ ) is greater than ( $C^*_0$ ) and the internal friction angle of the nailed-soil ( $\phi^*$ ) is smaller than one of the un-reinforced soil ( $\phi'$ )

### 3.3 THEORETICAL MODELS FOR EVALUATING THE ROLE OF BENDING STIFFNESS

To evaluate the shear forces and bending moments in the nails as a result of the mobilized passive soil resistance, two approaches have been proposed:

(a) Elastic approach (Schlosser, 1982)

(b) Plastic approach (Jewell and Pedley, 1990a, 1992)

Schlosser(1982) proposed an elastic analysis for the passive interaction between the soil and nail by adopting the closed form solutions derived by Hetenyi (1946) for an infinitely long laterally loaded pile. The analysis resulted in the following relationship between the maximum shear force ( $T_c$ ) and maximum moment ( $M_{max}$ ) in the nail:

$$T_c = \frac{4.9M_{max}}{l_s} \quad (3.1)$$

Where,  $l_s$  is the shear width (distance between the points on the reinforcement on either side of the shear plane in the soil that experience the maximum moment as in Fig.3,4.

$$l_s = \frac{\pi}{2} l_0 = \frac{\pi}{2} \sqrt{\frac{4EI}{K_s d}} \quad (3.2)$$

Where,  $K_s$  =modulus of sub-grade reaction for the soil

E= Young's modulus of the nail

I = moment of inertia

d= Width of diameter of the nail

$l_0$  =Transfer length

In the analysis, the strength of the nail is assumed to be governed by the Tresca's failure criteria at point 'A' in Fig-3.4

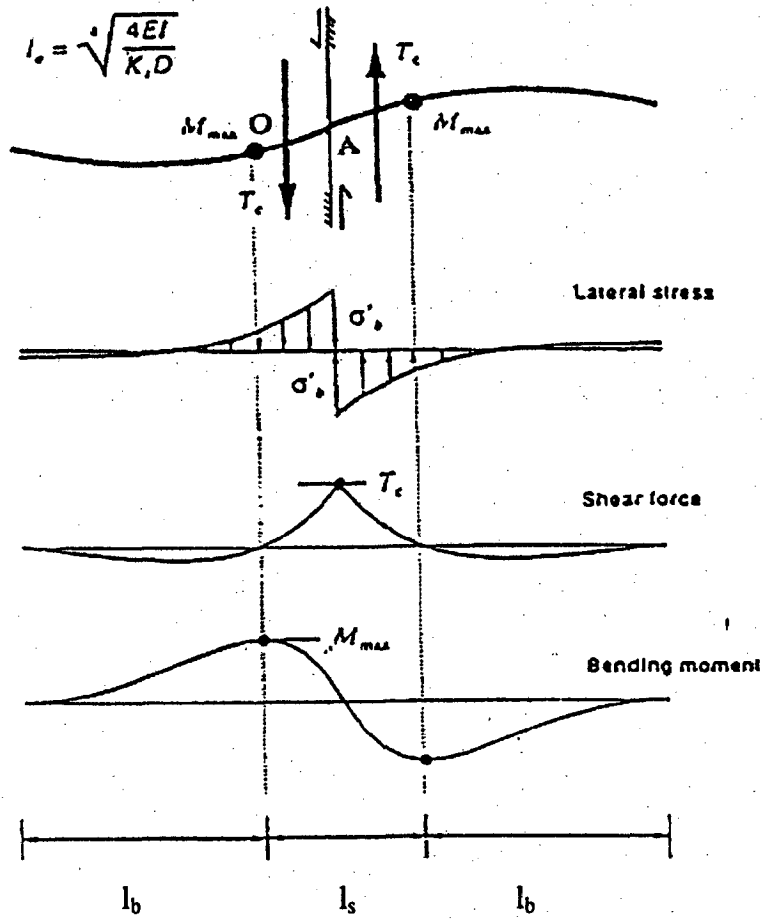


Fig-3.4 Elastic Analysis for Nail Bending Stiffness (Schlosser, 1982)

$$\left(\frac{T}{T_p}\right)^2 + \left(\frac{T_c}{T_n}\right)^2 = 1 \quad (3.3)$$

Where,  $T$  is the tensile force in the nail,  $T_p$  is the tensile strength of the nail and  $T_n$  is the shearing strength of the nail  $= \frac{T_p}{2}$ .

Jewell and Pedley (1990a) presented a plastic analysis which assumes plastic condition in the soil for a nail under lateral loading as shown in Fig-3.5 and derived the following relationship.

$$T_c = \frac{4M_{\max}}{l_s} \quad (3.4)$$

$$\sigma_b = \frac{8M_{\max}}{l_s^2 d} \quad (3.5)$$

The following criteria for the limiting combination of moment and axial force in the bar was used at point 'O' in Fig-3.5

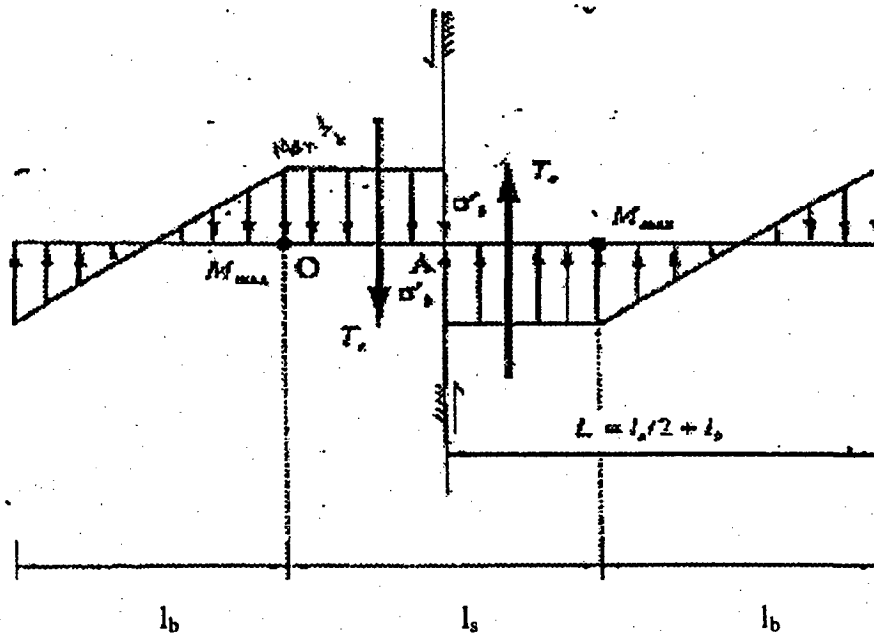


Fig-3.5 Plastic Analysis for Nail Bending Stiffness (Jewell and Pedley, 1992)

$$\frac{M}{M_p} + \left( \frac{T}{T_p} \right)^2 = 1 \quad (3.6)$$

Where,  $T_p$  is the fully axial force and  $M_p$  is the fully plastic moment

For a nail carrying axial force  $T$  and moment  $M=M_{\max}$

Eq 3.4 and 3.5 lead to:



$$l_s^2 = \frac{8M_p}{\sigma_b d} \left( 1 - \left( \frac{T}{T_p} \right)^2 \right) \quad (3.7)$$

Where,  $\sigma_b$  is the limit bearing stress between the soil and nail. For a circular bar,

$$M_p = \frac{\sigma_y d^3}{6} \quad (3.8)$$

Where,  $\sigma_y$  is the yield stress of the nail material.

From Eq. 3.7 and Eq 3.8 we have

$$\left( \frac{l_s}{d} \right)^2 = \frac{4\sigma_y}{3\sigma_b} \left( 1 - \left( \frac{T}{T_p} \right)^2 \right) \quad (3.9)$$

Jewell and Pedley (1990a) presented the following lower, safe estimate of the bearing stress  $N_b$  as a function of the soil internal friction angle ' $\phi$ ' and overburden pressure  $\sigma_v$ , assuming a punching shear failure of the soil around the bar.

$$\sigma_b = \sigma_v \left( \frac{1+K_a}{2} \right) \tan \left( \frac{\pi}{4} + \frac{\phi}{2} \right) \exp \left[ \left( \frac{\pi}{2} + \phi \right) \tan \phi \right] \quad (3.10)$$

The corresponding upper estimate is for fully developed plastic shear in the soil around the bar which appears almost never to be achieved (Jewell et al.1984) which is given by

$$\sigma_b = \sigma_v N_q$$

Where,  $N_q$  is the bearing capacity factor

Eq 3.1 and Eq 3.4 can be rewritten as

$$\frac{T_c}{M_p} = \frac{CM_{\max}}{l_s M_p} \quad (3.11)$$

Where C=4.9 for elastic analysis and 4 for plastic analysis.

For a circular bar,  $\frac{M_p}{T_p} = \frac{2d}{3\pi}$  (3.12)

The limiting combinations of shear force  $T$ , normalized by  $T_p$  is given (from Eq 3.6 and 3.11, with  $M=M_{max}$ ) by :

$$\frac{T_c}{T_p} = \frac{C.2d}{l_s.3\pi} \left[ 1 - \left( \frac{T}{T_p} \right)^2 \right] \quad (3.13)$$

Eq.3.13 was written in terms of shear and axial force rather than moment and axial force because the maximum moment ( $M_{max}$ ) at point 'O' and the maximum shear force ( $T_c$ ) at point 'A' in Fig-3.4 are related by Eq-3.11. The improvement in the soil shearing resistance stemming from the nail bending stiffness (Jewell and Pedley (1990a) depends directly on the magnitude of the shear force  $T_c$ .

They concluded that only a relatively small magnitude of shear force ( $T_c$ ) compared to the plastic axial force ( $T_p$ ) can be mobilized in the nails and the values of  $T_c$  calculated using the limiting combination of shear force (Eq.3.3) can overestimate the likely magnitude of the shear force in a soil nail by a factor of 10 to 20.

### 3.4 DISTRIBUTION OF SHEAR STRESSES ALONG THE FAILURE SURFACE

A certain displacement is required in order to generate an efficient soil-reinforcement interaction. This displacement depends essentially on the normal stresses

at the failure surface and on the rigidity and the density of the reinforcing element. In order to ensure the stability of nailed soil structures it is necessary to establish design criteria based on the concept of an admissible displacement. These design criteria should enable an appropriate choice of the relative rigidity of the bars with respect to the soil. This relative rigidity can be characterized by the transfer length of the bar (Juran et al 1981):  $l_0 = \sqrt[4]{4EI/k_s\phi}$  ( $k_s$  being the coefficient of lateral earth pressure). Fig-3.6 shows the effect of the transfer length ( $l_0$ ) on the displacement ( $\delta$ ) necessary to generate the required shear force ( $T_0$ ) and a required increase of the shearing resistance  $\Delta F/F_s$  ( $F_s$  being the shearing resistance of the un-reinforced soil) at a normal stress of  $\sigma = 0.1 \text{ Mpa}$ . The displacement decreases as the transfer length increases.

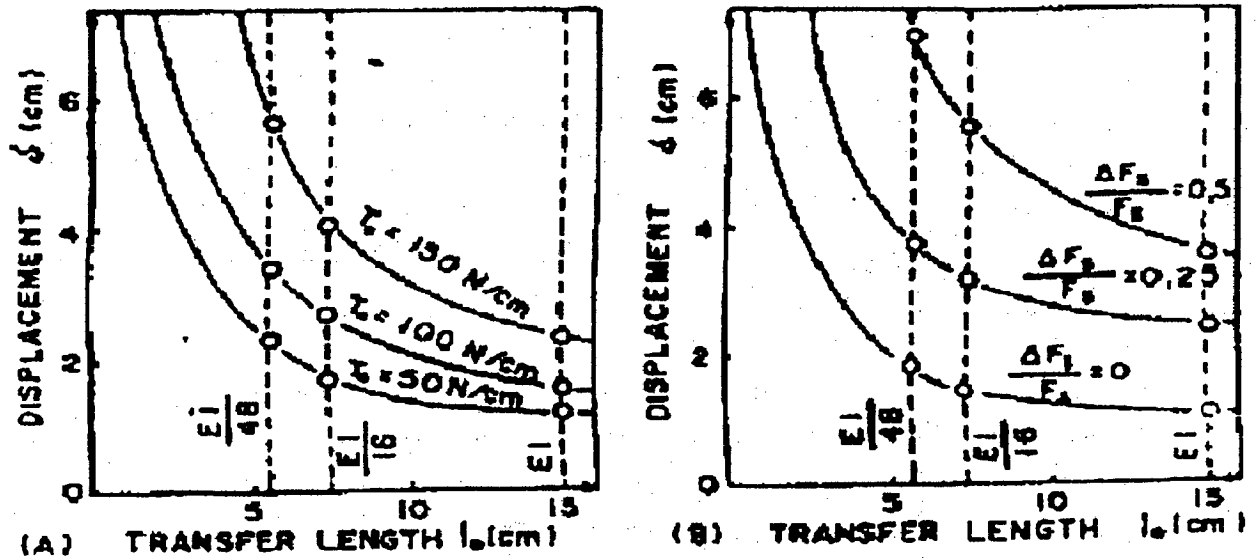


Fig-3.6 Effect of the Transfer Length on the Displacement Necessary to Mobilize a) Shear force in bars; b) Increase of the overall shear resistance.

### **3.5 DATA REQUIRED FOR SOIL NAILING DESIGN**

To perform a soil nail wall design, knowledge of the wall face and the foundation soil supporting the wall face is required. It also requires the knowledge of the project geometry, loading and surcharge condition, ground water conditions, the properties of soil nailing and soil parameter. The quality of a soil nail wall system will be a function of the soil being reinforced. Since a soil nail wall is comprised of over 98% soil, the characteristic of that soil (shear strength, consolidation, permeability, corrosion potential) will greatly influence the soil nail design and the wall performance. The shear strength of the retained soil must also be determined since this will determine what load will be applied to the back of the soil nail wall. The shear strength of the foundation soil will determine what length the soil nails will need to be to resist bearing and sliding failure modes for a wall of a given height.

- Mechanical properties of the in-situ soil, particularly the soil type, angle of internal friction, dilation characteristics and cohesion.
- Mechanical properties of the nails especially the tensile and shear capacities of the nail section and the bending stiffness.
- Parameters related to the soil-nail interaction by friction, particularly the limit skin friction  $f_1$ , which can be mobilized along the inclusion in the specific ground under consideration. This limit skin friction can be computed using the methods adopted for friction pile design. In-situ pull-out tests are strongly recommended to determine this parameter.
- Parameters related to the development of lateral earth thrust on the nail surface especially the limit passive pressure of the soil and modulus of soil reaction.
- Geometric properties of the nails such as thickness, shape and length, the horizontal and vertical spacing of the nail and inclination of the nail
- Parameters related to the method of nail inclination and grouting method etc.

- Type and thickness of facing and connection to be used at the nail-facing junction.
- External loads including surcharges, embankment slopes, water flow & seepage forces and also seismic factors.

### **3.6 STEPS FOR THE DESIGN OF NAILED-SOIL STRUCTURES**

- I. For the specific structure geometry (depth and cut slope inclination) ground profile and boundary (surcharge) loading, estimate working nail forces and location of the potential sliding surface.
- II. Select the reinforcement type (type, cross-sectional area, length, inclination and spacing) and verify local stability at each reinforcement level, that is, verify that nail resistance (strength and pull-out capacity) is sufficient to withstand the estimated working force with an acceptable factor of safety.
- III. Verify that the global stability of the nailed-soil structure and the surrounding ground is maintained during and after excavation with an acceptable factor of safety.
- IV. Estimate the system of forces acting on the facing (lateral earth pressure and nail forces at the connection) and design the facing for specified architectural and durability criteria.
- V. For permanent structures, select corrosion protection relevant to site condition.
- VI. Select the drainage system for ground water piezometric level

The working nail forces in the structure can be estimated by selecting an appropriate earth pressure diagram depending on the nature and magnitude of tolerable ground movements. Observations on instrumented soil nailed walls (Juran&Elias, 1990) showed that the anticipated displacements are comparable to those measured in braced excavations. The empirical earth pressure diagrams proposed by Terzaghi and Peck (1967) for the design of braced excavations can be used to estimate the working nail forces. Juran and Elias (1987) modified these earth pressure diagrams based on

observations on scale nailed soil walls by introducing some empiricism. The maximum tensile force ( $T_{max}$ ) in the nail is expressed in a non-dimensional form:

$$TN = \frac{T_{max}}{\gamma H S_h S_v}$$

in which  $H$  is the total structure height,  $S_h$  and  $S_v$  are the horizontal and vertical nail spacing. These empirical earth pressure diagrams can not be used to assess the effect of design parameters such as the facing and nail inclinations, rigidity of the nails, surcharge and ground water effects on the working tensile forces in the nails.

The available design methods for soil nailed retaining structures can be broadly classified into two main categories

- A. Limit equilibrium design methods or modified slope stability analyses, which are used to evaluate the global safety factor of the nailed structures with respect to a rotational or translational failure along potential sliding surfaces, taking into account the shearing, tension or pull-out resistance of the inclusions crossing the potential failure surface.
- B. Working stress design methods, which are used to estimate the tension and shear forces generated in the nail during construction under the design loading conditions and evaluate the local stability at each level.

All the design methods are based on the consideration of the two distinct zones (Elias and Juran, 1991):

- a) An active zone (or sliding) which tends to separate from the rest of the soil mass
- b) A resistant (or stable) zone into which the generated nail forces are transferred as shown in Fig-3.7

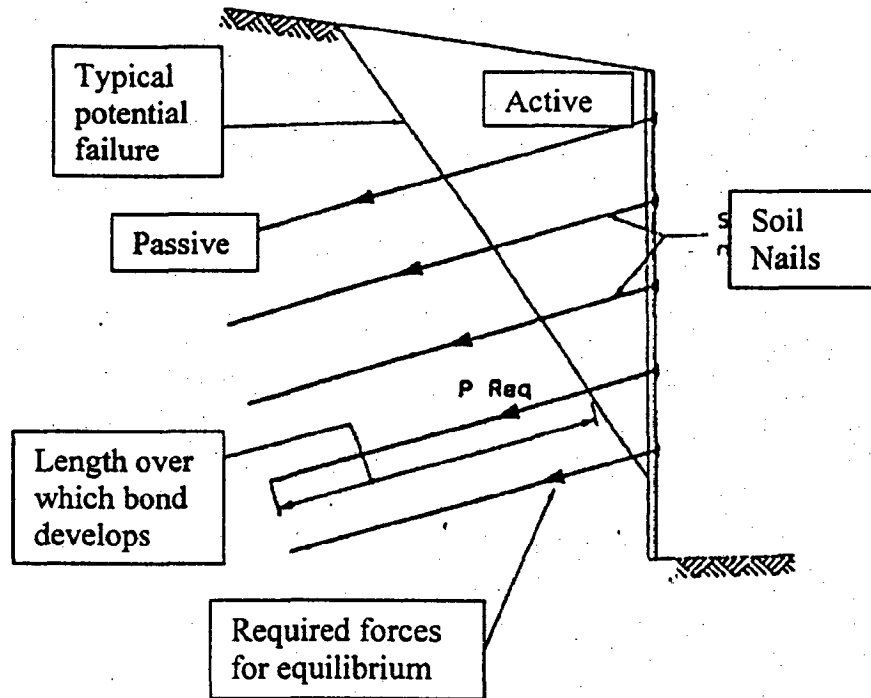


**Fig-3.7 Soil Nailed Wall Showing all the Components**

The well published design methods and their main features are presented in Table – 3.1. This table will also include a new method proposed by Bridle and Barr (1990b). Juran et al. (1990a) Elias and Juran (1991) evaluated the Davis, French and the Kinematical design methods through comparative analysis. The conclusions from such a comparative study are:

- a) For most of the cases considered in the study, the Davis method with  $F_c = F_\phi = F_p = 1.5$  yields more conservative structure geometries as compared with the French method. The modified Davis method with  $F_c = F_\phi = 1$  and  $F_p = 2$  and the French method yields similar design schemes.
- b) All methods except the German method predict a potential failure surface crossing all nails for nailed retaining structures under self weight or small surcharge loads. The location of this potential failure surface varies significantly from method to method (being nearest to the facing by the kinematical method).

- c) The analysis showed that for soil nailed excavations, the factors of safety with respect to soil strength are generally close to one. The use of residual soil strength parameters appears to be unnecessarily conservative.
- d) The kinematical method can be used to adequately analyze the effect of nail bending stiffness while predictions based on the French method are not consistent with experimental results.
- e) The choice of methods used to calculate global stability appears to be noncritical as all methods in their simplest form yield in most cases reasonably comparable results under the same definition of factor of safety. However for pullout failure predictions, the modified Davis method provides the best approximation of the critical height
- f) For satisfactory design, Juran et.al. (1990a) recommended both a local stability analysis using kinematical method and a global stability analysis using the French method (with  $F_c=F_\phi=F_p=1.5$ ) or the modified (with  $F_c=F_\phi=1$  and  $F_p=2$ )
- g) Gassler (1988) has shown through comparative stability analysis that the bi-linear failure mechanism (used in the German method) is applicable only in cohesionless soils under local surcharges. For nailed soil structures, which are subjected mainly to self-weight, the bilinear failure surface yields a failure zone which is substantially larger than those observed on actual structure.

### 3.7 COMPARATIVE ANALYSIS OF VARIOUS DESIGN METHODS

The comparative analysis by Juran et al. (1990a) of the various design methods suggested that all the methods give comparable results under the same definition of factor of safety. Thus the choice of the method appears to be noncritical. However an assessment of the design assumptions of all the methods leads to the following observation.

Since all the methods are based on the equilibrium of a failing wedge(s) either by translational or rotational mode, the nails intersected by the failure surface will be



subjected to significant lateral displacements. This will result in a mobilization of shear forces in the nails. How significant these shear forces will be depends on the soil-nail interaction mechanism.

- a) All the methods involve some assumptions regarding the allocation of forces to the boundaries between the active wedges. In the Davis method, the reaction between the wedges is assumed to be normal to the boundary between them and the magnitude is assumed to be equal to the lateral thrust on the boundary. In the German method the reaction between the wedges is assumed to be inclined at an angle equal to the soil friction angle, the magnitude of which can be determined from force equilibrium of the wedge in the unreinforced soil. Long et al. (1990) based on a comparative analysis of limit equilibrium methods concluded that the factor of safety is sensitive to the interwedge force inclination (higher interwedge force inclination results in higher factor of safety). The German and Davis methods give the same failure height under the assumption of same interwedge forces. In the absence of any concrete evidence on the magnitude and direction of the interwedge forces, a single wedge mechanism would simplify the analysis.
- b) All the methods for soil nailing design so far considered only a wedge failure mechanism. Since the primary objective of reinforcing the soil is to improve the overall shear strength of the soil leading to a coherent soil mass, external failure modes such as block sliding and overturning must also be considered particularly for walls with smaller L/H ratio.
- c) The Kinematical method stressed the significance of the local stability of the soil nailed wall. Other than the model tests by Juran et al. (1984) there is hardly any evidence of the local stability governing the design. Failure of soil nailed walls in France (Schlosser, 1991) usually occurred during the final stages of excavation prior to installing the latest row of nails but not due to local stability being critical at any particular nail level.
- d) The kinematical analysis method explicitly assumes that the failure surface (coinciding with the locus of maximum nail tension) is always inside the reinforced mass. Large-scale tests by Plumelle et al (1990) in which the wall was failed by saturation and not by external load support this assumption. However

large scale tests by Stocker et al (1979) showed that under large surcharge loads, the failure surface meets the ground behind the top rows of nails.

- e) The Kinematical method also assumes that the shearing resistance of stiff inclusions is mobilized in the direction of sliding surface in the soil. This assumption may be more relevant for soil nailing used for slope stabilization where nails are commonly installed perpendicular to the failure surface (Mitchell and Villet, 1987). In retaining walls, the shear forces generated in the nails will be normal to the nail axis due to the mobilization of passive resistance normal to the nail surface.

**TABLE - 3.1 (Comparison of Design Methods)**

Features	German method (Stocker et al, 1979)	Davis method (Shen et al, 1981b)	French method (Schlosser, 1982)	Modified Davis method (Elias and Juran, 1980)	Kinematical method (Juran et al. 1990b)	Bridle and Barr's method (Bridle and Barr, 1990b)
Analysis	Limit force equilibrium Global stability	Limit force equilibrium Global stability	Limit moment equilibrium Global stability	Limit force equilibrium Global stability	Working stress analysis Local stability	Limit moment equilibrium Global stability
Input material properties	Soil parameter (c, $\phi$ ), interface friction	Soil parameter (c, $\phi'$ ), limit nail forces, interface friction	Soil parameter (c, $\phi'$ ), limit nail forces, bending stiffness.	Soil parameter (c, $\phi'$ ), limit nail forces, interface friction	Soil parameter (c, $\phi'$ ), non-dimensional bending stiffness parameter (N)	Soil parameter (c, $\phi'$ ), limit nail forces, bending stiffness
Nail forces	Tension	Tension	Tension, shear, moments	Tension	Tension, shear, moments	Tension, shear, moments
Failure surface	Bilinear	Parabolic	Circular, any input shape	Parabolic	Log-spiral	Log-spiral
Failure mechanism	Pull-out	Mixed	Mixed	Mixed	Non-applicable	Mixed
Soil strength (F, F <sub>s</sub> )	1 (residual shear strength)	1.5	1.5	1	1	1

Pull-out resistance, $F_p$	1.5 to 2	1.5	1.5	2	2	#
Tension Bending	Yield stress	Yield stress	Yield stress, Plastic moment	Yield stress	Yield stress, Plastic moment	Yield stress, Fracture stress
Design output	GSF, CFC	GSF, CFC	GSF, CFC	GSF, CFC	Mobilized nail forces, CFS	GSF, Weight of each slice, CFS
Ground water	No	No	Yes	No	Yes	No
Soil stratification	No	No	Yes	No	Yes	No
Loading	Slope surcharge	Uniform surcharge	Slope, any surcharge	Slope, uniform surcharge	Slope	Slope, uniform surcharge
Structure geometry	Inclined facing, Vertical facing	Vertical facing	Any input geometry	Inclined facing, Vertical facing	Inclined facing, Vertical facing	Inclined facing, Vertical facing

Mixed failure mechanism: Limit tension force in each nail is governed by either its pull out resistance factored by the safety factor or the nail yield stress, whichever is smaller.

Pull out failure mechanism: Limit tension forces in all the nails are governed by their pull out resistance factored by the safety factor. In other words the tension breakage made of the nail is not considered.

Definition of safety factors used in this analysis:

For soil strength,  $F_c = c/c_m$ ,  $F_\phi = (\tan\phi/\tan\phi_m)$  where  $c$  and  $\phi$  are the soil cohesion and friction angle respectively, while  $c_m$  and  $\phi_m$  are the soil cohesion and friction angle mobilized along the potential sliding surface. However, Shen et al. (1981b) used  $F_\phi = \phi/\phi_m$

For nail pull out resistance,  $F_p = f_l/f_m$ , where  $f_l$  and  $f_m$  are the limit interface shear stress and the mobilized interface shear stress respectively.

GSF: Global safety factor, CFS: Critical failure surface

Present design capabilities, # No specific value recommended.

**ANALYSIS OF SOIL NAILING WALL WITH FRICTION CIRCLE METHOD**

The principle of the method is explained with reference to trial circle of rotation 'O' as shown in Fig-4.1

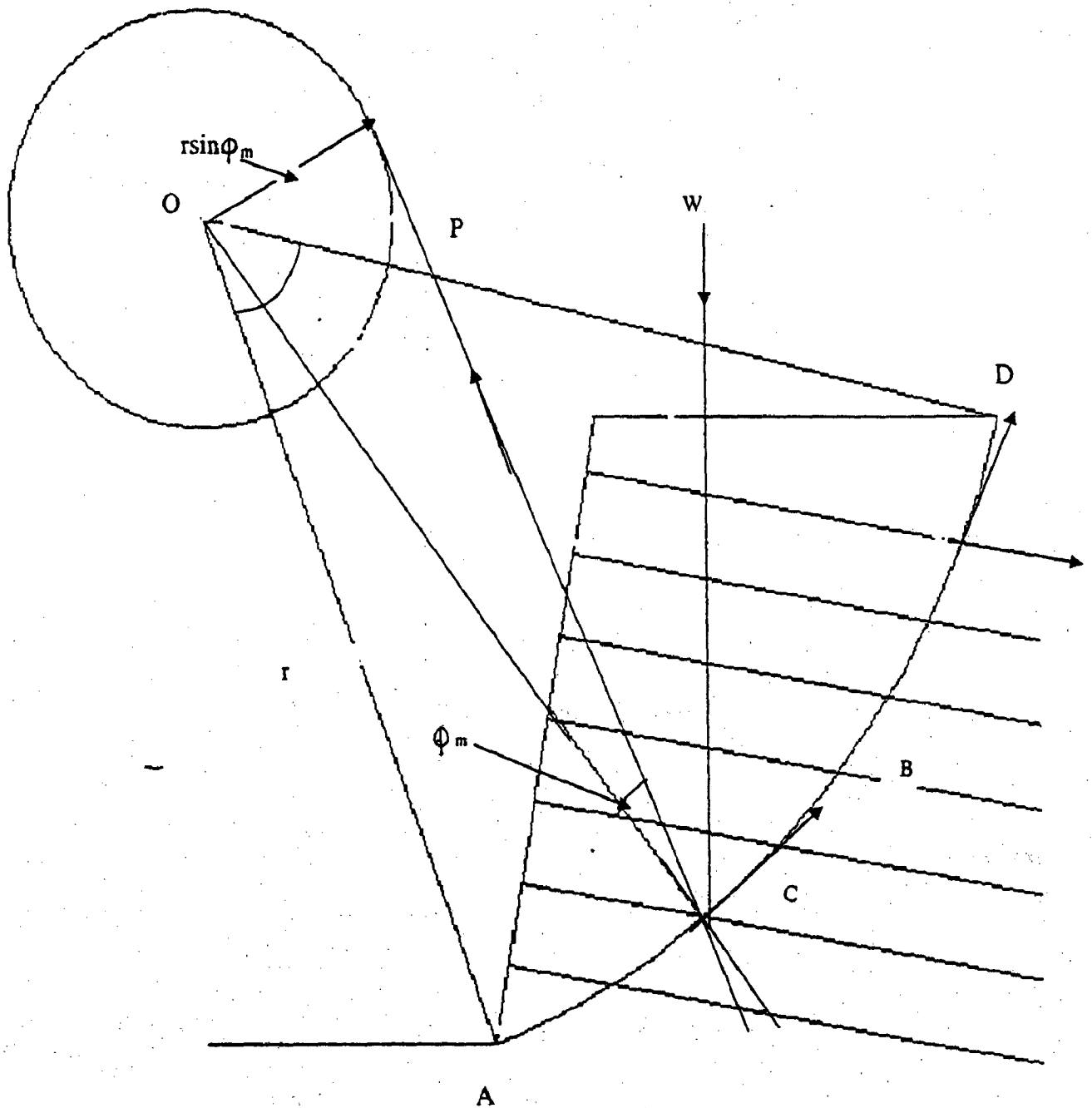


**Fig-4.1 Principle of Friction Circle.**

With center 'O' and radius  $r \sin \phi_m$ , where 'r' is the radius of trial circle, a circle is drawn. Any line tangent to the inner circle must intersect the trial circle at an angle ' $\phi_m$ '. This inner circle is called friction circle or  $\phi$ -circle.

### (A) Resisting Forces

#### (i) The resultant cohesive force

Let the length of arc A'B'D' be designated as 'l', length of chord A'D' is ' $l_c$ ', let length 'l' be divided into a number of small elements and let the mobilized cohesive force on these elements be designated as  $C_1, C_2, C_3, C_4, C_5$  and  $C_6$  as shown in Fig-4.2

The resultant of all these forces is shown by force polygon in Fig-4.2. The resultant is A'D' which is parallel and equal to the chord length A'D'. All the mobilized cohesive forces along the arc is therefore,  $C = C_m l_c$ , where  $C_m = C / F_c$

$C$  = limit cohesion

$F_c$  = Factor of safety with respect to cohesion.

The line of action of 'C' may be determined by moment consideration. The moment of the total cohesion is expressed as  $C_m l r = C_m l_c l_a$

Where  $l_a$  = moment arm

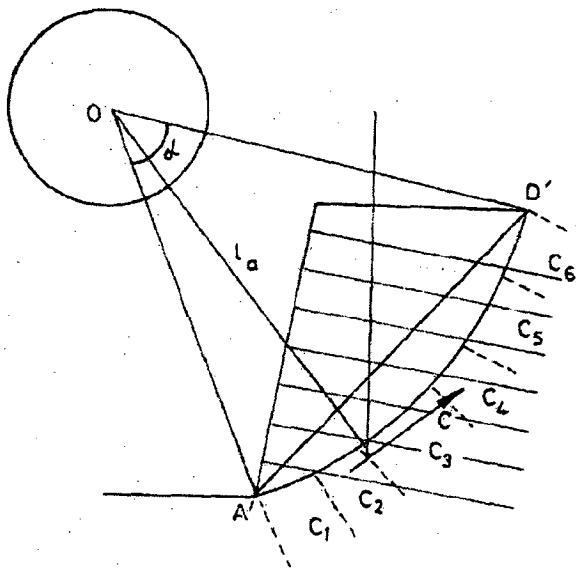
Therefore

$$l_a = r l / l_c$$

From geometry (Fig-4.2),  $l_c = 2r \sin(\alpha/2)$

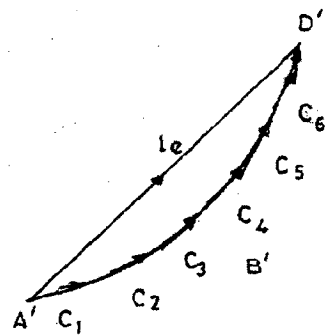
Where ' $\alpha$ ' is the arc angle .

$$l_a = \frac{r \pi \alpha}{360 \times \sin \frac{\alpha}{2}}$$



(a)

Fig.4.2 (a) Resultant Cohesive Force



(b)

(b) Force Polygon

Resisting moment about 'O' due to cohesive forces

$$= C_m r l = \frac{\pi^2 \alpha}{180} \times \frac{C}{F_c} \quad (4.1)$$

**(ii) Resultant inter-granular forces (reaction)**

The forces considered are (Fig-4.3):

- 1 The total weight 'W' of the mass above the trial circle is acting through the center of mass. The center of mass may be determined by any of the known methods.
- 2 Surcharge load acting on the failure zone
- 3 The resultant inter-granular forces 'P' acting on the boundary.
- 4 Cohesive force
- 5 Nail axial force
- 6 Nail shear force acting perpendicular to the nail axis.

Friction circle is drawn with a radius of  $r \sin \phi_m$  (Fig-4.3), where  $\tan \phi_m = \frac{\tan \phi}{F_\phi}$ . The

resultant of intergranular forces has a tendency to miss the tangency to the ' $\phi_m$ '

circle by an amount of  $r k \sin \phi_m$ , where  $k = \frac{1 - \left(\frac{2\alpha}{\pi}\right)^2}{\cos \alpha}$  (4.2)

Line of action of weight 'W' from center of rotation 'O' is 'X'. This can be calculated from equation-(4.16) then

$$\theta_2 = \sin^{-1} \left( \frac{X}{l_a} \right) \quad (4.3)$$

P= Resultant of boundary inter-granular forces(reaction)

$\theta_2$  = Angle between line of action of weight 'W' and line passing through center of rotation that is perpendicular to the line of action of resultant cohesive forces.

'q' = Intensity of surcharge load acting on the wall.

's' = Length on which surcharge load is acting.

Considering the equilibrium of all the forces in the vertical direction.

$$P \cos(\theta_2 - \phi_m) + C_m r l \cos(90 - \theta_2) = W + q s$$

$$P = \frac{W + qs - C_m r l \cos(90 - \theta_2)}{\cos(\theta_2 - \phi_m)}$$

$$P = \frac{W + qs - \frac{C \pi r^2 \alpha \cos(90 - \theta_2)}{F_c \times 180}}{\cos(\theta_2 - \phi_m)}$$

$$P = \frac{W + qs - \frac{C \pi r^2 \alpha \sin(\theta_2)}{F_c \times 180}}{\cos(\theta_2 - \phi_m)} \quad (4.4)$$

Resisting moment about 'O' due to inter-granular forces ( $M_{res}$ ):

$$M_{res} = P k r \sin \phi_m = \frac{W + qs - \frac{C \pi r^2 \alpha \sin \theta_2}{F_c \times 180}}{\cos(\theta_2 - \phi_m)} \times k r \sin \phi_m \quad (4.5)$$

### (iii) Axial force

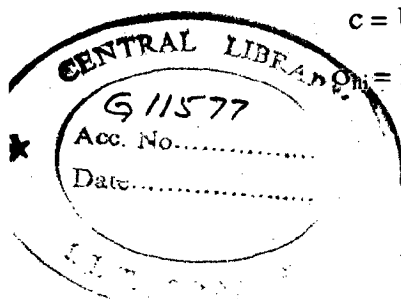
Axial force/ pull - out resistance of the length of nails behind the slip surface is given by:

$$\begin{aligned} T_i &= (c + \sigma_{ni} \tan \delta) p_i l_{ei} / S_h \\ &= f_1 p_i l_{ei} / S_h \end{aligned} \quad (4.6)$$

Where  $f_1$  = Limit bond stress of the soil nail interface from pull-out tests

$c$  = Unit soil cohesion

$\sigma_{ni}$  = Normal stress at mid depth of nail in the length  $l_{ei}$





$\delta$  = Mobilized soil / nail interface friction angle

$p_i$  = Perimeter of the nail

$l_{ei}$  = Length of nail behind the failure surface

**(iv) Shear stress that acts normal to the nail axis**

The mobilized shear  $T_{ci}$  in the 'i'th nail which acts normal to the nail axis at its intersection with the slip surface is given by Jewell and Pedley (1990a):

$$T_{ci} = \frac{CM_p}{l_{si}S_h} \left[ 1 - \left( \frac{T_i}{T_p} \right)^2 \right] \quad (4.7)$$

In which  $C = 4$ ;

$l_{si}$  = shear width (it is the distance between the points on the reinforcement on either side of the reinforcement on the either side of the shear plane in the soil that experiences the maximum moment.)

$$l_{si} = \sqrt{\frac{8M_p}{\sigma_b d} \times \frac{d}{D} \left( 1 - \frac{T}{T_p} \right)^2} \quad (4.8)$$

Where,  $T$  = Axial force in the nail at the point of maximum bending moment

$$= \sigma_v \times \pi d \, dL \tan \delta \quad (\text{for circular nail section}) \quad (4.9)$$

$T_p$  = Fully plastic axial force

= Nail yield stress ( $\sigma_y$ ) x Cross sectional area of nail

$$\text{Cross sectional area} = \frac{\pi}{4} d^2$$

$d$  = Dia of nail

$D$  = grout hole dia

For grouted nails,  $D \neq d$ .

For driven nails,  $D = d$ .

$M_p$  = Fully plastic moment capacity of nail (depend on the shape of nail and material property of nail)

$$\frac{M_p}{T_p} = \frac{2d}{3\pi} \quad (4.10)$$

Jewell and Pedley (1990a) presented the following lower, safe estimate of the bearing stress  $\sigma_B$ , as a function of the soil internal friction angle ' $\phi$ ' and the overburden stress  $\sigma_v$  assuming a punching shear failure of the soil around the bar.

$$\sigma_B = \sigma_v \left( \frac{1 + K_A}{2} \right) \tan \left( \frac{\pi}{4} + \frac{\phi}{2} \right) \exp \left[ \left( \frac{\pi}{2} + \phi \right) \tan \phi \right] \quad (4.11)$$

$\sigma_v = \gamma \times \text{depth of nail from the top}$

$\sigma_B$  should be calculated at the intersection of the nail with the slip surface.

#### Assumptions:

1. The foundation and body of the nailed wall are assumed homogenous. Therefore slip circles are assumed to pass through toe
2. Factor of safety with respect to cohesion ( $F_c$ ) and factor of safety with respect to friction ( $F_\phi$ ) are assumed 1.5.
3. Only internal stability is considered.
4. While considering force equilibrium in the vertical direction, nail axial force and nail tension have not been considered.
5. The analysis is based on moment and force equilibrium.
6. The shear resistance of the nail due to nail bending stiffness is taken care of by using the plastic analysis method suggested by Jewell and Pedley (1990a). The shear resistance mobilized in the nail is calculated by limiting the soil bearing pressure to safe value given in equation (4.7).
7. The deformation of the soil in the active zone is sufficient to fully mobilize the shear strength of the soil over the entire failure surface.

- 8 The internal failure mode of the wall is either by pullout or excessive bending leading to the formation of a plastic hinge in the nail whichever is critical.
- 9 Mobilized soil and nail interface friction angle ( $\delta$ ) is assumed to be  $(2/3)$  of the value of angle of repose of soil

(B) Driving forces

(a) Driving force due to weight

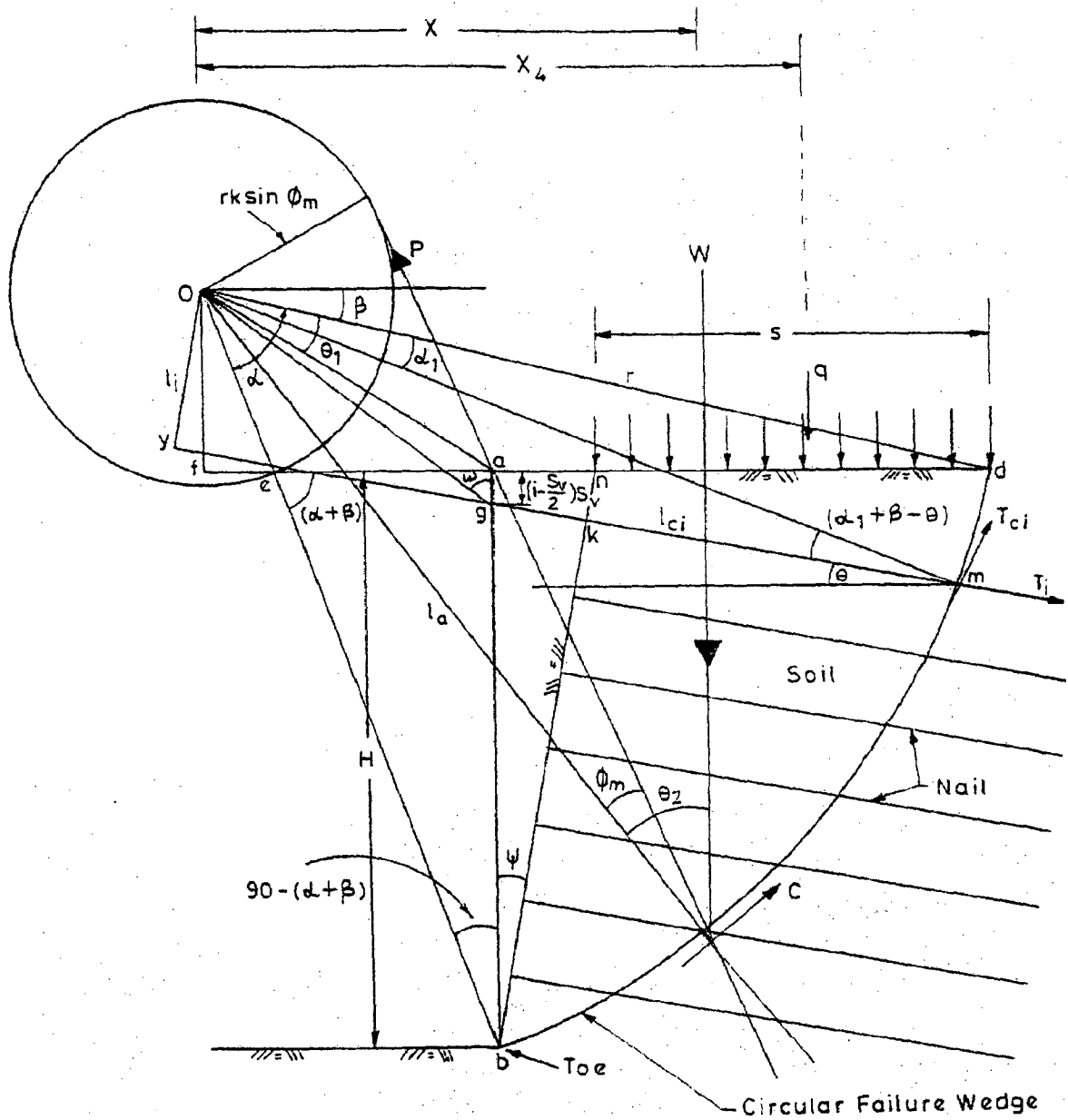


Fig.4.3. Nailed Soil Wall Showing all the Forces

(4.12)

From Fig-4.3

$$W_1 = \text{wt of wedge 'abd'}$$

$$W_1 = \frac{\pi^2 \alpha \gamma}{360}$$

Moment of the Circular type wedge 'abd' about 'O' =  $M_1$   
Where,  $\alpha$  is the arc angle of circular wedge  
 $\gamma$  is the unit weight of soil

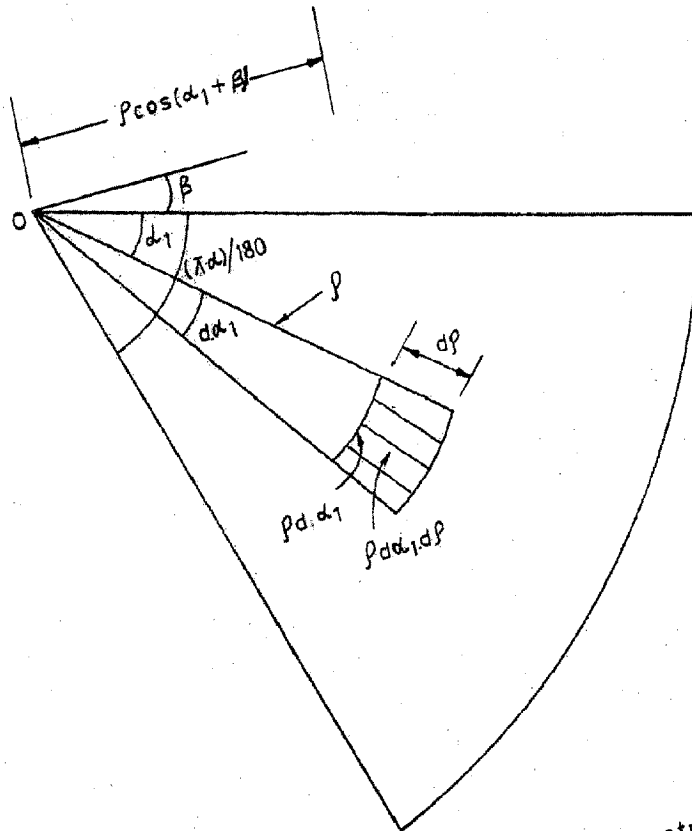


Fig-4.4 Circular Wedge to Find out the Centre of Gravity

Let us consider one elementary area (Fig-4.4) having dimension  $d\rho$  and  $\rho d\rho$ ,  $\rho$  being the radial distance of that element,  $\rho \cos(\alpha_1 + \beta)$  is the centro-dial distance from

'O'. Now integrating for the total arc having radius 'r' and angle  $\frac{\pi\alpha}{180}$ , we get

$$X_1 = \frac{\int_0^{\frac{\pi\alpha}{180}} \int_0^r \rho \cos(\alpha_1 + \beta) \cdot \rho d\rho \cdot d\alpha_1}{\int_0^{\frac{\pi\alpha}{180}} \int_0^r \rho d\rho \cdot d\alpha_1}$$

$$X_1 = \frac{\int_0^r \rho^2 d\rho \int_0^{\frac{\pi\alpha}{180}} \cos(\alpha_1 + \beta) d\alpha_1}{\int_0^r \rho d\rho \int_0^{\frac{\pi\alpha}{180}} d\alpha_1}$$

$$\text{Assume } \alpha_1 + \beta = \varepsilon$$

Since 'β' is constant, hence after differentiating  $d\alpha_1 = d\varepsilon$

Changing the limit,

When  $\alpha_1 = 0$ , then  $\varepsilon = \beta$  and

When  $\alpha_1 = \frac{\pi\alpha}{180}$ ,  $\varepsilon = \frac{\pi\alpha}{180} + \beta$

Now putting the limit in the above equation

$$X_1 = \frac{\frac{r^3}{3} \int_{\beta}^{\frac{\pi\alpha}{180} + \beta} \cos \varepsilon d\varepsilon}{\frac{r^2}{2} \left( \frac{\pi\alpha}{180} - 0 \right)}$$

$$= \left( \frac{120r}{\pi\alpha} \right) \left( \sin \left( \frac{\pi\alpha}{180} + \beta \right) - \sin \beta \right)$$

$$= \left( \frac{120r}{\pi\alpha} \right) \left( \sin \frac{\pi\alpha}{180} \cos \beta + \cos \frac{\pi\alpha}{180} \sin \beta - \sin \beta \right) \quad (4.13)$$

From Fig-4.3

$$M_1 = W_1 \times X_1 \quad (4.14)$$

where,  $X_1$  is the moment arm for  $W_1$  which can be calculated from equation (4.13)

$$de = H \cot(\alpha + \beta) + H \tan \psi + s$$

$$ef = r \cos \beta - \{ H \cot(\alpha + \beta) + s + H \tan \psi \}$$

$$fo = r \sin \beta$$

$W_2 =$  Wt of wedge 'oed'

$$W_2 = \frac{1}{2} \times fo \times df \times \gamma - \frac{1}{2} \times fo \times ef \times \gamma$$

=

$$\gamma \left( \frac{1}{2} \times (r \sin \beta) \times (r \cos \beta) - \frac{1}{2} \times (r \sin \beta) \times (r \cos \beta - \{ H \cot(\alpha + \beta) + s + H \tan \psi \}) \right) \quad (4.15)$$

$$M_2 = \frac{1}{2} \times fo \times df \times \frac{1}{3} \times df \times \gamma - \frac{1}{2} \times fo \times ef \times \frac{1}{3} \times ef \times \gamma$$

Where  $M_2 =$  Moment due to  $W_2$  about 'O'

$$= \gamma \left\{ \frac{1}{2} \times (r \sin \beta) \times \frac{1}{3} (r \cos \beta) \times (r \cos \beta) - \frac{1}{2} (r \sin \beta) (ef) \frac{1}{3} (ef) \right\} =$$

$$\frac{1}{6} \times \gamma \times r \sin \beta \left[ r^2 \cos^2 \beta - (r \cos \beta - (H \cot(\alpha + \beta) + s + H \tan \psi))^2 \right]$$

$$= \frac{1}{6} \times \gamma \times r \sin \beta \left[ H \cot(\alpha + \beta) + s + H \tan \psi \right] \times \left[ 2r \cos \beta - (H \cot(\alpha + \beta) + s + H \tan \psi) \right] \quad (4.16)$$

$W_3 =$  Weight of wedge 'abe'

In  $\Delta$  abe

$$W_3 = \frac{1}{2} \times ae \times ab \times \gamma$$

$$= \frac{1}{2} \times H^2 \times \cot(\alpha + \beta) \times \gamma \quad (4.17)$$

$$M_3 = \frac{1}{2} \times ae \times ab \times X_2 \times \gamma$$

Where,  $M_3$  = Moment due to  $W_3$  about 'O'

$$M_3 = \frac{1}{2} \times H^2 \times \cot(\alpha + \beta) \times \gamma \times X_2$$

Where  $X_2$  = Lever arm of weight of  $\Delta$  abe

$$= ef + \frac{2}{3} (ae)$$

$$= (r \cos \beta - (H \cot(\alpha + \beta) + s + H \tan \psi)) + \frac{2}{3} H \cot(\alpha + \beta)$$

$$X_2 = (r \cos \beta - H \tan \psi - \frac{1}{3} H \cot(\alpha + \beta) - s)$$

$$M_3 = \frac{1}{2} \times H^2 \times \cot(\alpha + \beta) \times \gamma \times \left( r \cos \beta - s - \frac{1}{3} \times H \times \cot(\alpha + \beta) - H \tan \psi \right) \quad (4.18)$$

In  $\Delta$  abn

$W_4$  = Wt of wedge  $\Delta$  abn

$$W_4 = \frac{1}{2} \times H \times H \tan \psi \times \gamma \quad (4.19)$$

$$W = W_1 - W_2 - W_3 - W_4 \quad (4.20)$$

$$M_4 = \frac{1}{2} \times H \times H \tan \psi \times \gamma \times X_3$$

Where  $M_4$  = Moment due to  $W_4$  about 'O'

$X_3$  = Lever arm of weight of  $\Delta$  abn

$$= (r \cos \beta - s) + \frac{2H \tan \psi}{3}$$



$$\text{or, } M_4 = \frac{1}{2} \times H^2 \times \gamma \times \tan \psi \times \left( r \cos \beta - s + \frac{2H \tan \psi}{3} \right) \quad (4.21)$$

$$X = \frac{M_1 - M_2 - M_3 - M_4}{W} \quad (4.22)$$

$$\text{In } \Delta \text{ ode, } \frac{r}{\sin(\alpha + \beta)} = \frac{de}{\sin \alpha} = \frac{eo}{\sin \beta}$$

$$de = H \cot(\alpha + \beta) + s + H \tan \psi$$

From first and second ratios

$$s = \frac{r \sin \alpha}{\sin(\alpha + \beta)} - H \cot(\alpha + \beta) - H \tan \psi \quad (4.23)$$

From first and third ratios,

$$eo = \frac{r \sin \beta}{\sin(\alpha + \beta)}$$

$$be = H \operatorname{cosec}(\alpha + \beta)$$

$$r = eo + be$$

$$= \frac{r \sin \beta}{\sin(\alpha + \beta)} + H \operatorname{cosec}(\alpha + \beta)$$

$$\text{or, } r \left( 1 - \frac{\sin \beta}{\sin(\alpha + \beta)} \right) = \frac{H}{\sin(\alpha + \beta)}$$

$$\text{or, } r \left( \frac{\sin(\alpha + \beta) - \sin \beta}{\sin(\alpha + \beta)} \right) = \frac{H}{\sin(\alpha + \beta)}$$

$$\text{or, } r = \frac{H}{\sin(\alpha + \beta) - \sin \beta} \quad (4.24)$$

Putting different values of  $\alpha$ ,  $\beta$  and  $H$  in equation (4.24) different values of 'r' may be obtained.

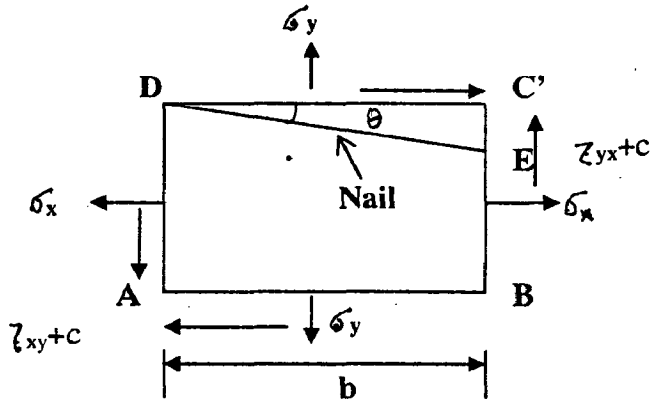


Fig- 4.5 Calculation of Normal Stress on Inclined Nail Face

Let us consider a rectangular block ABC'D having width 'b', thickness 't' and nail inclination ' $\theta$ ' subjected to normal stress  $\sigma_x$  and  $\sigma_y$  and tangential stress  $\tau_{xy}$  as shown in Fig. 4.5.

Total shear force on C'D,  $Q_1$

$$Q_1 = (\tau_{xy} + c) \times b \times t$$

Total shear force on C'E,  $Q_2$

$$\begin{aligned} Q_2 &= (\tau_{xy} + c) \times C'E \times t \\ &= (\tau_{xy} + c) \times C'D \tan\theta \times t \\ &= (\tau_{xy} + c) \times b t \tan\theta \end{aligned}$$

Normal force ( $P_x$ ) on C'E =  $\sigma_x \times C'E \times t$

$$= \sigma_x b t \tan\theta$$

Similarly normal force ( $P_y$ ) on C'D

$$P_y = \sigma_y b t$$

If the normal and tangential force on the plane DE be  $\sigma_{ns}$  and  $\tau_{ns}$  respectively, then

$$\begin{aligned} \sigma_{ns} &= \sigma_n \times DE \times t \\ &= \sigma_n \times (C'D / \cos\theta) \times t \end{aligned}$$

$$\sigma_{ns} = \frac{\sigma_n \times b \times t}{\cos \theta}$$

$$\text{Similarly, } \tau_{ns} = \frac{\tau_n \times b \times t}{\cos \theta}$$

From equilibrium of wedge C'DE, resolving forces parallel to  $\sigma_{ns}$  and  $\tau_{ns}$  we get

$$\sigma_{ns} = P_x \cos(90-\theta) + P_y \cos \theta + Q_1 \cos(90-\theta) + Q_2 \cos \theta$$

$$\frac{\sigma_n \times b \times t}{\cos \theta} = \sigma_x \times b \times t \tan \theta \sin \theta + \sigma_y \times b \times t \times \cos \theta + (\tau_{xy} + c) \times b \times t \times \sin \theta + (\tau_{xy} + c) \times b \times t \tan \theta \times \cos \theta$$

$$\text{or, } \sigma_n = \sigma_x \sin^2 \theta + \sigma_y \cos^2 \theta + (\tau_{xy} + c) \sin 2\theta$$

(4.25)

Similarly,

$$\tau_{ns} = -P_x \cos \theta + P_y \cos(90-\theta) - Q_1 \cos \theta + Q_2 \cos(90-\theta)$$

$$\frac{\tau_n \times b \times t}{\cos \theta} = -\sigma_x \times b \times t \tan \theta \cos \theta + \sigma_y \times b \times t \times \sin \theta - (\tau_{xy} + c) \times b \times t \times \cos \theta + (\tau_{xy} + c) \times b \times t \tan \theta \times \sin \theta$$

$$\text{or, } \tau_n = -\sigma_x \sin \theta \cos \theta + \sigma_y \sin \theta \cos \theta - (\tau_{xy} + c) \cos^2 \theta + (\tau_{xy} + c) \sin^2 \theta$$

$$\text{or, } \tau_n = \left( \frac{\sigma_y - \sigma_x}{2} \right) \sin 2\theta - (\tau_{xy} + c) \cos 2\theta$$

(4.26)

From Coulomb's theory

$$\tau_n = c + \sigma_n \tan \delta;$$

(4.27)

By rearranging the terms from equation (3.25)

$$\tau_{xy} + c = \left[ \left( \frac{\sigma_y - \sigma_x}{2} \right) \sin 2\theta - \tau_n \right] \frac{1}{\cos 2\theta}$$

(4.28)

From equations (3.26), (3.27) & (3.28);

$$\sigma_n = \sigma_x \sin^2 \theta + \sigma_y \cos^2 \theta + \left[ \left( \frac{\sigma_y - \sigma_x}{2} \right) \sin 2\theta - \tau_n \right] \tan 2\theta$$

$$\text{or, } \sigma_n = (\sigma_x \sin^2 \theta + \sigma_y \cos^2 \theta) + \left[ \left( \frac{\sigma_y - \sigma_x}{2} \right) \sin 2\theta - (c + \sigma_n \tan \delta) \right] \tan 2\theta$$

$$\sigma_n (1 + \tan \delta \tan 2\theta) = (\sigma_x \sin^2 \theta + \sigma_y \cos^2 \theta) + \left( \frac{\sigma_y - \sigma_x}{2} \right) \sin 2\theta \cdot \tan 2\theta - c \tan 2\theta$$

$$\sigma_n = \frac{\sigma_x \sin^2 \theta + \sigma_y \cos^2 \theta}{1 + \tan \delta \tan 2\theta} + \frac{\sigma_y - \sigma_x}{2} \times \frac{\sin 2\theta \tan 2\theta}{1 + \tan \delta \tan 2\theta} - \frac{c \tan 2\theta}{1 + \tan \delta \tan 2\theta}$$

(4.29)

To calculate  $l_{ei}$

From Fig.4.3:

$$\text{In } \Delta oad, \quad \frac{r}{\sin(\beta + \theta_1)} = \frac{s + H \tan \psi}{\sin \theta_1} = \frac{ao}{\sin \beta}$$

From above,

$$\frac{r}{\sin(\beta + \theta_1)} = \frac{s + H \tan \psi}{\sin \theta_1}$$

$$\frac{r}{H \tan \psi + s} = \cos \beta + \cot \theta_1 \sin \beta$$

$$\cot \theta_1 = \left[ \frac{\frac{r}{s + H \tan \psi} - \cos \beta}{\sin \beta} \right]$$

$$\text{or, } \cot \theta_1 = \frac{r - s \cos \beta - \cos \beta \cdot H \tan \psi}{s + H \tan \psi \sin \beta}$$

$$\text{or, } \cot \theta_1 = \frac{r - s \cos \beta - \cos \beta \cdot H \cdot \tan \psi}{\sin \beta (s + H \tan \psi)}$$

$$\text{or, } \tan \theta_1 = \frac{\sin \beta (s + H \tan \psi)}{r - s \cos \beta - \cos \beta H \tan \psi}$$

$$\text{or, } \theta_1 = \tan^{-1} \left( \frac{\sin \beta (s + H \tan \psi)}{r - s \cos \beta - \cos \beta H \tan \psi} \right) \quad (4.30)$$

$$ao = \frac{r \sin \beta}{\sin(\theta_1 + \beta)} \quad (4.31)$$

In Fig 4.3 in  $\Delta oag$   $\frac{ao}{\sin \omega} = \frac{go}{\sin(90 + \beta + \theta_1)} = \frac{\left(i - \frac{S_v}{2}\right) S_v}{\sin(180 - 90 - \beta - \theta_1 - \omega)}$

From first and third ratios:

$$\frac{ao}{\sin \omega} = \frac{\left(i - \frac{S_v}{2}\right) S_v}{\sin(90 - \beta - \theta_1 - \omega)}$$

$$\frac{ao}{\sin \omega} = \frac{\left(i - \frac{S_v}{2}\right) S_v}{\cos(\beta + \theta_1 + \omega)}$$

$$\frac{\cos(\beta + \theta_1 + \omega)}{\sin \omega} = \frac{\left(i - \frac{S_v}{2}\right) S_v}{ao}$$

$$\text{or, } \frac{\cos(\beta + \theta_1) \cos \omega}{\sin \omega} - \frac{\sin(\beta + \theta_1) \sin \omega}{\sin \omega} = \frac{\left(i - \frac{S_v}{2}\right) S_v}{ao}$$

$$\text{or, } \cos(\beta + \theta_1) \cot \omega - \sin(\beta + \theta_1) = \frac{\left(i - \frac{S_v}{2}\right) S_v}{ao}$$

$$\text{or, } \cot \omega - \tan(\beta + \theta_1) = \frac{\left(i - \frac{S_v}{2}\right) S_v}{ao \cdot \cos(\beta + \theta_1)}$$

$$\text{or, } \cot \omega = \frac{\left(i - \frac{S_v}{2}\right) S_v}{ao \cdot \cos(\beta + \theta_1)} + \tan(\beta + \theta_1)$$

$$\text{or, } \cot \omega = \frac{\left(i - \frac{S_v}{2}\right) S_v + \tan(\beta + \theta_1) ao \cdot \cos(\beta + \theta_1)}{ao \cdot \cos(\beta + \theta_1)}$$

$$\text{or, } \tan \omega = \frac{ao \cdot \cos(\beta + \theta_1)}{\left(i - \frac{S_v}{2}\right) S_v + \tan(\beta + \theta_1) ao \cdot \cos(\beta + \theta_1)} \quad (4.32)$$

From first and second ratios

$$go = \frac{ao \cdot \cos(\beta + \theta_1)}{\sin \omega} \quad (4.33)$$

In  $\Delta ogm$ ,

$$\frac{r}{\sin(90 + \omega + \theta)} = \frac{go}{\sin(\alpha_1 + \beta - \theta)} = \frac{gm}{\sin(180 - 90 - \omega - \alpha_1 - \beta)}$$

From first and second ratios,

$$\sin(\alpha_1 + \beta - \theta) = \frac{gO}{r} \times \sin(90 + \omega + \theta)$$

$$\text{or, } \sin(\alpha_1 + \beta - \theta) = \frac{gO}{r} \times \cos(\omega + \theta)$$

$$\text{or, } \alpha_1 = \sin^{-1}\left(\frac{gO}{r} \times \cos(\omega + \theta)\right) - \beta + \theta \quad (4.34)$$

From second and third ratios, we find the value of gm after putting all those known values found from above.

$$gm = \frac{gO \times \cos(\omega + \alpha_1 + \beta)}{\sin(\alpha_1 + \beta - \theta)} \quad (4.35)$$

$$km = gm - \left[H - \left(i - \frac{S_v}{2}\right) \times S_v\right] \sin(\Psi) \quad (4.36)$$

Where 'i' is the number of nail rows.

Length of nail behind failure surface,  $l_{ci} = L - km$

Where 'L' is the length of nail provided

From  $\Delta omy$

$$om = r \quad (4.37)$$

$$oy = l_i = r \sin(\alpha_1 + \beta - \theta) \quad (4.38)$$

$$my = l_{ci} = r \cos(\alpha_1 + \beta - \theta) \quad (4.39)$$

#### (b) Driving force due to surcharge load

Let surcharge load of intensity  $q$  kN/m<sup>2</sup> acting over a length of 's'.

$$\text{So, moment of forces about O, } P_1 X_4 = q \times s (r \cos\beta - 0.5 \times s) \quad (4.40)$$

Where 'P<sub>1</sub>' is the total surcharge load acting on the mid point of 's' and X<sub>4</sub> is the moment arm from center of rotation 'O'.

The factor of safety is defined as

$$FOS = \frac{\sum_{i=1}^n T_i l_i + \sum_{i=1}^n T_{cl} l_{cl} + M_c + M_{res}}{WX + P_1 X_4} \quad (4.41)$$

Assuming different slip surface having radius 'r', the minimum value of factor of safety can be found.

**Computer program in FORTRAN language for computing FOS with the help of Eq.4.41 is enclosed in appendix-A. Effects of different design parameters on FOS are reflected in following graphs:**



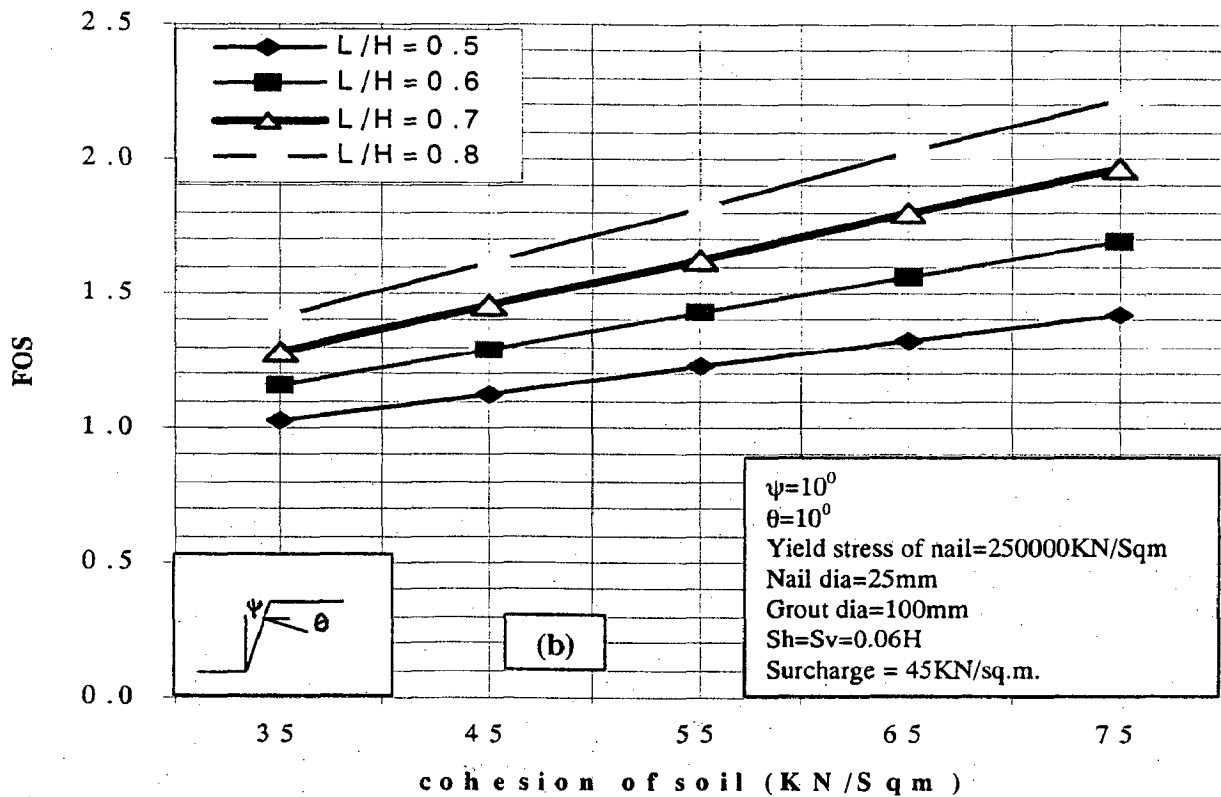
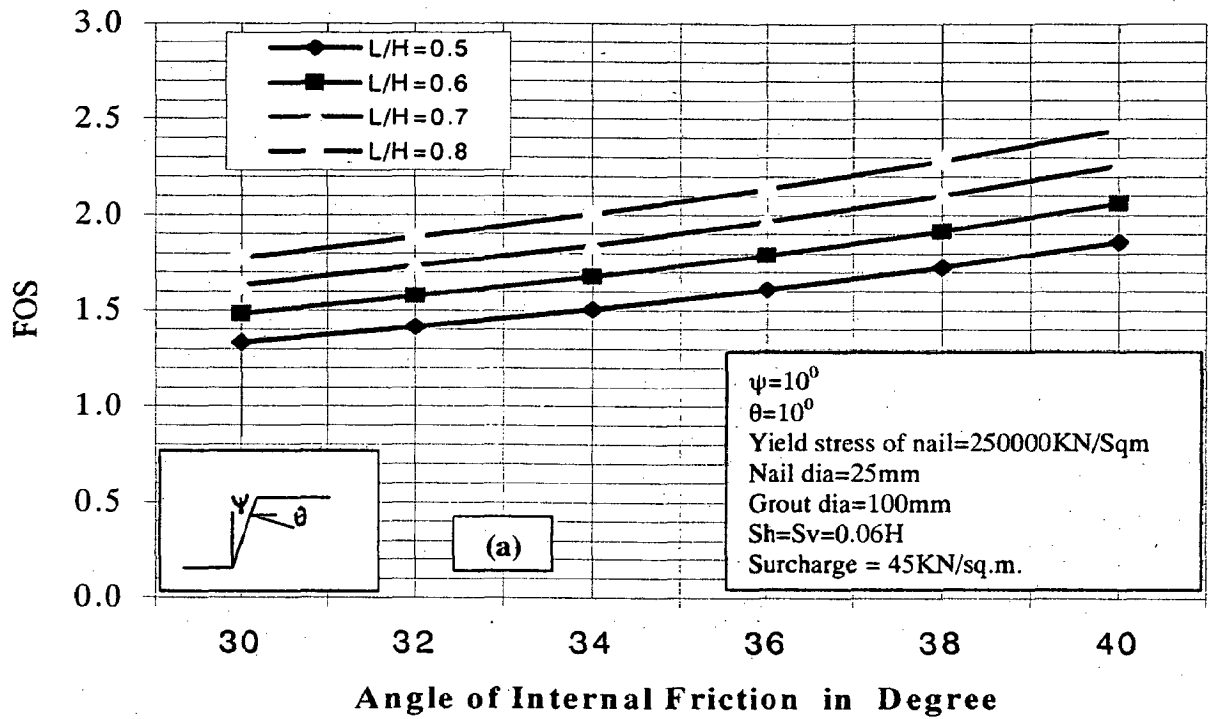


Fig-4.6(a) FOS VS Angle of Internal Friction ( $c=0$ ), (b) FOS VS Cohesion ( $\phi=0$ )

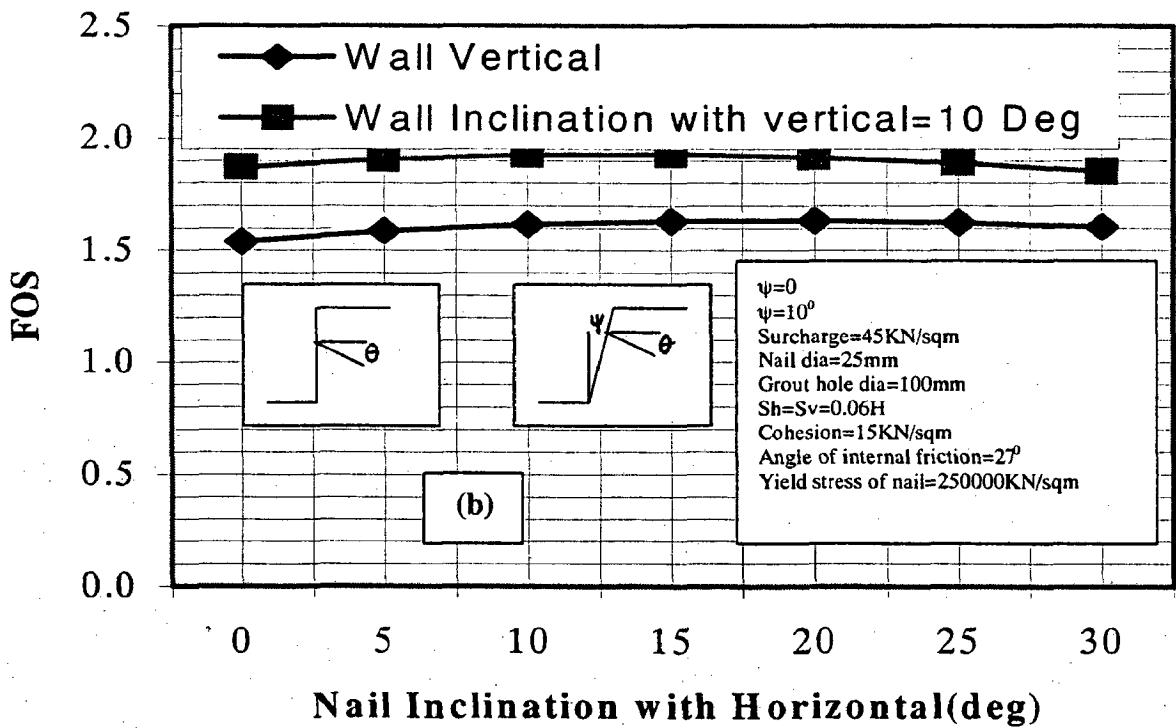
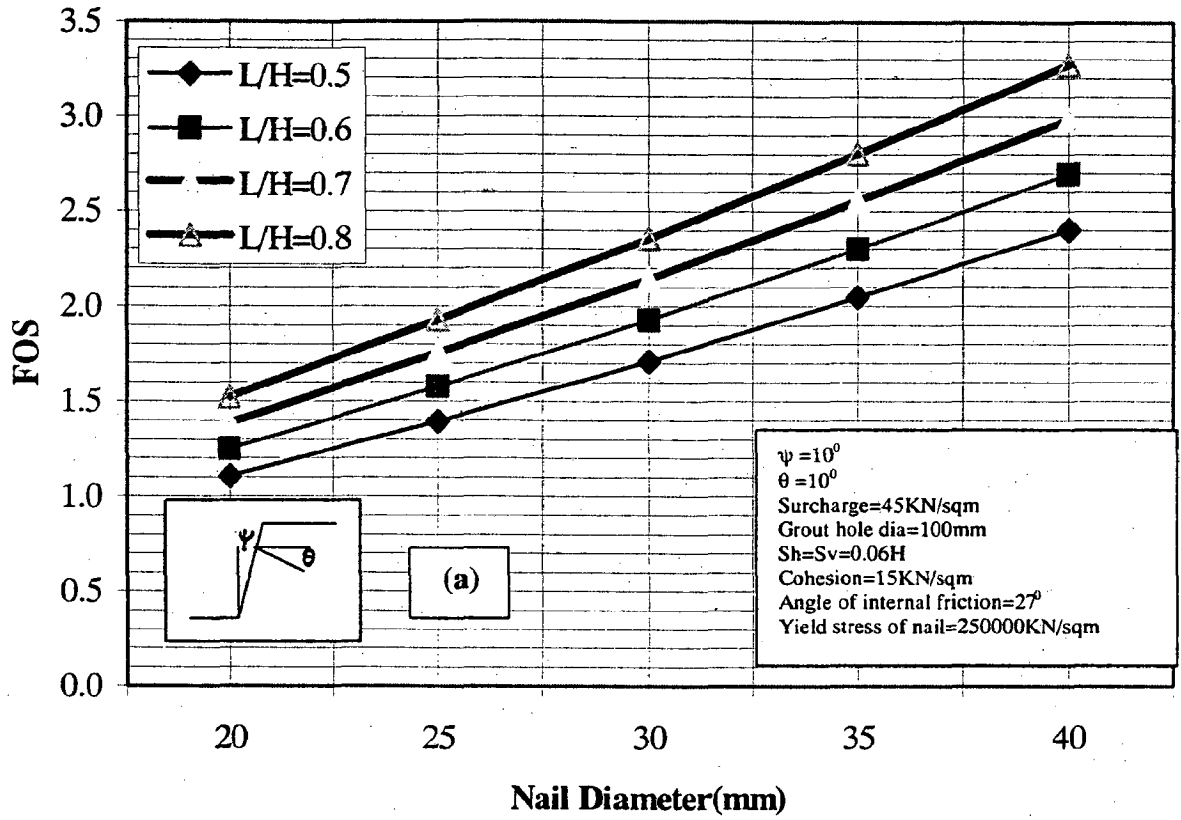


Fig-4.7(a) FOS VS Nail Diameter (b) FOS VS Nail Inclination (L/H = 0.8)

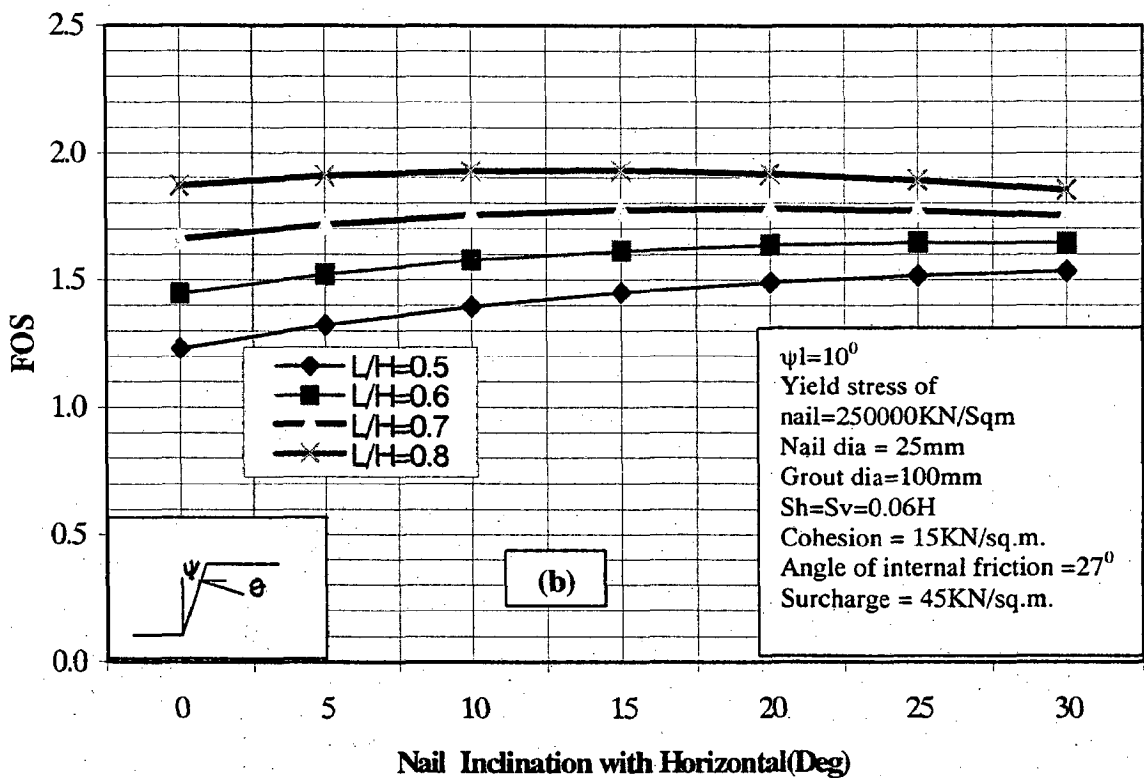
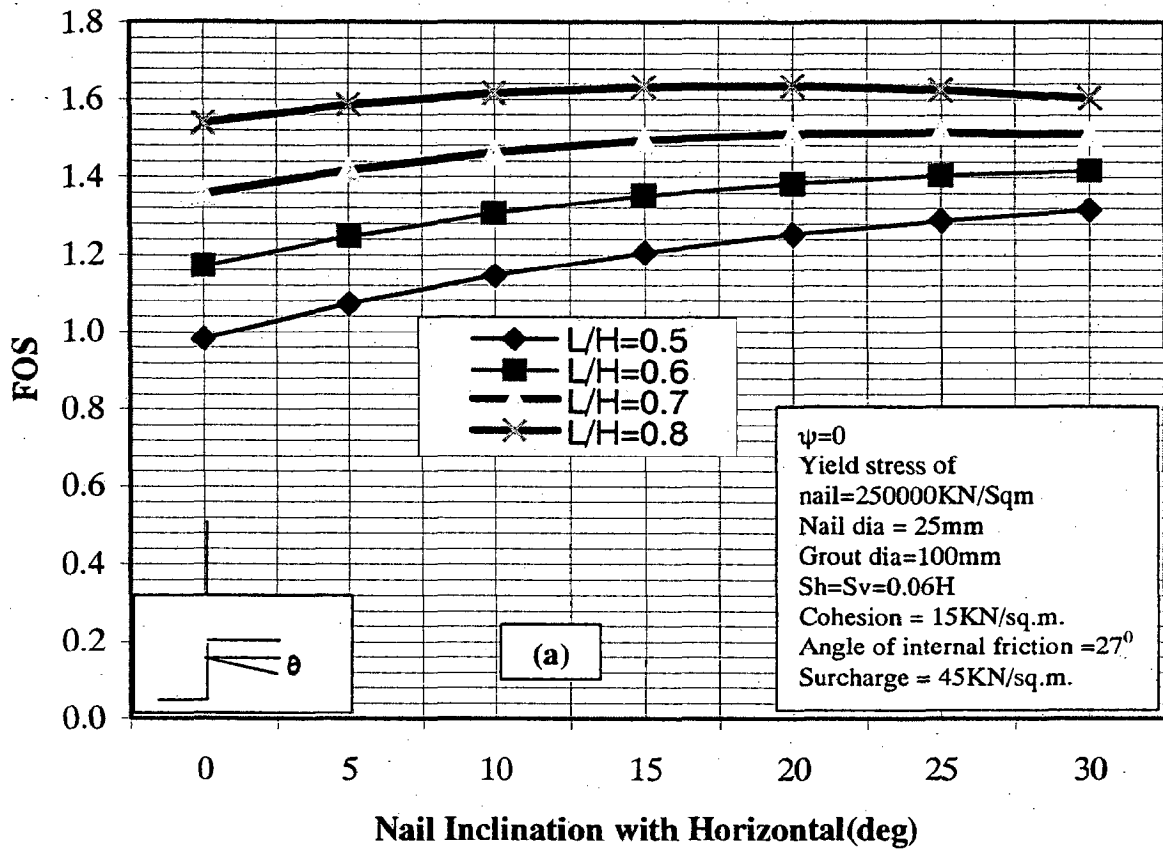


Fig-4.8(a) FOS VS Nail inclination (wall vertical) (b) FOS VS Nail Inclination

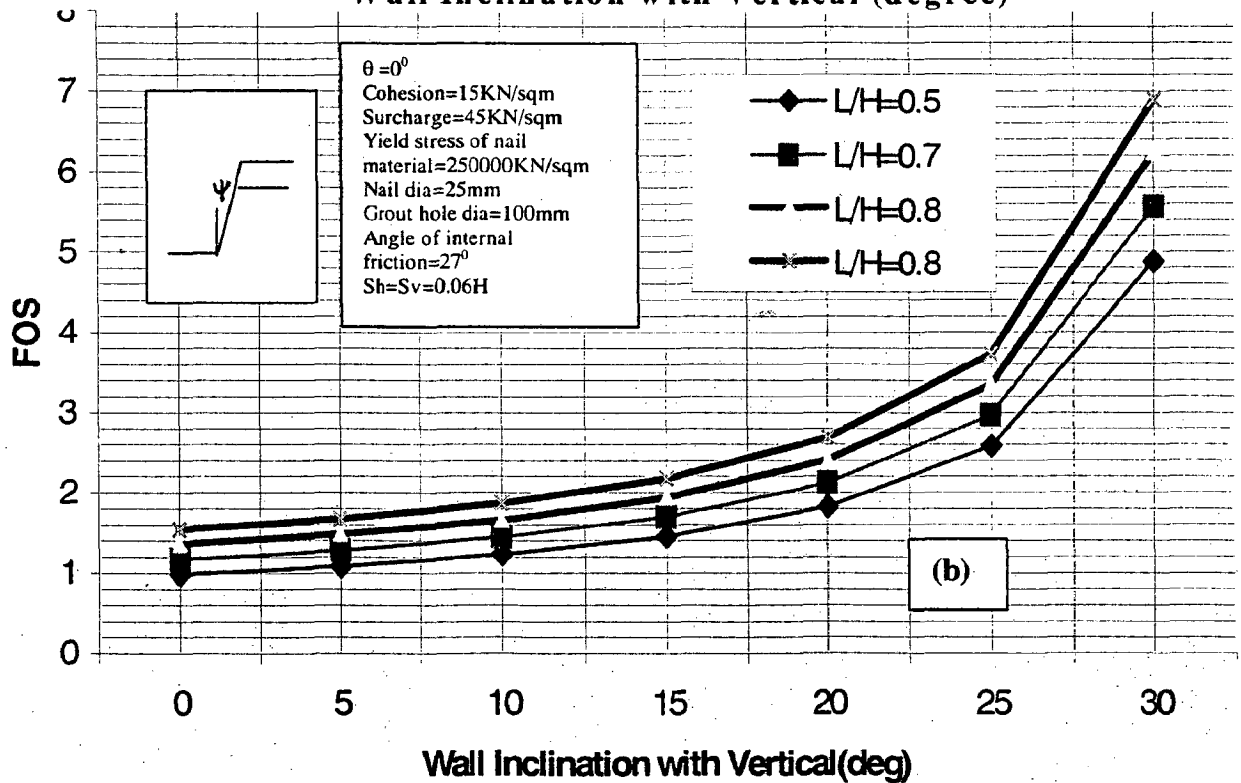
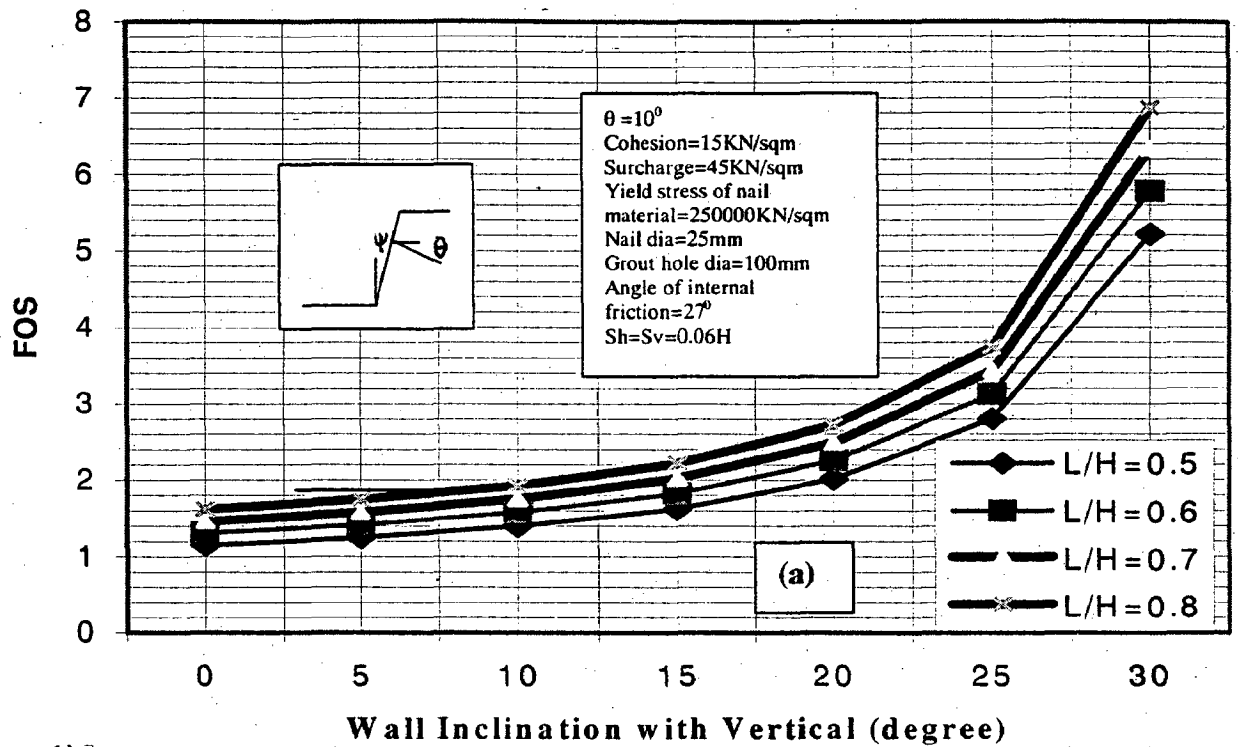
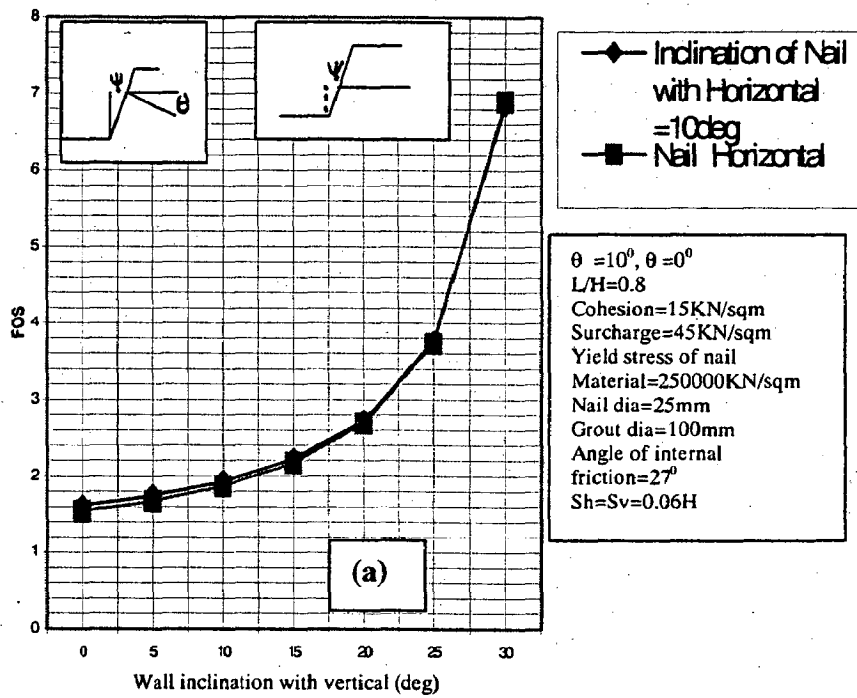
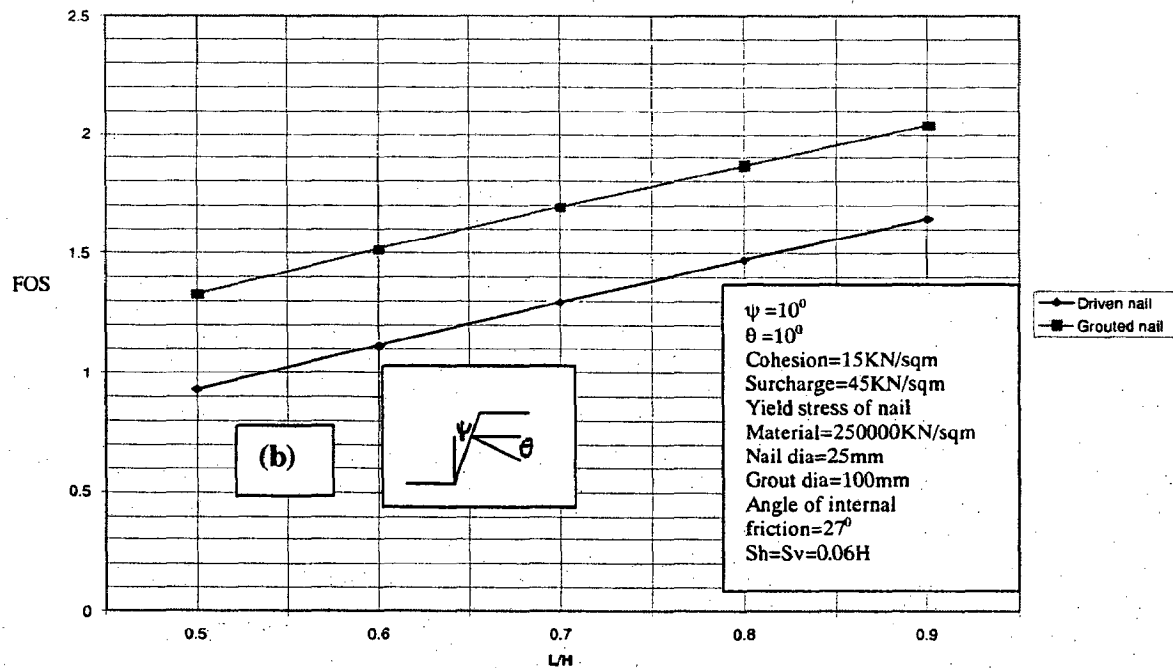


Fig-4.9(a) FOS VS Wall Inclination (for inclined nail) (b) FOS VS Wall Inclination (for horizontal nail)



**Fig-4.10(a) FOS VS wall Inclination**



**Fig-4.10(b) FOS VS L/H ratio**

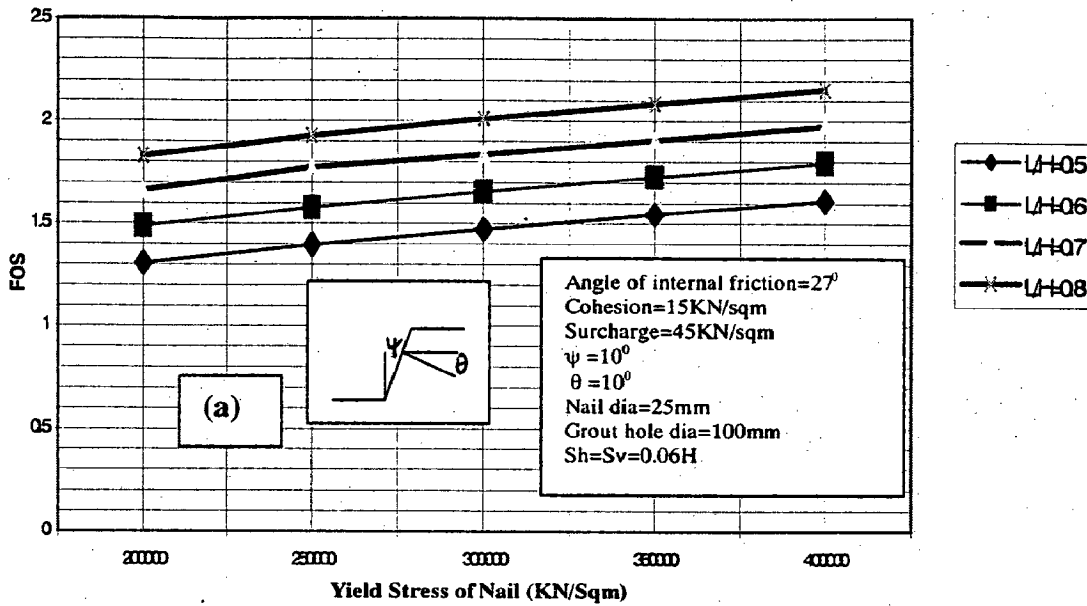


Fig-4.11(a) FOS VS Yield Stress of Nail (for different L/H ratio)

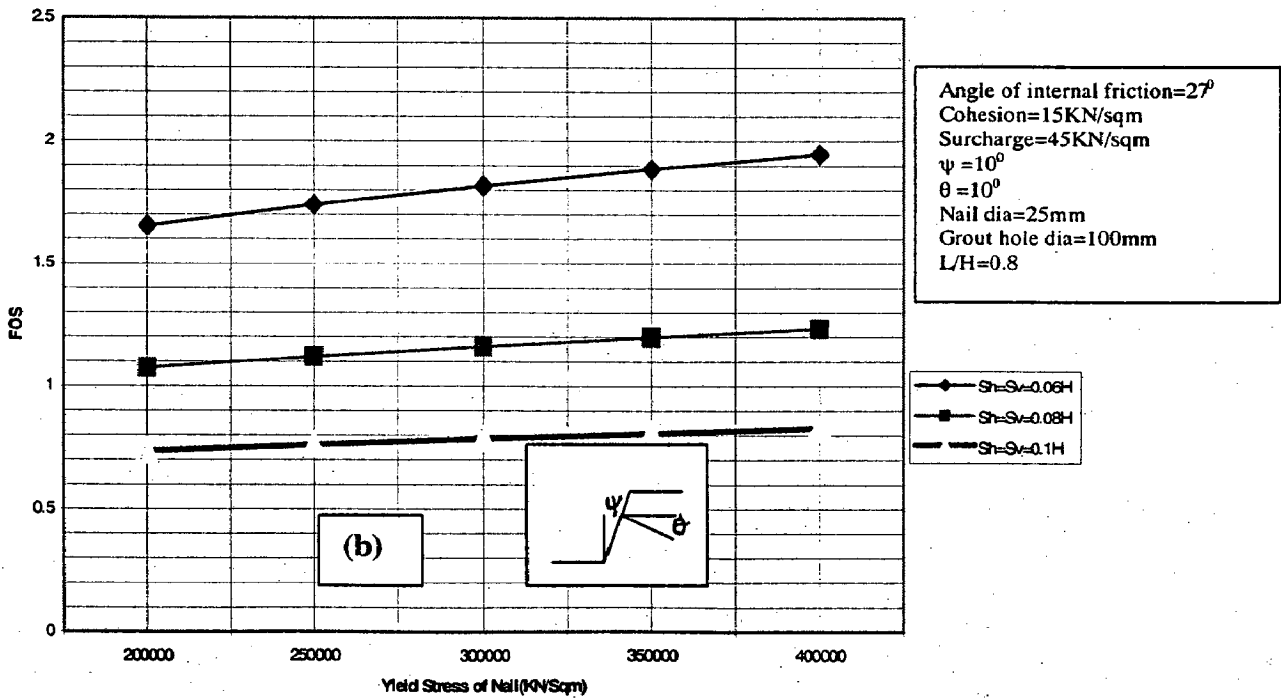


Fig-4.11(b) FOS VS Yield Stress of Nail (for different nail spacing)

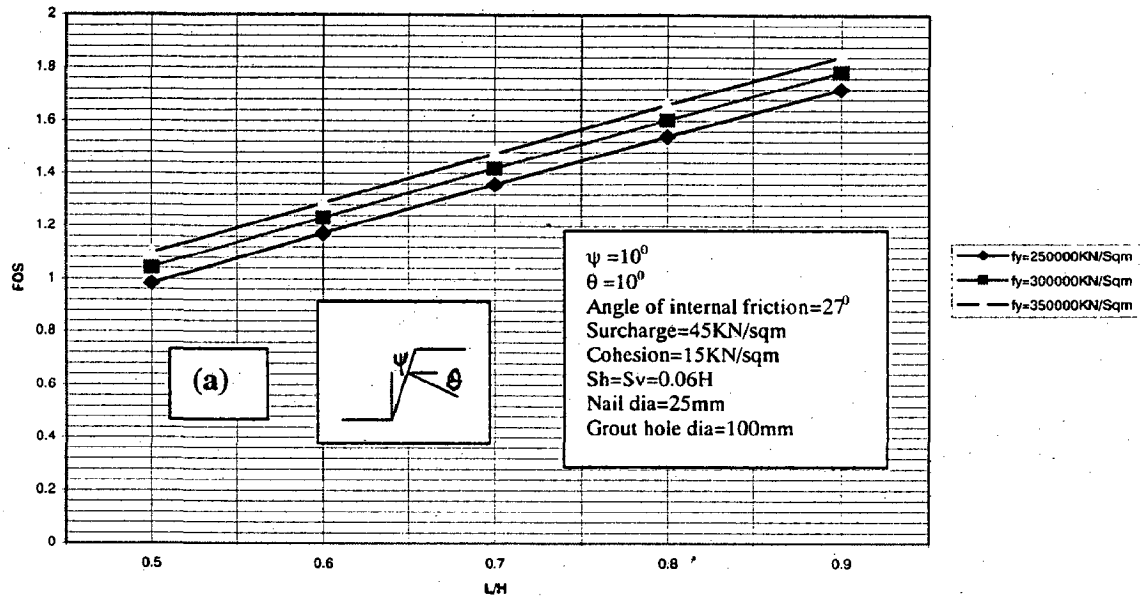


Fig-4.12 (a) FOS VS L/H Ratio for Different Yield Stress of Nail

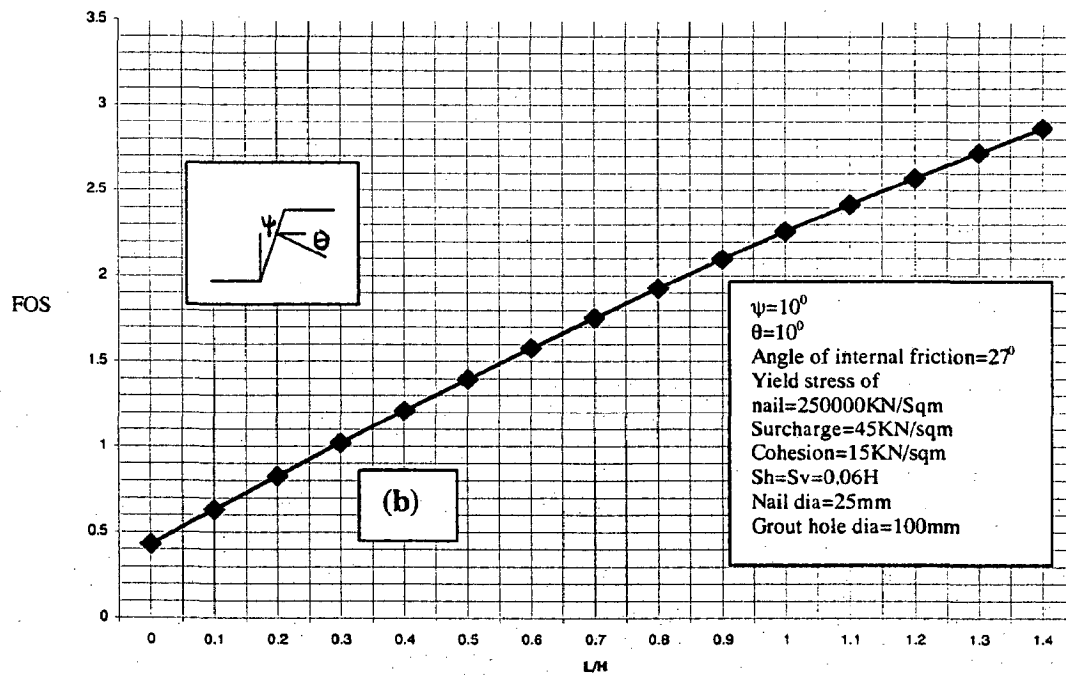


Fig-4.12(b) FOS VS L/H Ratio

## SOIL NAILING IN EROSION CONTROL

---

### 5.1 SOIL NAILING TECHNIQUE IN RAINFALL EROSION CONTROL

Nailing technique can be used in stabilizing a slope experiencing rockfall and superficial sliding. This technique has been successfully used in a project located along side the Ruhr River at the foot of Kahlenberg in Germany, the rock and soil slope was approximately 445m long and 12m high at its highest point. To stabilize the surface, high tensile steel wire mesh was used in combination with nailing. The slope was also vegetated. Because of this, no further surface erosion took place.

Rock breakouts and superficial sliding occurred several times in January and February and road traffic was closed for safety reason. Many trees standing at an angle or growing in a bow as well as cracks of several centimeters wide in the footpath indicated that a creeping deformation of the soil layer was in progress. Based on the geological situation the overall stability of the slope was not endangered.

Because of the high tensile mesh and optimal interaction between the mesh and the system spike, it was possible to select horizontal and vertical spacing of nails as 2.5m c/c in the steep section of the cutting and 3.3m c/c in the flatter portion of the slope. GWEI-type nails of 28mm in diameter were used for the nailing. The overall nail length was 4.0m

The mesh size was 83mmX143mm. Diameter of the wire mesh was 3mm. Mesh was of high power tensile steel, around three times higher in strength than the normal steel. Therefore, the mesh is really an economic alternative of wire-rope nets. Moreover, if a mesh is used before using nailing, nail pattern can be freely selected.



## **5.2 SOIL NAILING IN RIVER BANK EROSION CONTROL**

Soil Nailing technique is suitable above ground water table. In river bank/bed erosion process, turbulence of water, velocity and shear stress are involved. In nailing technique stability of nailed wall comes due to shear force of each nail and axial force due to soil-nail interface action. If nails are inserted into the river bank i.e. below water table soil-nail interface relation will be weak and as such the technique will not be cost effective also.

Below HFL River bank erosion may be protected by articulated concrete block. Obviously in this case bank should be flatter. These blocks are anchored with the bank material to provide extra factor of safety. This anchor is known as nails. In addition to this, selfweight of concrete block provides additional protection against erosion due to velocity, tractive force. Virtually speaking, the technique is not suitable in riverbank/bed erosion control under water.

**Soil nailing may be successfully used above HFL to protect riverbank sliding and rainfall erosion control**

## **GEOSYNTHETICS IN EROSION CONTROL**

---

### **6.1 INTRODUCTION**

Geosynthetic materials are being increasingly used throughout the world in civil engineering works. The reason for this wide use is that they are

- Good alternative to conventional design
- Some times the only means of construction
- Easy to install

It has wide use in water resources projects especially in erosion control. Geosynthetic components such as geotextile, geo-jute, gabions, polymer wire rope, polymer flexible rope, Reno mattress, jute bag/synthetic bag filled with cement or soil are being successfully used in erosion control.

### **6.2 HISTORICAL DEVELOPMENT OF GEOSYNTHETICS**

The first use of a woven synthetic fabric for erosion control was in 1950's in Florida by Barrette. In 1960's, geotextiles were extensively used for erosion control both in Europe as well as in U.S.A. Later in 1969, Giroud used non-woven fabrics as a filter in the upstream face of the earthen dam.

### **6.3 FUNCTION OF GEOTEXTILE**

Functions of geo-textiles in constructions are:

- Separating, geo-textiles provide separation between layers of different grain size.
- Filtering, it can retain particles and allows water to pass through.
- Draining, it functions as a drain because it has a higher permeability than the surroundings.
- Reinforcing, it increases the stability of soil body.

### **6.4 GEOTEXTILE SPECIFICATION**

Specifications for geo-textile should include the following items (Murray and Mc-Gown, 1982)

- (i) Identification of design procedures to be followed for specific applications

(ii) Limiting values of geo-textile properties, measured according to standard test procedure, which may be adopted in design.

(iii) Procedures for transporting, storing and handling geotextiles.

(iv) Construction, installation procedure

(v) Limiting values of geotextile properties measured according to standard test procedures for the purpose of quality control.

**Some properties of geo-textile are listed below.**

**(a) Basic physical properties**

(i) Constituent material and method of manufacture

(ii) Mass per unit area

(iii) Thickness

(iv) Roll width/roll length

**(b) Mechanical properties**

(i) Tensile strength

(ii) Tensile modulus

(iv) Seam strength

(v) Interface friction

(vi) Fatigue resistance

**(c) Hydraulic properties**

(i) Compressibility

(ii) Opening size

(iii) Permittivity

(iii) Transmissivity

**(d) Constructability/survivability properties**

(i) Burst resistance

(ii) Puncture resistance

(iii) Tear strength

(iv) Biological stability

(v) Wetting & drying stability

Hydraulic properties have to be satisfied when geotextile will be used in riverbank protection works as filter material.

## 6.5 GEOTEXTILE IN FILTRATION AND EROSION CONTROL.

Geo-textiles may be used in the following environments:

- In fairly steady unidirectional flow (Land drainage filter)
- Reversing flow with moderate cycle time (Rivers and Coastal defense filter)
- Reversing flow with a very short cycle time (Anti pumping filters)

Depending upon the gradation of riverbank or bed materials, the following criteria should be ratified to select filter fabric.

- (i) Granular material containing 50% or less fines by weight, the following ratio should be satisfied.

$$\frac{\text{85\% passing size of bed material (mm)}}{\text{equivalent opening size of fabric}} \geq 1$$

Where, according to Calhoun,  $O_{95}$  is the equivalent opening size of woven geo-textile.  $O_{95}$  is known as the 95% opening size and corresponds to the size where 95% of the geo-textile openings are the same size or smaller. For non-woven geo-textile  $O_{95}$  or  $O_{90}$  is used and even a conservative value of  $O_{50}$  is used.

In order to reduce the possibility of clogging, no fabric should be specified with an equivalent opening size smaller than 0.149mm and should be equal to or less than 85% passing size of the bed materials.

- (ii) For bed material containing at least 50% but not more than 85% fines by weight, the equivalent opening size of filter should not be smaller than sieve no 100 (0.149mm) and should not be larger than sieve no. 70 (0.211mm)
- (iii) Filter fabric should not be placed where 85% or more of the bed materials are fines i.e. finer than 0.074mm (No. 200 sieve).

Char et al. (1989) has reported the successful use of geotextile in bank protection in Farakka Barrage project, West Bengal of India. Stone gabion caged with Netlon geogrids are used for bank protection in Dhadhan estuary at Gandhar area, Gujarat (Desai et al. 1989). It was protected from upstream because outgoing tides reportedly causing major damage. Non-oven geotextile is also used as a filter layer in between gabions and base soil.

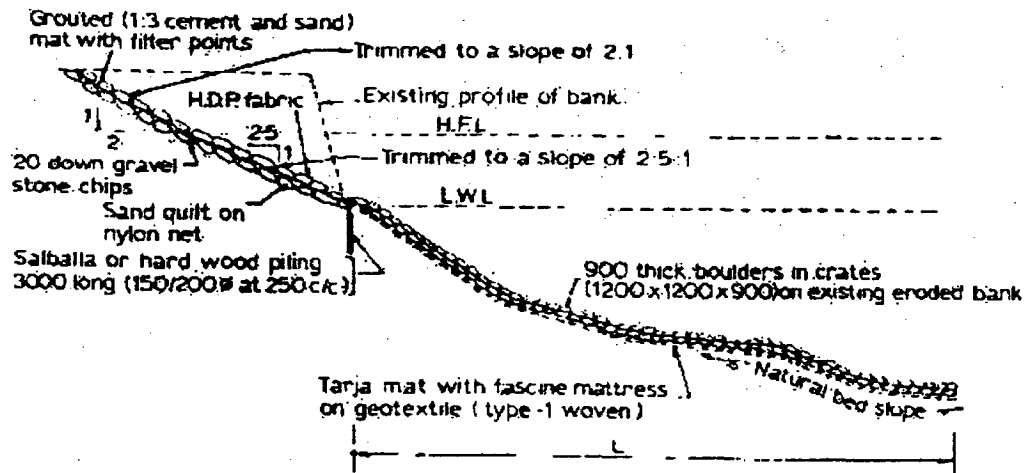


Fig-6.1 Geo-textile in Erosion Control at Farakka (Char et al.1989)

## 6.6 EROSION CONTROL ON SLOPES OF CANALS, RIVER BANKS DRAINS/WATER WAYS.

Erosion control can be accomplished by the following ways.

- Rip rap (broken blocks) or heavy armor stones
- Concrete blocks
- Articulated concrete mattresses
- Gabion mattresses
- Jute bag/synthetic bag filled with cement or soil.

In conventional method, granular filter layer is used between cover layer and sub layer. Geo-textile is good alternative to these filter materials which are difficult and expensive to install especially if this is required to be placed under moving water.

### **6.6.1 Riprap Protection**

Riprap has been described as a layer or facing of rock, dumped or hand-placed to prevent erosion, scour, sloughing of a structure or embankment. Materials other than rock are also referred to as riprap, e.g. rubble, broken concrete slabs and performed concrete shapes (slabs, blocks, rectangular prisms etc.). Riprap is a flexible revetment. Flexibility of the riprap mass is due to individual particles acting independently. The most commonly used, in riverbank protection is bonded riprap laid over geo-textile. This type of riprap is less susceptible to wave induced movement than loose riprap.

### **6.6.2 Concrete Block/Articulated Concrete Mattresses**

Concrete blocks are used in bank protection work. They may be used over geo-textile filter or granular filter. They are placed above water surface and are dumped in the water to make a toe wall and apron. These types of revetment works are extensively used in bank protection works in Bangladesh. Even in dry season, rivers are not dried up. So it is not possible to make toe and apron in the dry condition.

In large rivers, precast concrete blocks held together by steel rods or cables can be used to form flexible articulated mats. Block sizes may vary to suit the contour of the bank. It is particularly difficult to make a continuous mattress of uniform size to fit sharp curves. The open spacing between blocks permits removal of bank material unless a filter blanket of gravel or plastic filter cloth is used underneath. For embankments that are subjected to only occasional flood flows, the spaces between blocks may be filled with earth and vegetation can be established. The articulated concrete is flexible, strong and durable and ensures complete coverage of the riverbank when properly placed.

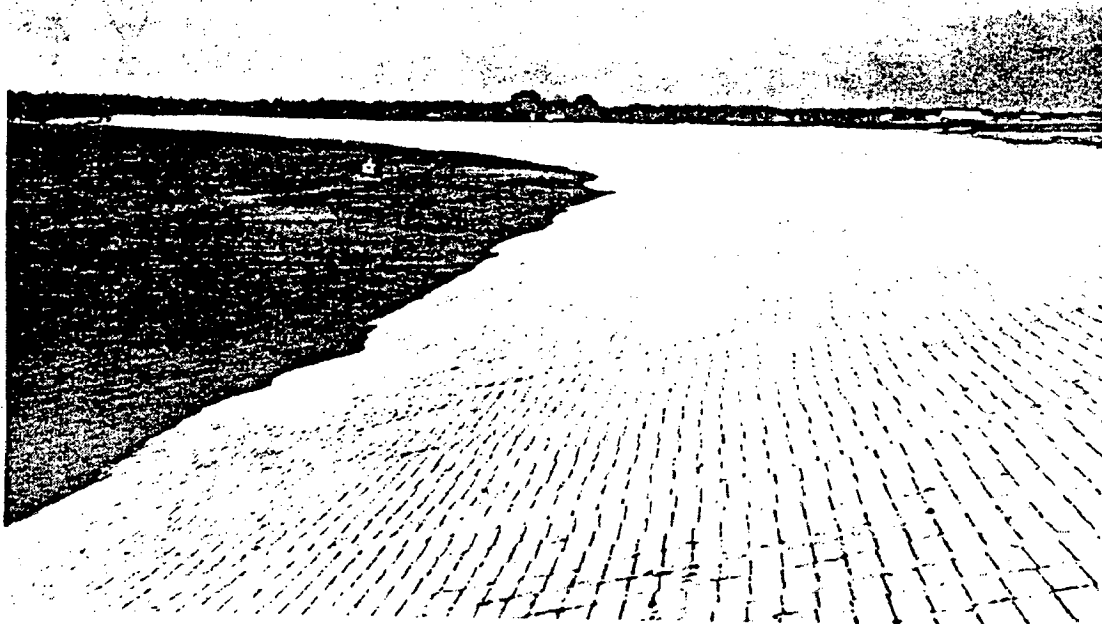


**Fig-6.2 Bank Protected with Articulated Concrete Mattress, Lower Mississippi River. (Source: U.S Army Corps of Engineers, Vicksburg District)**

### **6.6.3 Gabion Protection**

Gabions are mesh baskets, which are filled with relatively small rocks from being washed away by wave action as it completely encases them. These gabion boxes may be used over granular filter or any fabric filter. Box gabions are commonly stacked on relatively steep slope to form a massive structure capable of resisting the forces of both river flows and unstable bank line materials. The flexibility of their mesh and filler stones allows them to maintain their structural integrity even after some degree of displacement, undercutting or settlement. Box gabions structures generally are aligned either along the stream bank toe to form a retaining wall for the bank materials or out from bank to form dikes for diverting flows away from the banks

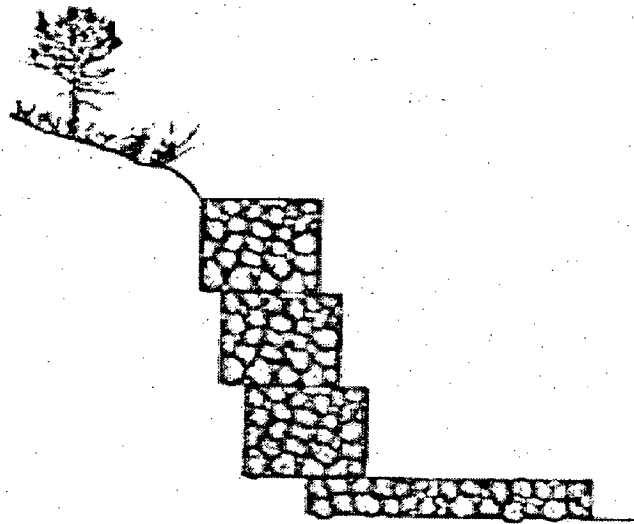


**Fig-6.3 Gabion Boxes in Erosion Control**

**6.6.4 Geo-Jute**

Synthetic geo-textiles have already been widely used in bank protection works but are too costly to be used on a larger scale in developing countries. This is why an indigenous jute geo-textile (geo-jute) comparatively much cheaper and easily available has been substituted in bank protection work on the Hoogly estuary in the state of West Bengal of India. This estuary is plagued by eroding banks of submerged sand flats and numerous unstable inlands, one of which is Nayachara Island. The Western face of this Island has been undergoing severe erosion to deterioration of the navigation channel that leads to the port of Haldia.

**Table-6.1**

**Some physical properties of the Jute Geo-textile**

Material	Mass per Unit area (g/m <sup>2</sup> )	Breaking strength (KN/5cm)		Elongation at break (%)		Pore Size (. m)
		Warp	Weft	Warp	Weft	
Bitumen - Coated Jute geo-textile	1538	1.7	1.4	11.8	13.5	150



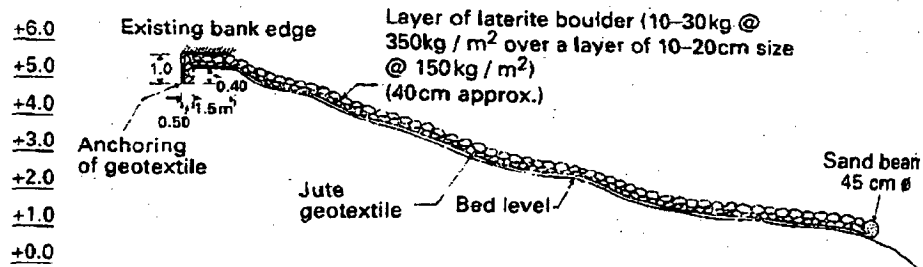


**Fig-6.4 Cross-sectional View of Bank Protection Work using Geo-jute at Hoogly Estuary**



**Fig-6.5 (a) Placement of Riprap over Geo-jute (b) Construction of Toe of the Slope**

### 6.6.5 Synthetic Gunny Bags/Jute Bags

Synthetic bags filled with cement and sand have been used to form revetment. Since jute bags have less longevity, synthetic bags being used instead. These are placed directly on the sloping surface to be protected. This type of protection is used where there is scarcity of riprap. Soil is locally available. That is why protection is also cheap. A soil-cement blanket with 8%-15% cement may be an economical and effective stream bank protection method for use in areas where vegetation is difficult to establish in sandy bank materials. This type of protection has three disadvantages: impermeability, low strength, and susceptibility to temperature variation

Synthetic bag or gunny bag filled with locally available soil are used in closing breach of flood control embankment or to control erosion on an emergency basis. During high flood, generally there is maximum head difference between the water in the river and in the project side, when embankment is breached water with high velocity enters into the project area. With the passage of time, erosion takes place from embankment side and from bottom of streambed. Boulders are required to stop the flow of water. Since boulders are not easily available in alluvial flood plain. Synthetics or jute gunny bags filled with locally available soils have become an economical alternative along with bamboo piling as well as brush wood. For instance, in Bangladesh the same is extensively used in closing of breach in the flood control embankment as well as protecting overtopping of the same.



**Fig-6.6 Sand Cement Bag Revetment (after U.S Army Corps of Engineers, 1981)**

#### **6.6.6 Gabion Mattresses Protection**

Gabion mattresses are flexible version of the boxes. They are used in single layer to form a protective cover to a soil surface. They are most popular all over the world as

or synthetic filter and additional things have been discussed for gabion types of revetment work.

### 7.3 ESTIMATION OF SCOUR

River Engineers have to deal with different types of scour. These are as follows:

- General scour (lowering) of riverbed during flood
- Downstream progressing degradation owing to the removal of sediment from the flow
- Upstream progressing degradation when downstream bed level is lowered i.e. by the drop in level of main river
- Scour due to constriction of river
- Scour due to bend.
- Scour due to local obstruction.

#### 7.3.1 Local Scours Around Bridge Piers

(a) Laursen (1962) formula

$$\frac{b}{D_0} = 5.5 \frac{D_s}{D_0} \left( \frac{1}{11.50} \times \frac{D_s}{D_0} + 1 \right)^{1.7} - 1 \quad (7.1)$$

$D_s$  = Depth of scour below mean bed elevation.

$b$  = width of pier normal to flow.

$D_0$  = Mean depth flow upstream of pier.

(b) Neill (1969) formula

$$\frac{D_s}{b} = 1.5 \left( \frac{D_0}{b} \right)^{0.3} \quad (7.2)$$

(c) Shen et al. (1969) method

$$\frac{D_s}{b} = 3.4(F_0)^{2/3} \left( \frac{D_0}{b} \right)^{1/3} \quad (7.3)$$

$$\text{Where, } F_0 = \frac{u_0}{(gD_0)^{1/2}}$$

$F_0$  = Froude number

$U_0$  = mean upstream velocity

$D_0$  = mean depth flow upstream of pier.

(d) Colorado State University formula reported in Federal Highway Administration manual:

$$\frac{D_s}{D_0} = 2.2 \left( \frac{b}{D_0} \right)^{0.65} (F_0)^{0.43} \quad (7.4)$$

(a) Jain and Fischer (1979)

For Circular Piers

$$\frac{D_s}{b} = 2.0(F_0 - F_c)^{0.25} \left( \frac{D_0}{b} \right)^{0.5} \quad \text{for } F_0 - F_c > 0.2 \quad (7.5)$$

$$\frac{D_s}{b} = 1.84 \left( \frac{D_0}{b} \right)^{0.3} (F_0)^{0.25} \quad \text{for } F_0 > F_c \quad (7.6)$$

For rectangular piers

$$\frac{D_s}{b} = 2.2(F_0 - F_c)^{0.25} \left( \frac{D_0}{b} \right)^{0.5} \quad \text{for } F_0 - F_c > 0.2 \quad (7.7)$$

Where,  $F_c$  is the critical Froude number for incipient sediment motion. For  $0 < (F_0 - F_c) < 0.2$ , the larger value from both formula is used. The procedure for computing  $F_c$  is as follows.

- Determine  $\tau_c$  from the shields diagram based on the estimated median diameter of bed material (Fig.7.1 or Fig-7.2)

- Compute laminar sub-layer thickness  $\sigma$  from equation  $\delta = 11.6 \frac{v}{u_*}$  and obtain the ratio  $\frac{\delta}{d_{50}}$
- Select correction factor X in the logarithmic velocity distribution (Fig.7.3)
- Compute mean critical velocity formula equation.

$$U_c = 2.5 \left( \frac{\tau_c}{\rho} \right)^{1/2} \ln \left( \frac{11.02 D_0 X}{d_{50}} \right) \quad (7.8)$$

- Compute  $F_c$  from  $\frac{U_c}{(gD_0)^{1/2}}$

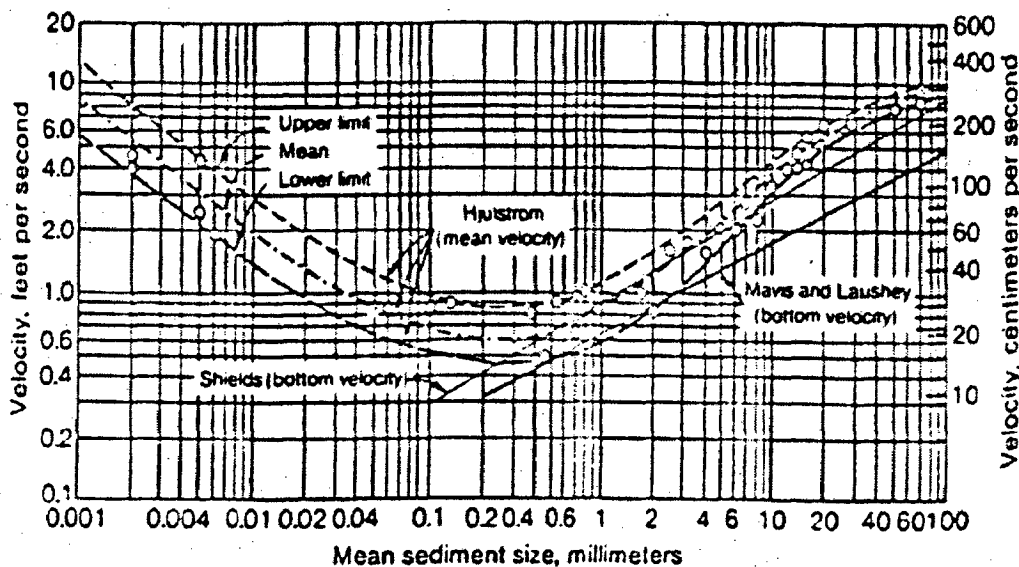


**Fig-7.1 Critical Water Velocity for Quartz Sediment as Function of Mean Grain Size(after ASCE Task Committee,1967)**

Synthetic bag or gunny bag filled with locally available soil are used in closing breach of flood control embankment or to control erosion on an emergency basis. During high flood, generally there is maximum head difference between the water in the river and in the project side, when embankment is breached water with high velocity enters into the project area. With the passage of time, erosion takes place from embankment side and from bottom of streambed. Boulders are required to stop the flow of water. Since boulders are not easily available in alluvial flood plain. Synthetics or jute gunny bags filled with locally available soils have become an economical alternative along with bamboo piling as well as brush wood. For instance, in Bangladesh the same is extensively used in closing of breach in the flood control embankment as well as protecting overtopping of the same.

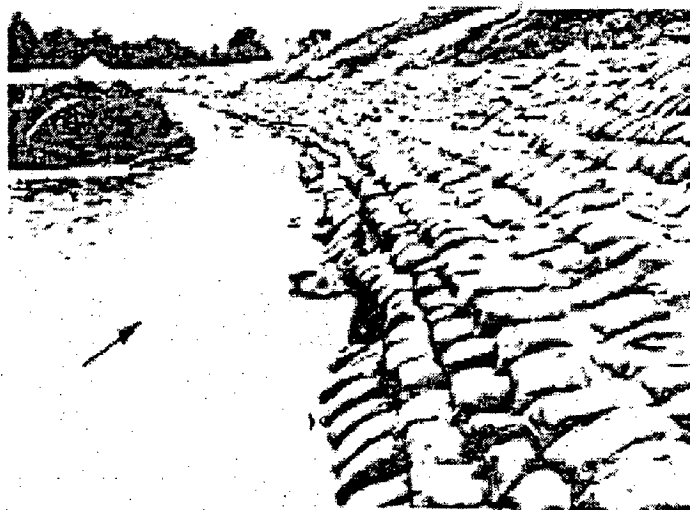


**Fig-6.6 Sand Cement Bag Revetment (after U.S Army Corps of Engineers, 1981)**

#### **6.6.6 Gabion Mattresses Protection**

Gabion mattresses are flexible version of the boxes. They are used in single layer to form a protective cover to a soil surface. They are most popular all over the world as

the Reno mattress. The mattresses are filled in-situ in dry or in shallow (< 0.5 m depth) water. In deeper water, they must be filled prior to placing by crane or sliding into place from tilled platform. Platform may be installed either on the bank or on pontoons. Mattress gabions are shaped into shallow, broad baskets are tied together side by side to form a continuous blanket of protection. They are normally placed on a smoothly graded riverbank slope.

Gabions and mattresses are among the more expensive methods of stream bank erosion protection. However, their record of satisfaction is making them more and more popular.

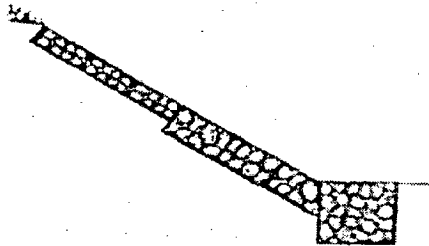


**Fig-6.7 Gabion Mattresses in Erosion Control**

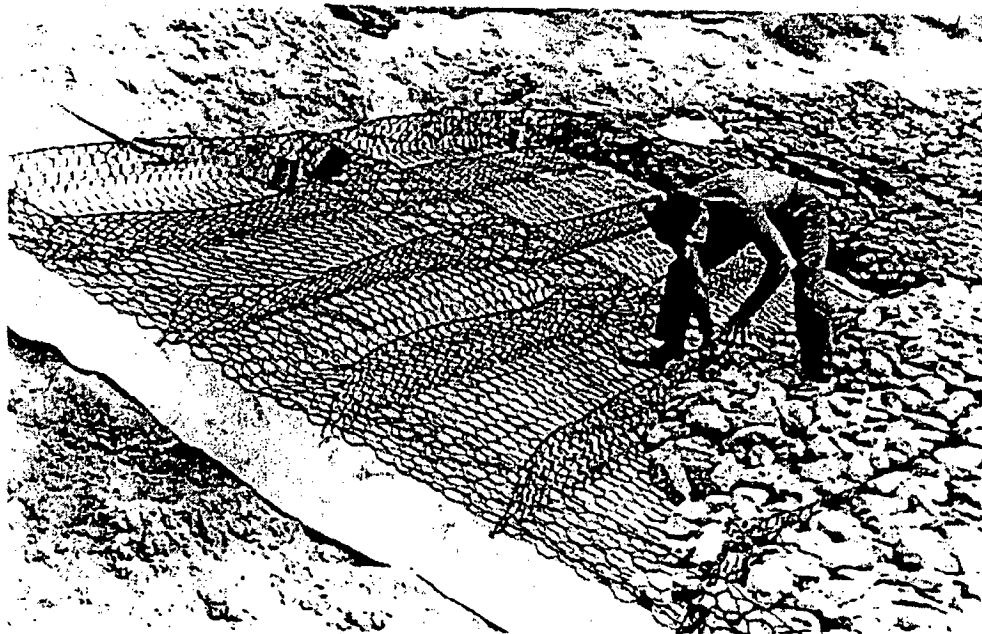


**Fig-6.8 Rock and Wire Mattress Revetment**

## RIVER TRAINING TECHNIQUE

---

### 7.1 GENERAL

In the past, river improvement works were based on observation and practical experience. However, in recent times, a technology based on mathematical and physical sciences has been achieved. These modern tools cannot always guarantee great accuracy in the results of river projects. The effects of engineering projects, which involve important changes in the morphological appearance of a river, may be very difficult to predict. This is because some phenomena in the formation and deformation of river channels are still not yet understood and mathematical models or scale models cannot give fully reliable solutions. Therefore, results so obtained require careful interpretation. In some situations, especially where modern equipment and construction materials are limited the old river regulation techniques are still valuable. Maintenance of the original river having sharp and meanders is difficult, some time impossible.

### 7.2 RIVER REGULATION

The purpose of river training works is to stabilize the channel along a certain alignment with cross-section for one or more of the following objectives.

- (a) Safe and expeditious passes of flood.
- (b) Efficient transportation of suspended and bed load
- (c) Stable river course with minimum bank erosion.
- (d) Sufficient depth and good coarse for navigation
- (e) Direction of flow through a certain defined stretch of river.

The equilibrium of the bed in the longitudinal profile of a river is controlled by the balance between the sediment load contributed to channel and transport capacity of the flow. River training works are required to resist the current and protect the channel against the changes. **In this chapter, design criteria of different types of revetment works in bank protection activity including granular filter as well as**



or synthetic filter and additional things have been discussed for gabion types of revetment work.

### 7.3 ESTIMATION OF SCOUR

River Engineers have to deal with different types of scour. These are as follows:

- General scour (lowering) of riverbed during flood
- Downstream progressing degradation owing to the removal of sediment from the flow
- Upstream progressing degradation when downstream bed level is lowered i.e. by the drop in level of main river
- Scour due to constriction of river
- Scour due to bend.
- Scour due to local obstruction.

#### 7.3.1 Local Scours Around Bridge Piers

(a) Laursen (1962) formula

$$\frac{b}{D_0} = 5.5 \frac{D_s}{D_0} \left( \frac{1}{11.50} \times \frac{D_s}{D_0} + 1 \right)^{1.7} - 1 \quad (7.1)$$

$D_s$  = Depth of scour below mean bed elevation.

$b$  = width of pier normal to flow.

$D_0$  = Mean depth flow upstream of pier.

(b) Neill (1969) formula

$$\frac{D_s}{b} = 1.5 \left( \frac{D_0}{b} \right)^{0.3} \quad (7.2)$$

(c) Shen et al. (1969) method

$$\frac{D_s}{b} = 3.4(F_0)^{2/3} \left( \frac{D_0}{b} \right)^{1/3} \quad (7.3)$$

$$\text{Where, } F_0 = \frac{u_0}{(gD_0)^{1/2}}$$

$F_0$  = Froude number

$U_0$  = mean upstream velocity

$D_0$  = mean depth flow upstream of pier.

(d) Colorado State University formula reported in Federal Highway Administration manual:

$$\frac{D_s}{D_0} = 2.2 \left( \frac{b}{D_0} \right)^{0.65} (F_0)^{0.43} \quad (7.4)$$

(a) Jain and Fischer (1979)

For Circular Piers

$$\frac{D_s}{b} = 2.0(F_0 - F_c)^{0.25} \left( \frac{D_0}{b} \right)^{0.5} \quad \text{for } F_0 - F_c > 0.2 \quad (7.5)$$

$$\frac{D_s}{b} = 1.84 \left( \frac{D_0}{b} \right)^{0.3} (F_0)^{0.25} \quad \text{for } F_0 > F_c \quad (7.6)$$

For rectangular piers

$$\frac{D_s}{b} = 2.2(F_0 - F_c)^{0.25} \left( \frac{D_0}{b} \right)^{0.5} \quad \text{for } F_0 - F_c > 0.2 \quad (7.7)$$

Where,  $F_c$  is the critical Froude number for incipient sediment motion. For  $0 < (F_0 - F_c) < 0.2$ , the larger value from both formula is used. The procedure for computing  $F_c$  is as follows.

- Determine  $\tau_c$  from the shields diagram based on the estimated median diameter of bed material (Fig.7.1 or Fig-7.2)

- Compute laminar sub-layer thickness  $\sigma$  from equation  $\delta = 11.6 \frac{v}{u_*}$  and obtain the ratio  $\frac{\delta}{d_{50}}$
- Select correction factor X in the logarithmic velocity distribution (Fig.7.3)
- Compute mean critical velocity formula equation.

$$U_c = 2.5 \left( \frac{\tau_c}{\rho} \right)^{1/2} \ln \left( \frac{11.02 D_0 X}{d_{50}} \right) \quad (7.8)$$

- Compute  $F_c$  from  $\frac{U_c}{(gD_0)^{1/2}}$

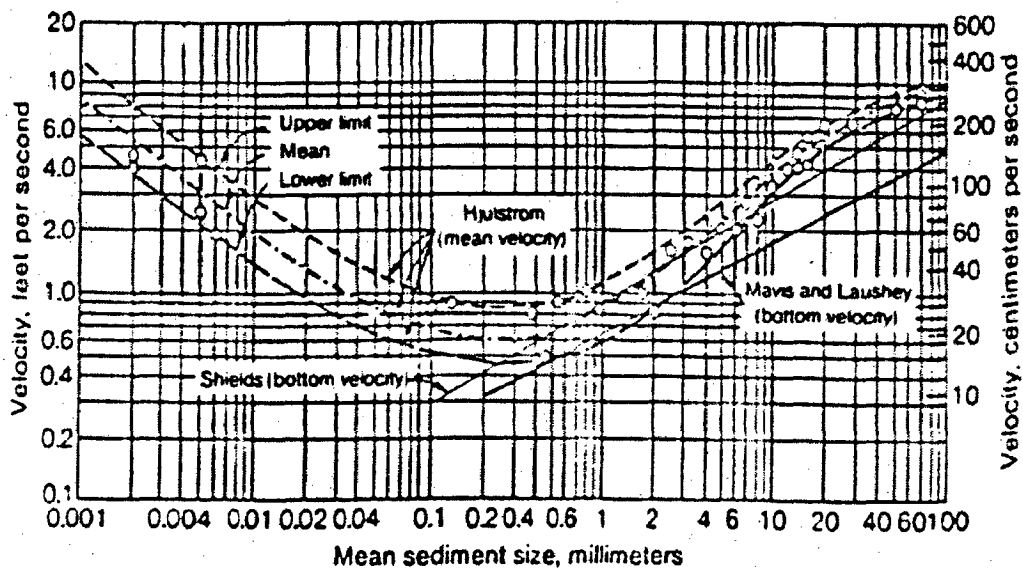


**Fig-7.1 Critical Water Velocity for Quartz Sediment as Function of Mean Grain Size(after ASCE Task Committee,1967)**

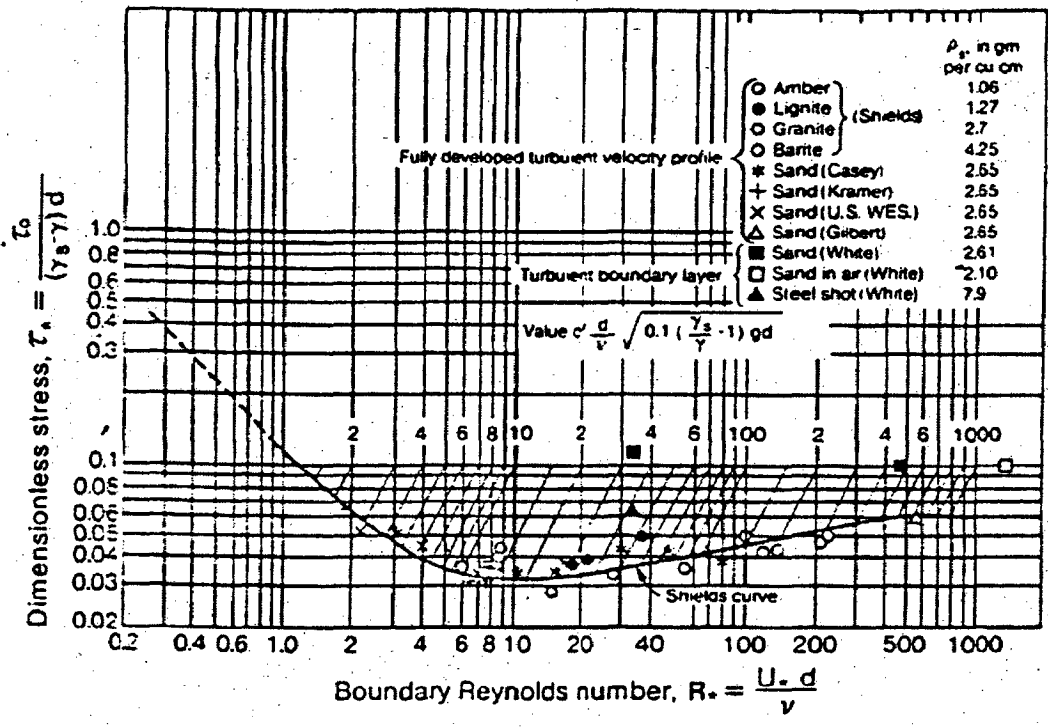


Fig-7.2 Shields Diagram for Incipient Motion

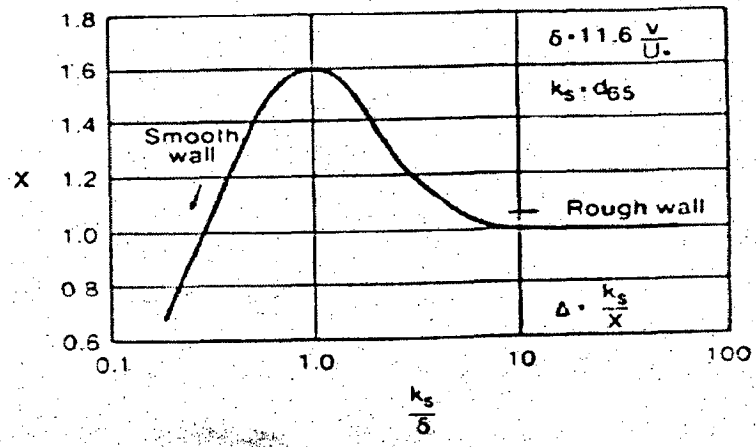


Fig-7.3 Correction Factor in Logarithmic Velocity Distribution (Einstein, 1950)

The scour around bridge piers, abutments, is due to the obstruction of flow. Many formulae have been developed for predicting local scour. Such formulae contain limited number of variables such as flow depth, effective pier width, Froude number, shear stress, and critical shear stress.

### 7.3.2 Local Scour Around Embankments

(a) Liu et.al (1961) presented the following equation for the equilibrium scour depth in sand in subcritical flow

$$\frac{D_s}{D_0} = C \left( \frac{a}{D_0} \right)^{0.40} (F_0)^{0.33} \quad \text{if } 0 < \frac{a}{D_0} < 25 \quad (7.9)$$

$D_s$  = Equilibrium scour depth measured from mean bed level.

$a$  = embankment length normal to the wall of flumes

$D_0$  = approaching depth

$F_0$  = Froude number of the approaching flow

$C = 1.1$  at a spill slope

$C = 2.15$  if the embankment terminates at a vertical wall and has a vertical wall on the upstream side.

(b) Colorado State University (1975) presented the following equation.

$$\frac{D_s}{D_0} = 4(F_0)^{0.33} \quad \text{if } \frac{a}{D_0} > 25 \quad (7.10)$$

Maximum scour depth = equilibrium scour depth + 30% of that

### 7.3.3 Scour Due to Long Constriction

Due to the construction of groynes, bridge crossing, river may experience long constriction and as a result there will be scour.

(a) Komura (1971b) used the following equation for relative depth of scour along the constricted reach with width  $B_1$ , and the water depth  $h$ .

$$\frac{\Delta Z}{h} = (1 + 1.2F^2) \left[ \left( \frac{B}{B_1} \right)^{2/3} - 1 \right] \quad (7.11)$$

$B$  = channel width

$B_1$  = channel width after constriction

$h$  = depth of flow in meter

$F$  = Froude number

$\Delta Z$  = Relative scour depth

(b) Meyer-Peter and Muller's formula developed by Michiue et. al (1984):

$$\frac{\Delta Z}{h} = \left[ \left( \frac{B_1}{B} \right)^{-4/7} - 1 \right] + (0.5)F^2 \left[ \left( \frac{B_1}{B} \right)^{6/7} - 1 \right] \quad (7.12)$$

Notations have the same meaning as in Eq-7.11

(c) Formula proposed by Straub (1934) and developed by Gill (1972):

$$\frac{\Delta Z}{h} = \left( \frac{B_1}{B} \right)^{-6/7} \left[ \left( \frac{B_1}{B} \right)^{-P} \left( 1 - \frac{\tau_c}{\tau} \right) + \frac{\tau_c}{\tau} \right]^{-3/7} - 1 \quad (7.13)$$

$\tau_c$  = critical shear stress of the bed material.

$\tau$  = bed shear stress upstream of the constriction.

$P$  = co-efficient = 2/3

### 7.3.4 Local Scour at Groynes

Copeland (1983) investigated groynes in a concave bend of a meandering stream. Location of groynes within the concave bank is a very important factor, which can lead

maximum scour depth in comparison with a groyne located along a straight reach. After comparison of twenty formulae for scour depth calculation the one suitable for gravel bed rivers is given by Neill (1973, 1980)

$$H' = \frac{2.1 \sim 2.75}{h} \left[ \frac{2.5q^2}{D^{0.318}} \right]^{0.333} \quad (7.14)$$

The range of validity of this equation is

$$0.1 \leq D_{50} \leq 200 \text{ mm}$$

h = depth of flow (m)

D is in mm

q = flow in cumec per meter

### 7.3.5 Estimation of Scour Depth in Alluvial Channel

According to Lacey

$$R = 1.35 \left( \frac{q^2}{f} \right)^{1/3} \quad (7.15)$$

Where, r = depth of scour in meter from top of water surface

q = discharge per meter run

$$f = \text{silt factor} = 1.76 \sqrt{d_{50}}$$

Where,  $d_{50}$  in mm.

Recommended scour depth

**Table-7.1 (Factor for scour depth calculation)**

<b>Reach Type</b>	<b>Factor</b>
Straight reach	1.25 R
Moderate bend	1.50 R
Severe bend	1.75 R
Right angled bend	2.00 R

Depth of scour from minimum bed level of river

$$D = xR - Y$$

Where, x = factor given in the above table depending upon river condition

Y = Depth of flow in meter.

### **7.3.6 Armoring In River Bed**

Armoring of the bed layer refers to coarsening of bed material size because of degradation of well-graded sediment mixtures. The selective erosion of finer particles of bed material leaves the coarser fraction of the mixtures on the bed to induce coarsening of the bed material. When the applied bed shear stress is sufficiently larger to mobilize the larger bed particles, degradation continues; when the applied bed shear stress can not mobilize the coarse bed particles, an armor layer forms on the bed surface. The armor layer becomes coarser and thicker as the bed degrades until it is sufficiently thick to prevent any further degradation. The armor layer is representative of stable bed condition and can be mobilized only during large flood. Three conditions need to be satisfied to form armor layer:

- (1) The stream must be degrading
- (2) The bed material must be sufficiently coarse
- (3) There must be a sufficient amount of bed coarse material



The second condition can be quantified as follows from Shields diagram (Fig-7.2). The incipient condition of motion with  $\tau_{*c} \approx 0.05$  can be rewritten in terms of minimum grain size at the beginning of motion

$$d_{sc} \approx 10hs.$$

Where,  $d_{sc}$  = minimum grain diameter

$h$  = flow depth

$S$  = longitudinal slope of river

The unit of grain size is the same as those of flow depth.

The third condition refers to the fraction of material  $\Delta P_c$  coarser than  $d_{sc}$  available in the bed material. When this percentage is large, armor layer will form rapidly and extent of degradation is minimum.

We can consider that an armor layer of approximately twice the grain size will stabilize the bed. The scour depth  $\Delta z$  that will form an armor layer equal to  $2d_{sc}$  can be estimated from.

$$\Delta z = 2d_{sc} \left( \frac{1}{\Delta p_c} - 1 \right) \quad (7.16)$$

Once an armor layer has formed, it plays a very important role in channel stability and morphology. Indeed the riverbed is stable except under large flood and the armor layer protects the bed against further degradation.

#### 7.4 FLOW RESISTANCE IN RIVER

Flow resistance consists of two components: grain roughness and form roughness. The former is due to the shear force and the latter is due to the pressure difference in the

presence of layer elements. Roughness may be in terms of Manning's n, Chezy's C, friction factor 'f'.

**(a) Strickler's (1923) formula**

$$n = \frac{d_{50}^{1/6}}{21.1} \quad (7.17)$$

Where, d = diameter of uniform sand (m)

**(b) Meyer-Peter and Muller (1948) formula from sand mixtures**

$$n = \frac{(d_{90})^{1/6}}{26} \quad (7.18)$$

$d_{90}$  is the size in meter

In a channel paved with gravel, in the absence of bed forms, resistance may be mainly caused by grain roughness.

**(c) In gravel bed rivers, Federal Highway Administration formula was developed for rock riprap and that is as follows**

$$n = 0.0395(d_{50})^{1/6} \quad (7.19)$$

$d_{50}$  = medium size in feet

**(d) Limerinos formula (applicable in gravel bed river)**

$$n = \frac{0.113h^{1/6}}{1.16 + 2.00 \log\left(\frac{h}{d_{84}}\right)} \quad (7.20)$$

Where, h is the depth of flow in meter

$$(e) \quad n = \frac{0.1134d_a^{0.107}}{0.749 + 1.86 \log\left(\frac{d_a}{d_{50}}\right)} \quad \text{For } 1.5 < \frac{d_a}{d_{50}} < 185 \quad (54) \quad (7.21)$$

$$n = 0.023d_a^{0.167} \quad \text{For } 185 < \frac{d_a}{d_{50}} < 30000 \quad (7.22)$$

Where  $d_a$  = the average channel flow depth (m)

$d_{50}$  = the median bed material size(m)

$$n = 0.3225S_f^{0.38} R^{-0.16} \quad (7.23)$$

Where,  $S_f$  = Friction slope

$R$  = Hydraulic radius in meter

## 7.5 DESIGN OF COVER LAYER

### (A) Requirement due to current attack

Cover layer may be designed on the basis of the following

Velocity of flow

Tractive forces.

In practical field, velocity of flow can be measured easily. This approach is easier but measurement of tractive force is not so easy. Pilarczyk (1985) has given an integrated approach including both velocity and shear stress.

$$D_n = \frac{\phi_c k_T k_h}{\Delta m k_s} \times \frac{0.0035}{\theta_c} \times \frac{v^2}{2g} \quad (7.24)$$

Where,  $D_n$  = Nominal thickness of protection unit (m)

$\phi_c$  = stability factor

= 1.25 (for exposed edges of loose unit)

$\phi_c$  = 1.0 (for exposed edges of block-mats or mattresses)

$\phi_c$  = 0.75 (for continuous protection of loose unit)

$\phi_c$  = 0.50 (for continuous protection of block-mats/mattresses)

$k_T$  = Turbulence factor

$k_h$  = depth and velocity distribution factor

$\Delta m$  = Relative density of protection unit

$k_s$  = slope factor

$\theta_c$  = Critical dimensionless shear stress

$v$  = mean velocity (averaged over the local depth of  $h$  and time (m/s))

For rip-rap (stone/rock must not be too flat)

$$D_n = D_{n50} = (M_{50}/\rho_s)^{0.33} \text{ or } D_{n50} = 0.85 D_{50}$$

$$\Delta = (\rho_s - \rho) / \rho, \quad \rho_s = \text{density of riprap}$$

$\rho$  = density of water

For blocks:  $D_n = D$  = thickness of block

For mattresses (Gabion, stone mattresses)

$D_{n50} = d$ , where  $d$  is the average thickness of the mattresses.

$$\Delta m = \Delta(1 - n), \quad n = \text{porosity of the material inside the gabion.}$$

$k_T = 0.67$  (low turbulence, uniform flow)

$k_T = 1.0$  (normal turbulence in rivers along straight reach )

$k_T = 1.50$  (Non-uniform flow with increased turbulence as below stilling basin, bridge piers, concave bends with  $R_c/B > 2$ )

$k_T = 2.0$  (high turbulence, local disturbances, sharp concave bends  $R_c/B < 2$ , This will be applied only due to difficulties in defining local mean velocity and average mean velocity.

$K_T = 3.0$  (jet impact, screw-race velocity)

For a logarithmic velocity profile over a rough boundary

$$k_h = 2 \left[ \log \left( \frac{12h}{K_r} \right) + 1 \right]^{-2} \quad (7.25)$$

$h$  = Depth of water

$K_r$  = mean equivalent roughness height  $2D_n$  according to Pilarczyk for a non-fully developed velocity profile and rough, porous top-layer (flow passing bottom protection, crest of a dam)  $k_h$  factor can be expressed in more general form,

$$k_h = \left( \frac{h}{D_n} + 1 \right)^{-0.2} \quad (7.26)$$

$$K_s = \sqrt{1 - \frac{\sin^2 \alpha}{\sin^2 \phi}} \quad (7.27)$$

Where,  $\alpha$  = slope angle with horizontal,  $\phi$  = Angle of repose

$\theta_c = 0.035$ , for rip-rap

$\theta_c = 0.06 \sim 0.10$ , for gabions

The return current velocity will attack the lower point of the bank protection of the navigation waterways or a combination of the velocities caused by return current and

discharge. In such cases, according to Isbash formula, necessary diameter can be calculated as

$$D_{n50} = \frac{b}{k_s} \frac{u_b^2}{2g\Delta} \quad (7.28)$$

Where, b = stability factor incorporating turbulence

$$= 0.7 \sim 2.8,$$

b = 1.4 for a major turbulence

$u_b$  = bottom velocity or maximum return current velocity

$k_s$  = slope factor

If the screw-race is likely to cause damage (high turbulence), equivalent (nominal) diameter will

$$D_{n50} \approx \frac{1.3u_b^2}{gk_s\Delta} \quad (7.29)$$

Where,  $u_b$  = Screw – race velocity

According to Maynard (1993) equation for stone size when undermining the stable riprap

$$D_{30} = S_f C_s C_v C_T h \left[ \frac{\sqrt{\Delta U}}{\sqrt{k_1 g h}} \right]^{2.5} \quad (7.30)$$

Where,  $D_{30}$  = rip-rap size for which 30% is finer by weight

$S_f$  = Factor of safety = 1.1 (minimum)

$C_s$  = stability co-efficient for incipient failure = 0.3 for angular rock

= 0.375 for rounded rock

$C_v$  = velocity distribution co-efficient = 1.0 for straight channel, inside of bends

$C_v = 1.283 - 0.2 \log (R/W)$  for out side bends (1 for  $R/W > 26$ )

$C_v = 1.25$  down stream of concrete channels and end of dikes.

$R$  = the center line radius of bends,

$W$  = water surface width at upstream end of bend.

$C_T$  = Blanket thickness co-efficient

$k_1$  = side slope correction factor

$h$  = local depth

$U$  = depth averaged velocity

$\Delta$  = Relative density of rock.

From empirical relationship

$$k_1 = -0.672 + 1.492 \cot(\alpha) - 0.449 \cot^2 \alpha + 0.045 \cot^3 \alpha \quad (7.31)$$

Where,  $\alpha$  is side slope angle with horizontal

**(B) Requirement due to wave attack**

**(a) For Transversal stern waves (Laboyrie, 1986)**

Nominal stone diameter

$$D_{n50} > \frac{Z_{\max}}{1.5 \Delta \cot^{1/3} \alpha} \quad (7.32)$$

$Z_{\max}$  = total height of the transversal stern wave.

- (b) Nominal diameter required for interference peaks caused by secondary ship waves (Pilarczyk, 1985, Verhey, 1986).

$$D_{n50} \geq \frac{H_L \cos^{1/2} \beta}{1.8 \Delta} \quad (7.33)$$

$H_i$  = height of interference peak

$\beta$  = Angle between direction of wave propagation and normal to the bank.

- (c) Nominal diameter required for wind waves

- (i) According to Hudson (1953)

$$D_{n50} = \frac{H}{1.44 \Delta \cot^{1/3} \alpha} \quad (\text{only for regular waves}) \quad (7.34)$$

- (ii) According to Rozanov. et. al (1978)

$$D_{n50} \geq \frac{0.42(TH)^{2/3}}{\Delta(1 + \cot^3 \alpha)^{1/6}} \quad (\text{only for regular waves}) \quad (7.35)$$

H = wave height (regular waves)

T = wave period in second.

- (iii) According to Pilarczyk (1985,1989)

$$D_{n50} > \frac{H_s \sqrt{\xi_p}}{\phi_T \Delta} \quad (\text{for random wind waves}) \quad (7.36)$$

Where,  $H_s$  = significant wave height (m)

$$\text{Wave breaking parameter} = \xi_p = \frac{\tan \alpha}{\left(\frac{H_s}{L_p}\right)^{0.5}} = 1.25 \times T_p \tan \alpha H_s^{-0.5}$$

Where,  $T_p$  = wave peak period in second.



$H_s$  = Significant wave height (m)

$\phi_T$  = Total stability factor or stability function for the beginning of motion.

$\phi_T = 2.0$  for more or less absolute stability

$\phi_T = 2.25$  Loose rocks and stones

$\phi_T = 3.5$  Blocks connected to geotextile by pines

$\phi_T = 4.0$  Grouted blocks connected by geotextile

$\phi_T = 4.5$  Cabled closed blocks.

$\phi_T = 5.0$  Cabled open block; grouted concrete prisms

$\phi_T = 6.0$  Grouted cabled rocks; property design mechanically inter locked blocks.

Pilarczyk (1990) proposed following general design formula

$$\Delta m D_n = \frac{H_s \xi_p^b}{\psi_u \phi_r \cos \alpha} \quad (7.37)$$

or,

$$\frac{H_s}{\Delta m D_n} \leq \psi_u \left( \frac{\phi_r \cos \alpha}{\xi_p^b} \right) \quad (7.38)$$

Where,  $\Delta m$  = Relative density of a system

$D_n$  = Thickness of protection unit (m),

$H_s$  = significant wave height (m)

$\alpha$  = slope angle (deg)

$b$  = exponent related to the interaction between waves and revetment ( $0.5 \leq b \leq$

1.0)

$b = 0.5$  for rough and permeable revetment as rip-rap.

$b = 1.0$  for smooth and less permeable placed-block revetment

$b = 2/3$  for other system.

$\psi_u$  = System –determined (empirical) stability factor

- = 1.00 for riprap cover layer (two layers') and sub-layer granular
- = 1.50 for loose closed blocks  $H_b < 1.5\text{m}$  and sub-layer; geo-textile on sand.
- = 1.50 for loose closed blocks and sub layer; granular
- = 1.50 for blocks connected to geo-textile where sub-layer is granular
- = 2.0 for loose closed blocks  $H_b < 1.5$  where sub-layer is geo-textile.
- = 2~3.0 for gabion/mattresses as a unit where  $H_b < 1.5\text{m}$  and sub-layer geo-textile on sand
- = 2~2.5 stone fill in a basket where  $d_{\text{mini}} = 1.8 D_n$  and sub-layer is clay.

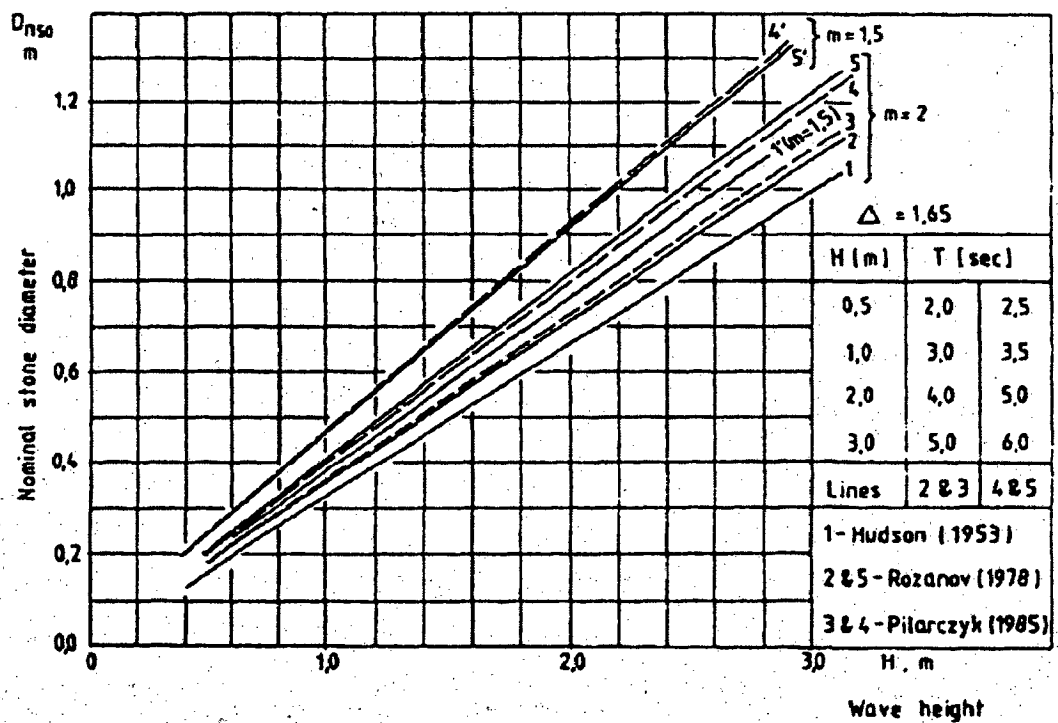
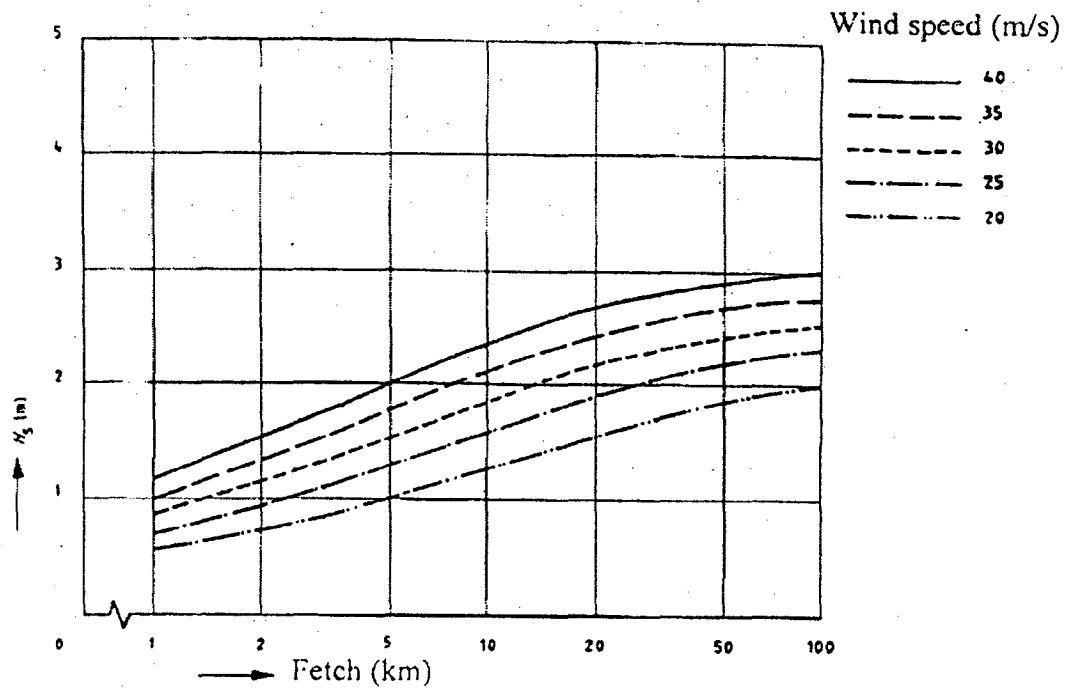
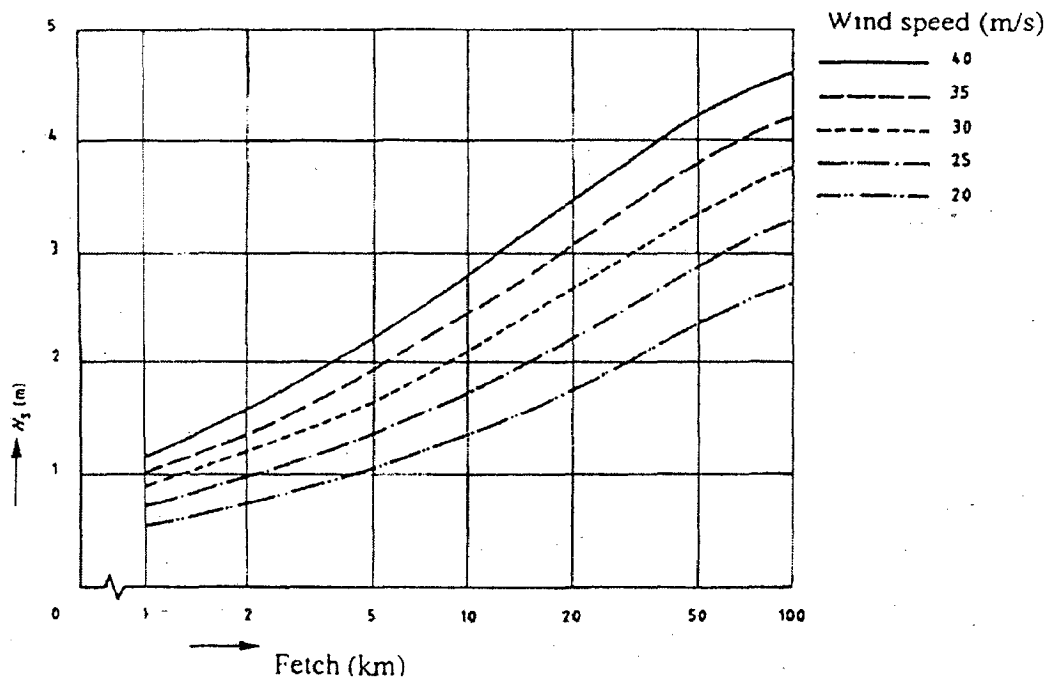


Fig-7.4 Comparison of Nominal Stone Diameter Calculated using Eq.7.34,7.36



**Fig -7.5 Significant Wave Height( $H_s$ ) as a Function of Fetch and Wind Speed with a Mean Water Depth of 10m.**



**Fig-7.6 Significant Wave Height( $H_s$ ) as a Function Of Fetch and Wind Speed with a Mean Water Depth of 20m.**

### 7.5.1 Selection Criteria of Thickness and Stone Size of Riprap

(i) The nominal diameter should be found for each type of current and wave and the greatest value should be finally selected. The riprap protection usually consists of two or three layers of stones. The actual depth of two layers of stones with the nominal diameter equals to  $(1.5\sim 1.8) D_{n50}$ . The total layer thickness must be greater than the largest stone taken. (Pilarczyk, 1985)

(ii) Simons', Li and associates (1982) suggested gradation for riprap. Under this gradation, the ratio of maximum size to median size  $d_{50}$  is about 2.

(iii) Thickness of stone blanket should be at least equal to the maximum stone size or at least 300 mm.

(iv) According to U.S Army Corps of Engineers (1970), thickness should be at least 1.5 times the spherical diameter of the  $W_{50}$  stone.

**Thickness determined by the above considerations should be increased by 50 percent when riprap is placed under water to overcome all uncertainties associated with this type of placement.**

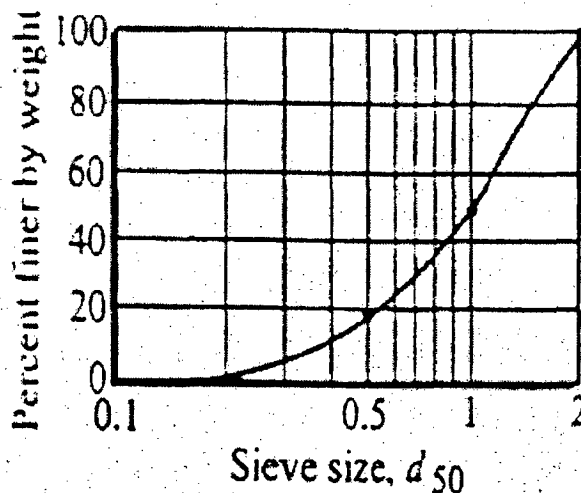


**Fig-7.7 Suggested Riprap Gradation Curve**

According to Scott Brown. A.

Riprap size required to resist particle erosion

$$D_{50} = 0.00594 \frac{V_a^3}{d^{0.5} k_1^{1.5}} \quad (7.39)$$

$D_{50}$  = median particle size to resist -erosion (m)

$V_a$  = average velocity in the main channel (m/s)

$d$  = average flow depth in the main flow channel (m)

$$k_1 = \text{slope correction factor} = \left[ 1 - \frac{\sin^2 \theta}{\sin^2 \phi} \right]^{0.5}$$

Shear stress approach (Lane's formula)

$$d_m = \frac{\tau_0}{\tau_{*c} (\gamma_s - \gamma) \left[ \cos \theta_1 \sqrt{1 - \frac{\tan^2 \alpha}{\tan^2 \phi}} \right]} \quad (7.40)$$

Where  $d_m$  = Effective size (m)

$\tau_0$  = Applied shear stress (N/m<sup>2</sup>)

$\tau_{*c}$  = Critical value of Shield number

$$\eta = \cos \theta_1 \sqrt{1 - \frac{\tan^2 \alpha}{\tan^2 \phi}}$$

$$\tau_0 = \gamma h s$$

### Velocity approach

On a side slope without secondary current the critical flow velocity  $V_c$  can be approximated by the following,

$$V_c = K_c \sqrt{2(G-1)gd_s} \left[ 1 - \frac{\sin^2 \theta_1}{\sin^2 \phi} \right]^{\frac{1}{4}} \quad (7.41)$$

With Critical velocity for the reach under study and slope 1:2  
Using graph (Fig-8,8) one can get value of  $d_s$ .

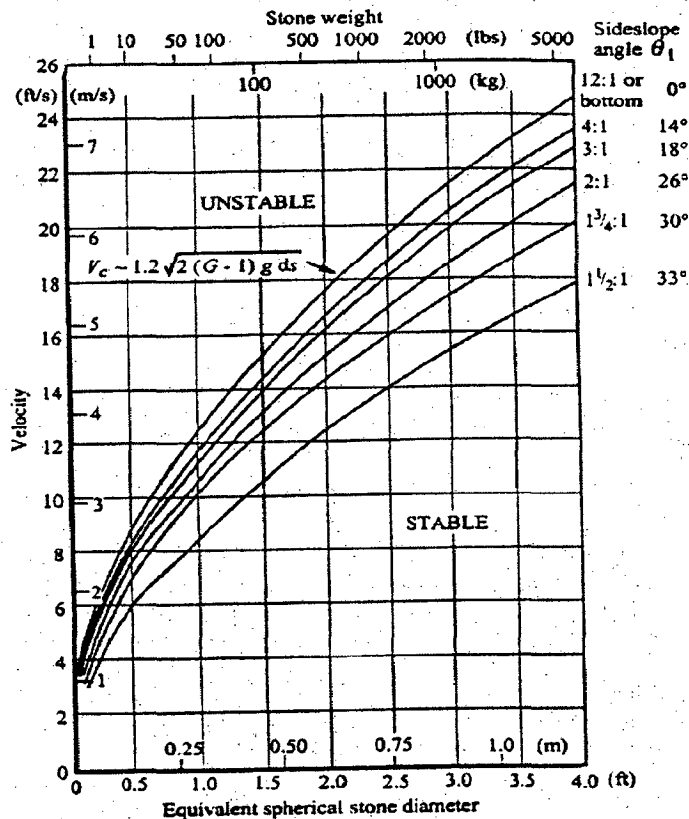


**Fig-7.8 Particle-stability Diagram**

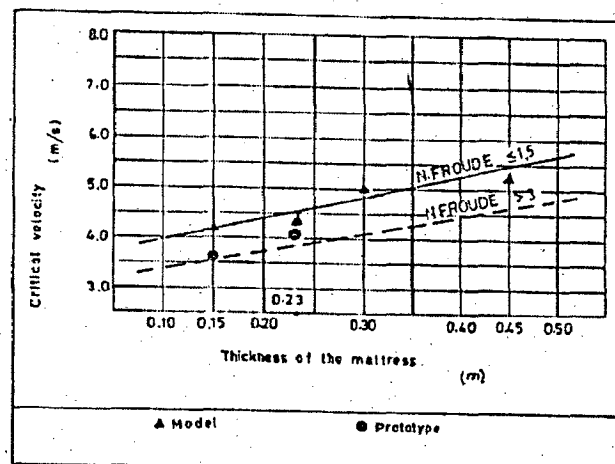
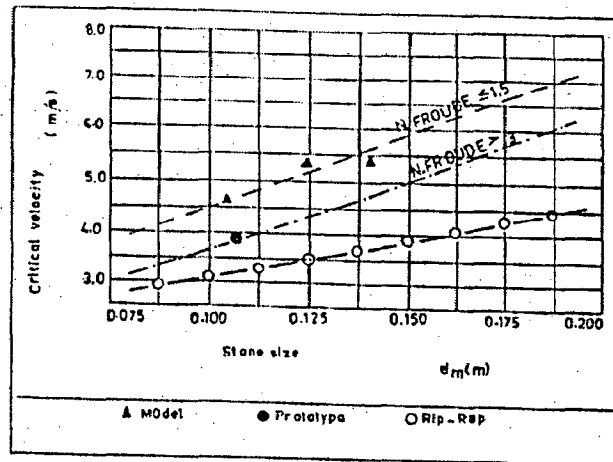


**Fig-7.9 Gabion Stone Size and Mattress Thickness Related to Velocity**  
 (Source: Maccaferri Flexible Reno mattress and Gabion linings)

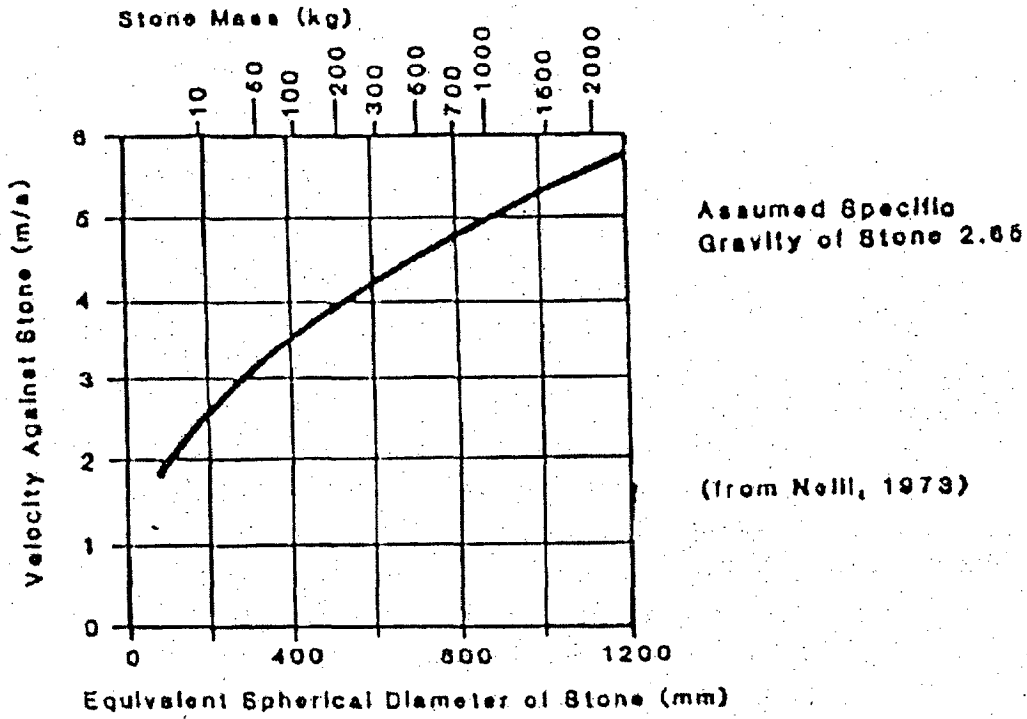


Fig-7.10 Neill's Curve for Size of Riprap Stone

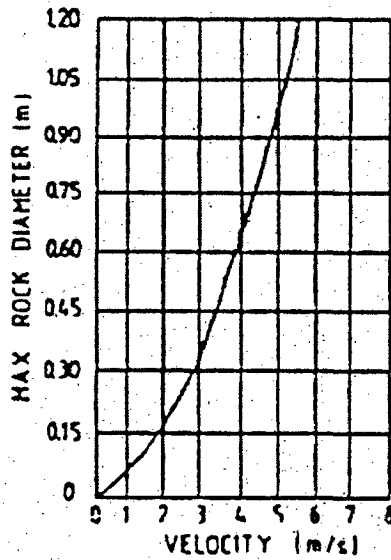


Fig-7.11 Maximum Stone Size for Riprap, according to USBR



**Escarameia and May(1992)-HR Wallingford**

$$D_{n50} = C \frac{U_b^2}{2g(S-1)} \quad (7.42)$$

$D_{n50}$  = Characteristic size of stone

$$= \text{Size of equivalent cube} = \left( \frac{w_{50}}{\rho_s} \right)^{\frac{1}{3}}$$

$w_{50}$  = Weight of particle

$\rho_s$  = Density of stone

$C = 12.3TI - 0.2$ ,  $TI = \text{Turbulence Intensity} = 0.2 < 0.5$

$$U_b = (-1.48 \times TI + 1.04) \times U_d \quad \text{for } TI < 0.5 \quad (7.43)$$

where,  $U_d$  = depth averaged velocity

$TI$  = Turbulence intensity

$U_b$  = Velocity near the bed (10% of the flow depth above bed)

$$U_b = (-1.48 \times TI + 1.36) \times U_d \quad \text{for } TI > 0.5 \quad (7.44)$$

**Table -7.2**

**Values of 'C' for use in Escarameia and May,s (1992) equation**

Type of revetment	Value of 'C'	observation
(i) Riprap	$12.3TI - 0.2$	Valid for $TI < 0.5$ and for design of bed and bank protection on slopes of 1:2 or flatter
(ii) Loose or interlocking	$9.22TI - 0.15$	Valid for $TI < 0.5$ and for design of bed and bank protection on slopes of 1:2.5 or flatter
(iv) Concrete blocks		
(v) Gabion Mattress	$12.3TI - 1.65$	Valid for $TI < 0.2$ and for design of bed and protection on slopes of 1:2 or flatter

## 7.6 DESIGN CRITERIA OF FILTER LAYER IN RIVER TRAINING WORK

The main function of filter is to retain the subsoil without generating excessive pore water pressure. This may act as a separation of layers as well as soil reinforcement. The pore size of fabric filter should be such that it will allow the pore water to pass through but not the subsoil particle. So the fabric must be soil light and permeable during its whole lifetime.

### 7.6.1 Soil Tightness

For uniformly graded soil, the fabric maximum pore size  $O_{90} < D_{90}$ . The filter criteria suggested by Ingold (1984) are

For  $1 < Cu < 50$

$$\frac{O_{90}}{D_{50}} = 2Cu \exp\left(1 - \frac{\sqrt{2}}{Cu}\right) \quad (7.45)$$

where  $Cu = \frac{D_{60}}{D_{10}}$  is the Co-efficient of non-uniformity.

For  $Cu < 5$

$$O_{90} < D_{90} \quad (7.46)$$

For  $5 < Cu < 50$

$$\frac{O_{90}}{D_{90}} = 2Cu \exp\left(0.2 - \frac{\sqrt{2}}{Cu}\right) \quad (7.47)$$

for non-cohesive soils containing more than 50% by weight of silt  $O_{90} < 0.2$  mm. Under cyclic hydraulic loads the fiber filter should retain as small particle as  $D_{15}$

### 7.6.2 Permeability

The permeability of geotextile is often characterized by the permittivity which may be defined as the seepage velocity per hydraulic head difference. The permittivity of a geotextile of thickness  $T_g$  can be expressed in the form.

$$\Psi = \frac{k}{T_g} \quad (7.48)$$

Where,  $k$  = Permeability Co-efficient

$T_g$  = thickness

$\Psi$  = Permittivity.

This should be in the range of  $10^{-2}S^{-1}$  to  $10S^{-1}$ .

For preliminary design the head loss is often taken as  $h = 0.1m$ . For this value the required permittivity of fabric should be

$$\Psi > 10 k_s i \quad (7.49)$$

Where,  $k_s$  = co-efficient of soil permeability,  $i$  = hydraulic gradient

Introducing clogging, blocking, compressibility of fabric

$$\Psi > (10^2 - 10^4) k_s i \quad (7.50)$$

When the hydraulic gradient in the sub soil is not known, it is possible to choose more simplified method

$$\eta k_g > k_s \quad (7.51)$$

$\eta$  = Reduction factor

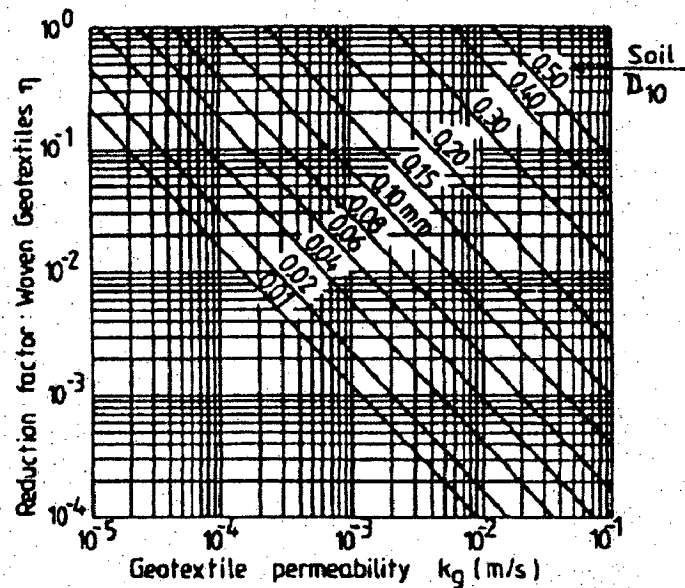


Fig-7.12 Reduction Factor  $\eta$  in Eq. 8.5 (after Veldhuijzen van Zanten et al.,1986)

### 7.6.3 Selection Criteria of Granular Filter

The requirements for granular filter developed by Terzaghi and latter on extended by U.S. Corps of Engineers at Vicksburg. This is presented below.

$$\frac{D_{15} \text{ filter}}{D_{85} \text{ soil}} < 5 \quad \text{Retention Criteria}$$

$$\frac{D_{50} \text{ filter}}{D_{50} \text{ soil}} < 25 \quad \text{Uniformity Criteria}$$

$$4 < \frac{D_{15} \text{ filter}}{D_{15} \text{ soil}} < (20 - 40) \quad \text{Permeability criteria}$$

While designing the filter the above criteria should be fulfilled. Size of filter will be determined from above conditions.

### 7.6.4 Thickness of Filter Layer

There is no hard and fast rule for determination of maximum thickness of filter layer. Most filters are constructed with thickness ranging from 200mm to 750mm. Following factors should be considered in determining thickness.

(a) Wave Action

Less wave in the river needs less thickness to layer.

(b) Gradation of riprap

If riprap is well graded with plenty of fines to fill the larger voids, there may be less thickness of filter layer.

(c) Gradation of bank material

If bank material is well graded with a clay binder, it needs less thickness of filter. If more than one filter layer is required, the same criterion is followed, the finer filter is considered as the base material for selection of the coarser filter. Horizontal filter may be of less thickness than the steeper one, minimum thickness is 150mm for sand and 300mm for gravel, in this case, if the filter contains excessive fines or coarse materials such that

$$\frac{D_{15}(\text{filter})}{D_{15}(\text{base})} > 4 \text{ but } < 5$$

$$\frac{D_{15}(\text{filter})}{D_{85}(\text{base})} > 5 > 6 \text{ the thickness}$$

Filter layer may be increased by 50 percent.

**According to Chang. H.**

The thickness of filter material ranges from 150mm to 380mm for a single layer or from 100mm to 200mm for individual layers of a multiple layer blanket.

## 7.7 DESIGN OF APRON IN BANK PROTECTION WORK

Design of apron depends on the scour depth. The following steps are followed in the design of apron.

- (1) Determine the thickness of cover layer; it may be of riprap, gabion or concrete block.
- (2) Determine the volume of material per meter run. This is calculated assuming that the apron will be launched at a slope 2:1 in gravel/sand bed, and in case of

concrete block it will be launched at a slope of 1 ½ : 1. So for unit meter thickness of apron,

For sand/gravel volume =  $\sqrt{5} \times \text{Depth of scour} \times \text{cover layer thickness} = \text{m}^3/\text{r.m}$

For concrete block volume =  $\sqrt{3.25} D \times \text{cover layer} = 1.8 D \times \text{cover layer}$ .

According to USBR  $V = 4.915 d^{1/2}$

Where,  $V = \text{Mean velocity of flow (m/s)}$

$D = \text{mean diameter of stone (m)}$

Blench recommended that thickness of apron should be (1.5~2) times the mean diameter of stone

According to Ahmad (1953)

Length of apron =  $L_a = 1.5 D$

$D = \text{Depth of scour}$ .

The apron thickness = 1.5 x thickness of the cover layer.

In case of dry streambed, edge of cover layer is protected by the toe trench. In designing, these estimates of scour depth are needed so that protective wall may be placed sufficiently below the streambed to prevent undermining. Depth of toe depends on the size of cover layer.

Toe depth is calculated as

$$d_s = 3.66 \text{ for } D_{50} < 0.0015\text{m} \quad (7.52)$$

$$d_s = 1.74 \overline{D}_{50}^{0.11} \text{ for } D_{50} > 0.0015\text{m} \quad (7.53)$$

Where  $d_s = \text{Anticipated depth of scour (m)}$

$D_{50} = \text{median diameter of bed material (m)}$ .

Slope of the toe trench may be 1:1.

### CASE STUDY

---

#### 8.1 PROBLEM OF PRESENT CASE STUDY

The Beas River originates from Beas Kund about 20 km upstream from Nehrukund. The total drop in bed elevation over a distance of 4.225 KM. in the river reach is 205.40 m and average slope is 0.0486 i.e. 1 in 20. As the river runs downstream, its slope becomes flatter. In the downstream it has got the uniform slope of 0.04 i.e. 1 in 25. This slope is considered in the present study reach near SASE, Manali.

Beas River near DRDO Guest House, Manali at SASE (Himachal Pradesh) India has been experienced severe erosion problem in the left bank. The river is snow-fed and its catchment at the inlet of study reach is about 325sq.km. It was found from local enquiry that the river bed has been continuously aggrading amounting to approximately five meters. In recent years, the channel has started migrating from one side to the other.

In the study reach, crates filled with stones were placed on the slope of the left bank as a protection measure. Now due to high velocity during high flood, river bed close to the crate work has been eroded. In some places scour is so intensive that crates work have slid into the river. As a remedial measure, apron has to be designed to prevent the sliding down of crate work.

## 8.2 ESTIMATION OF DESIGN FLOOD

31 years flood data of the Beas at Manali is available. To get flood discharge of 2yrs and 100yrs return period, frequency analysis has been done as given below.

**Table-8.1(Frequency Analysis)**

Year	Flow in cfs	Flow in cumec (X)	Y=logX	$(Y - \bar{Y})^2$	$(Y - \bar{Y})^3$
1965	4568	129.453	2.112	0.009	-0.001
1966	9093	257.687	2.411	0.042	0.008
1967	6734	190.835	2.281	0.005	0.000
1968	5526	156.602	2.195	0.000	0.000
1969	5716	161.986	2.209	0.000	0.000
1970	5328	150.990	2.179	0.001	0.000
1971	5655	160.257	2.205	0.000	0.000
1972	12351	350.016	2.544	0.113	0.038
1973	11343	321.450	2.507	0.090	0.027
1974	8133	230.481	2.363	0.024	0.004
1975	11921	337.830	2.529	0.103	0.033
1976	10072	285.431	2.456	0.062	0.015
1977	10200	289.058	2.461	0.064	0.016
1978	6540	185.337	2.268	0.004	0.000
1979	4566	129.396	2.112	0.009	-0.001
1980	5150	145.946	2.164	0.002	0.000
1981	1850	52.427	1.720	0.238	-0.116
1982	4348	123.218	2.091	0.014	-0.002
1983	3200	90.685	1.958	0.062	-0.016
1984	3380	95.786	1.981	0.051	-0.012
1985	4590	130.076	2.114	0.009	-0.001
1986	7240	205.175	2.312	0.011	0.001
1987	2350	66.597	1.823	0.147	-0.057
1988	5660	160.399	2.205	0.000	0.000
1989	6120	173.435	2.239	0.001	0.000
1990	4125	116.899	2.068	0.019	-0.003
1991	2910	82.467	1.916	0.085	-0.025
1992	2770	78.499	1.895	0.098	-0.031
1993	7095	201.066	2.303	0.009	0.001
1994	6065	171.876	2.235	0.001	0.000
1995	13200	374.075	2.573	0.134	0.049
	197799	5605.435	68.429	1.407	-0.068
<b>Total</b>		<b>180.8204977</b>	<b>2.207375758</b>		



For sample size  $n=31$  mean value for log series= $\bar{Y}$

$$\bar{Y} = \frac{1}{n} \sum_{i=1}^n Y_i = \frac{68.429}{31} = 2.207$$

For original series

$$\bar{X} = \frac{1}{n} \sum_{i=1}^n X_i = \frac{5605.435}{31} = 180.82$$

Standard Deviation  $S_y$  is given by the formula

$$S_y = \left[ \frac{1}{n-1} \sum_{i=1}^n (Y_i - \bar{Y})^2 \right]^{\frac{1}{2}}$$

$$S_y = \left[ \frac{1}{(31-1)} (1.407) \right]^{\frac{1}{2}}$$

$$= 0.21656$$

Coefficient of Skewness

$$C_s = \frac{n \sum_{i=1}^n (Y_i - \bar{Y})^3}{(n-1)(n-2)(S_y)^3}$$

$$= \frac{31 * (-0.068)}{30 * 29 * (0.2165)^3}$$

$$= -0.25$$

(1) Log normal distribution

$$S_y = 0.2166$$

$$C_s = -0.25$$

$$T = 100 \text{ ys}$$

$$P = \frac{1}{T} = \frac{1}{100} = 0.01 \quad [0 \leq P \leq 0.50]$$

$$\omega = \left[ \ln \left( \frac{1}{P^2} \right) \right]^{1/2} = \left\{ \ln \left( \frac{1}{(0.01)^2} \right) \right\}^{1/2} = 3.0348$$

$$K_T = Z = \omega - \left[ \frac{2.515517 + 0.802853\omega + 0.010328\omega^2}{1 + 1.432788\omega + 0.189269\omega^2 + 0.00130\omega^3} \right]$$

$$= 2.596723$$

$$y_{100} = \bar{y} + K_{100} S_y$$

$$= \bar{y} + 2.596723 \times 0.2166 = 2.207446 + 0.56246$$

$$= 2.76989$$

$$X_{100} = 10^{2.76989}$$

$$X_{100} = 588.70 \text{ m/s}$$

For return period,  $T = 2$  yrs.

$$P = \frac{1}{T} = \frac{1}{2} = 0.50$$

$$\omega = \left\{ \ln \left( \frac{1}{P^2} \right) \right\}^{1/2} = 1017741$$

Similarly

$$k_2 = Z = 0$$

$$y_2 = \bar{y} + k_2 S_y$$

$$= \bar{y} + 0 \times 0 = \bar{y} = 2.207446$$

$$X_2 = (10)^{2.207446} = 161.23 \text{ cumec}$$

(2) Log Pearson type-III

$$\bar{y} = 2.207$$

$$S_y = 0.2165$$

$$C_s = -0.25$$

(a)  $T = 2$  yrs

$$P = \frac{1}{T} = \frac{1}{2} = 0.50 \quad 0 \leq P \leq 0.50$$

Here  $C_s \neq 0$  so

$$K_2 = Z + (Z^2 - 1)K + V_3(Z^3 - 6Z)K^2 - (Z^2 - 1)K^3$$

$$+ ZK^4 + \frac{1}{3}K^5$$

Where  $K = \frac{C_5}{6} = -0.04012257$

$$\omega = \left\{ \ln \left( \frac{1}{0.5^2} \right) \right\}^{1/2} = 1.17741$$

$$Z = 1.17741 - \left[ \frac{2.515517 + 0.802853\omega + 0.010328\omega^2}{1 + 1.432788\omega + 0.189269\omega^2 + 0.001308\omega^3} \right] = 0$$

$$\therefore K_2 = 0.04012257 - 0.00006459 - 3.4659 \times 10^{-8} = 0.040058$$

$$y_2 = \bar{y} + k_2 S_y = 2.207446 + 0.040058 \times 0.216549 = 2.21612$$

$$X_2 = 164.48 \text{ cumec}$$

(b)  $T = 100 \text{ yrs}$

$$P = \frac{1}{T} = 0.01 \quad (0 \leq P \leq 0.50)$$

Here  $C_s \neq 0$  So,

$$k_{100} = Z + (Z^2 - 1)K + \frac{1}{3}(Z^3 - 6Z)K^2 - (Z^2 - 1)K^3 + ZK^4 + \frac{1}{3}K^5$$

$$K = \frac{C_5}{6} = -0.04012257$$

$$\omega = \left\{ \ln \left( \frac{1}{(0.01)^2} \right) \right\}^{1/2} = 3.0348$$

$$Z = 2.596723$$

$$K_{100} = 2.596723 - 0.2304227 + 0.001035269 + 0.00106636 \\ + 0.000006729 - 3.4659 \times 10^{-8} \\ = 2.3684$$

$$Y_2 = 2.207 + 2.36 \times 0.2165 = 2.72 \text{ cumec}$$

$$X_2 = 525.19 \text{ cumec}$$

(iii) Extreme Value Distribution

$$T = 2 \text{ yrs}$$

$$T = \frac{1}{P} = \frac{1}{0.5} = 0.5 \quad (0 \leq P \leq 0.5)$$

$$K_T = -\frac{\sqrt{6}}{\pi} \left[ 0.5772 - \ln \left\{ \ln \left( \frac{T}{T-1} \right) \right\} \right]$$

$$= -\frac{\sqrt{6}}{\pi} \left[ 0.5772 + \ln \left\{ \ln \left( \frac{2}{2-1} \right) \right\} \right]$$

$$K_2 = -0.164272$$

$$K_{100} = -\frac{\sqrt{6}}{\pi} \left[ 0.5772 + \ln \left\{ \ln \left( \frac{100}{100-1} \right) \right\} \right]$$

$$= 3.13668$$

$$X_2 = \bar{x} + k_2 S = 180.85 + (-0.164272 \times 86.95)$$

$$X_2 = 166.56 \text{ cumec}$$

$$X_{100} = \bar{x} + k_{100} S$$

$$= 180.85 + 3.13668 \times 86.95$$

$$= 453.61 \text{ m}^3/\text{s}$$

Frequency	Type Of Distribution		
	Log normal	Log pearson type-III	Extreme value distr.
2	161.23 cumce	164.48 cumec	166.56 cumec
100	588.70 cumce	525.10 cumec	453.61 m <sup>3</sup> /s

Hence log normal distribution gives maximum flood of 588.70 cumce discharge which can be treated as design flood.

### 8.3 HYDRAULICS OF BEAS RIVER

The flow in gravel bed Rivers is different from those flowing in plains. This is due to roughness of steep slope, high roughness co-efficient due to presence of big boulders, geologically influenced boundary conditions and high sediment inflow mass including big boulders.

In gravel bed rivers, flow velocity is generally high, turbulent and supercritical. Hydraulic jump formation is found in many locations within a short reach, whereas in rivers flowing in plain, the flow velocity is low, less turbulent and subcritical. Hydraulic jump is rear. Due to these reasons, hydraulic of mountain rivers is more difficult to understand.

To calculate Manning's roughness co-efficient, bed material distribution curve (Fig-8.1) of the river has been used.

$$n = \frac{(D_{50})^{\frac{1}{5}}}{21} = \frac{(0.70)^{\frac{1}{5}}}{21} = 0.045$$

To study the hydraulic profile of the river flow such as depth, top width, water surface level and energy level in different sections, one-dimensional program called HEC-6 has to be used. Since cross-sectional data is not available, we can take these results from previous study. In the present case 100 yrs discharge from distribution has been found as 588.7 cumec. In the previous study, river simulation (with dyke) has been carried out by HEC-6 considering 515.8 cumec as design discharge. River simulation (with dyke) result is as follows:

**In the study reach**

**For down stream section,**

HFL=1970.90m

EL=1971.37m

Velocity head= 0.47m

Top width =173.56m

Velocity=3.04m/s

**Upstream section,**

HFL= 1987.86m

El =1988.52m

Velocity head=0.66m

Top width=97.74m

Velocity=4.3m/s

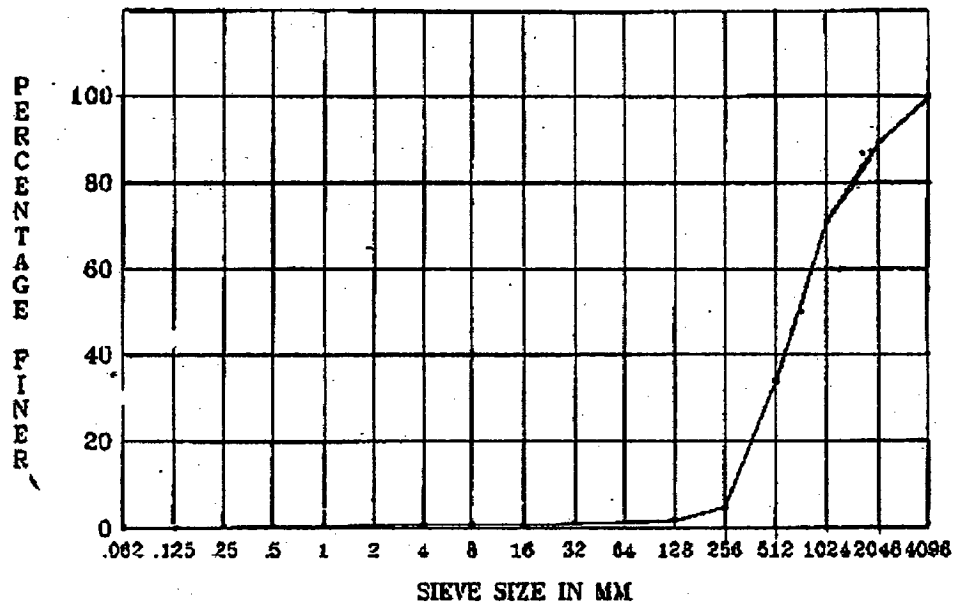


**Fig-8.1 Grain Size distribution Curve for Bed material**

**8.4 DESIGN OF EMBANKMENT (DETERMINATION OF CREST LEVEL) ALONG THE LEFT BANK OF RIVER**

At chainage 1000m

For flood of hundred year return period,  $Q_{100}=515.8\text{cumec}$

Bed level=1985.00m

HFL =1987.88m

$B_T$ = Top width of the river section (m)

$V=4.3\text{ m/s}$

In order to determine the height of required bank protection, super-elevation due to flow ( $Q_{100}$ ) in the curve is

$$Z = \frac{V^2 B_T}{g r_c} = 1.84\text{m}$$

(For average radius of curvature,  $r_c=100\text{m}$ )

Level of bank protection=1987.88+1.84=1989.7m

Considering Free board as 1.5m Top of

embankment=1989.7+1.5=1991.2m

## 8.5 DESIGN OF PROTECTIVE MEASURES IN SLOPE AND IN RIVER BED

### 8.5.1 Design of Rip-rap Cover Layer in Beas River (near chainage 1000 m)

Hydraulic Data

$$Q_{100} = 515.80 \text{ m}^3/\text{s}$$

$$\text{Av. velocity} = 4.30 \text{ m/s}$$

$$\text{Top width } B_T = 97.74 \text{ m}$$

$$\text{Energy level} = 1988.52 \text{ m}$$

$$\text{Flood level} = 1987.86 \text{ m}$$

$$\text{Bed level} = 1985.00 \text{ m}$$

$$\text{Normal depth of flood } h = 1987.86 - 1985.00 = 2.86 \text{ m}$$

$$\text{Area of flow } A = 119.95 \text{ m}^2$$

$$\text{Hydraulic mean depth} = R_n = \frac{A}{B_T} = \frac{119.95}{97.74} = 1.23 \text{ m}$$

$$\text{Energy slope (Assuming uniform flow conditions)} = 0.04$$

Average bed shear stress is given by

$$\tau = \gamma R_n S \text{ (N/m}^2\text{)}$$

$$= 9810 \times 1.23 \times 0.04 = 482.65 \text{ N/m}^2 \approx 483 \text{ N/m}^2$$

$$\text{Froude number.} = F = \frac{V}{\sqrt{gR_n}} = \frac{4.30}{\sqrt{9.81 \times 1.23}} = 1.24$$

(a) Thickness of cover layer for riprap protection according to Pilarczyk (1985)

$$D_n = \frac{\phi_c K_T K_h}{\Delta m k_s} \times \frac{0.035}{\theta_c} \times \frac{V^2}{2g}$$

Where  $\phi_c = 0.75$  (for stone rip-rap)

$K_T = 2.50$  (for high turbulent)

$$K_h = 2 \left[ \log \left( \frac{12 \times h}{K_r} \right) + 1 \right]^{-2}$$

$K_r =$  mean equivalent roughness height

$$= 1.50 \text{ m}$$

$$h = 2.86$$

$$K_n = 2 \left[ \log \left( \frac{12 \times 2.86}{1.50} \right) + 1 \right]^{-2} = 0.36$$

$$\begin{aligned} \Delta m &= \frac{(\gamma_s - \gamma)}{\gamma} \times (1 - n) \\ &= \frac{(2.65 - 1)}{1} \times (1 - 0.4) \\ &= 0.99 \end{aligned}$$

$$K_s = \sqrt{1.0 - \left( \frac{\sin 26.56}{\sin 40} \right)^2} = 0.72$$

$$\theta_c = 0.035 \text{ (for boulder rip-rap)}$$

$$\begin{aligned} D_n &= \frac{0.75 \times 2.50 \times 0.36}{0.99 \times 0.72} \times \frac{0.035}{0.035} \times \frac{(4.3)^2}{2 \times 9.81} \\ &= 0.90 \text{ m} \end{aligned}$$

**(b) According to Indian formulae**

$$t = 0.06 (Q)^{1/3} = 0.06 (515.8)^{1/3} = 0.48 \text{ m}$$

**(c) According to Neill (1973) (using graph, Fig-7.9)**

$$V = 4.3 \text{ m/sec}$$

$$D_{50} = 0.60 \text{ m}$$

**(d) According to USBR (using graph, Fig- 7.10)**

Maximum size of stone for velocity = 4.3 m/s is 0.75 m i.e.  $D_{100} = 0.75$

$$D_{50} = 0.85 \times 0.75 = 0.63 \text{ m}$$

**(e) Rip-rap size required to resist the particle erosion (Scott Brown.A., Eric Clyde S.)**

$$D_{50} = \frac{0.00594V_a^3}{d^{0.5} \times K_1^{1.5}}$$

Where  $D_{50}$  = median particle size to resist erosion (m)

$V_a$  = average velocity in the main channel (m/s)

$d$  = average flow depth in the main channel(m)

$$\begin{aligned} &= \frac{0.00594 \times 4.3^3}{2.86^{0.5} \times (0.72)^{1.5}} \\ &= 0.46 \text{ m} \end{aligned}$$



**(f) Shear stress approach (Lane's formula)**

$$d_m = \frac{\tau_0}{\tau_{*c}(\gamma_s - \gamma) \left[ \cos \theta_1 \sqrt{1 - \frac{\tan^2 26.56}{\tan^2 40}} \right]}$$

Where  $d_m$  = Effective size (m)

$\tau_0$  = Applied shear stress (N/m<sup>2</sup>)

$\tau_{*c}$  = Critical value of Shields number

$$\eta = \cos \theta_1 \sqrt{1 - \frac{\tan^2 26.56}{\tan^2 40}} = 0.72$$

$$\tau_0 = \gamma h s = 9810 \times 2.86 \times \frac{1}{34} = 825 \text{ N/m}^2$$

$$d_m = \frac{825}{0.047(2.65 - 1) \times 9810 \times 0.72} = 1.5 \text{ m}$$

**(g) Velocity approach**

On a side slope without secondary current the critical flow velocity  $V_c$  can be approximated by the following,

$$V_c = K_c \sqrt{2(G-1)gd_s} \left[ 1 - \frac{\sin^2 \theta_1}{\sin^2 \phi} \right]^{\frac{1}{4}}$$

Critical velocity for this reach = 4.3m/s and slope 1:2

Using graph (Fig-8.4) we get  $d_s = 0.5 \text{ m}$

**(h) Escarameia and May(1993)-HR Wallingford**

$$D_{n50} = C \frac{U_b^2}{2g(S-1)}$$

$D_{n50}$  = Characteristic size of stone

$$= \text{size of equivalent cube} = \left( \frac{w_{50}}{\rho_s} \right)^{\frac{1}{3}}$$

$w_{50}$  = weight of particle

$\rho_s$  = density of stone

$C = 12.3TI - 0.2$ ,  $TI = \text{Turbulence Intensity} = 0.2 < 0.5$

$$= 12.3 \times 0.2 - 0.2$$

$$= 2.26$$

$$U_b = (-1.48 \times TI + 1.04) \times U_d, \text{ where } U_d = 4.3 \text{ m/s}$$

$$= 3.199 \text{ m/s}$$

$$D_{n50} = 2.26 \frac{(3.199)^2}{2 \times 9.81 \times (2.65 - 1)}$$

$$= 0.71 \text{ m}$$

### (I) Maynard (1993)-US Army Corps of Engineers

$$D_{30} = S_f C_s C_v C_t y \left[ \left( \frac{1}{s-1} \right)^{0.5} \times \left( \frac{U_d}{\sqrt{K_1 g y}} \right) \right]^{2.5}$$

$s_f$  = factor of safety = 1.5

$c_s$  = 0.3 for angular rock

$c_v$  = 1.0 for straight channel

$c_t$  = 1.0 for standard design

$y$  = 2.86 m

$s$  = 2.65

$U_d$  = 4.3 m/s

$K_1$  = Slope correction factor =  $-0.672 + 1.492 \cot \alpha - 0.449 \cot^2 \alpha$

$K_1$  = 0.876, considering angle = 26.56 degree

$$D_{30} = 1.5 \times 0.3 \times 1.0 \times 1.0 \times 2.86 \times \left[ \left( \frac{1}{2.65 - 1} \right)^{0.5} \times \frac{4.3}{\sqrt{0.876 \times 9.81 \times 2.86}} \right]^{2.5}$$

$$D_{30} = 0.48 \text{ m}$$

$$0.75 \times D_{50} = 0.48 \text{ m}$$

$$D_{50} = 0.64 \text{ m}$$

Some of the values are very high that we are not considering. We can take thickness as 0.6m.

### 8.5.2 Design of Riprap Apron

To design of apron determination of scour depth is required.

Computation of scour depth is as follows:

(a) According to Komura (1971b), the relative scour depth

$$\frac{\Delta z}{h} = \left( 1 + 1.2 F^2 \right) \left[ \left( \frac{B}{B_1} \right)^{2/3} - 1 \right]$$

$$= \left(1 + 1.2 \times 1.24^2\right) \left[ \left(\frac{135.92}{97.74}\right)^{2/3} - 1 \right]$$

$$= 0.70$$

$$\Delta z = 0.70 \times 2.86 = 2.0 \text{ m}$$

**(b) According to Meyer-Peter and Muller's formula as developed by Michiue et.al. (1984)**

$$\begin{aligned} \frac{\Delta z}{h} &= \left[ \left(\frac{B_1}{B}\right)^{-4/7} - 1 \right] + (0.5F^2) \left[ \left(\frac{B_1}{B}\right)^{-6/7} - 1 \right] \\ &= \left[ \left(\frac{97.74}{135.92}\right)^{-4/7} - 1 \right] + (0.5 \times 1.24^2) \left[ \left(\frac{97.74}{135.92}\right)^{-6/7} - 1 \right] \\ &= 0.207 + 0.25 = 0.46 \end{aligned}$$

$$\Delta z = 2.86 \times 0.46 = 1.31 \text{ m}$$

**(c) According to formula as proposed by Straub (1944) and developed by Gill (1972)**

$$\frac{\Delta z}{h} = \left(\frac{B_1}{B}\right)^{-6/7} \left[ \left(\frac{B_1}{B}\right)^{-2/3} \left(1 - \frac{\tau_c}{\tau}\right) + \frac{\tau_c}{\tau} \right]^{-3/7}$$

$$K_s = \sqrt{1 - \frac{\sin^2 \alpha}{\sin^2 \phi}} = \sqrt{1 - \frac{\sin^2 26.56}{\sin^2 40}} = 0.72$$

$$\tau_c = \gamma \left[ \frac{v}{2.5 l_n \frac{12.3h}{K_s}} \right]^2$$

$$= 9810 \left[ \frac{4.30}{2.5 \ln \frac{12.3 \times 2.86}{0.72}} \right]^2 = 1919 \text{ N/m}^2$$

$$\tau = 483 \text{ N/m}^2 \text{ (already calculated)}$$

$$\frac{\Delta z}{h} = \left(\frac{97.74}{135.92}\right)^{-6/7} \left[ \left(\frac{97.74}{135.92}\right)^{-2/3} \left(1 - \frac{1919}{483}\right) + \frac{1919}{483} \right]^{-3/7} - 1$$

$$\Delta z = -0.64 \times 2.86 = -1.84 \text{ m (deposition)}$$

**(d) Scour Depth considering armoring effect (According to Pierre Y. Julien)**

Minimum grain size at the beginning of motion

$$d_{sc} = 10 \text{ hs,} \quad [\text{Assuming } \tau_{*c} = 0.05]$$

$h =$  Flow Depth during flood  $= 2.86$  m

$S = 1/34$  [ Slope of the River from 0 km – 1.0

km]

$$d_{sc} = 10 \times 2.86 \times 1/34 = 0.84 \text{ m}$$

From grain size distribution curve(Fig-8.1) to bed material percentage larger than 0.84 m  $= 100\% - 60\% = 40\%$

$$\begin{aligned} \text{Scour depth } \Delta Z &= 2 d_{sc} \left[ \frac{1}{\Delta P_c} - 1 \right] \\ &= 2 \times 0.84 \left( \frac{1}{0.4} - 1 \right) = 2.52 \text{ m} \end{aligned}$$

Maximum of the above scour value  $= 2.52$  m

Anticipated scour may be taken  $= 2.0 \times 2.52 = 5.04$ m

Factor 2.0 has been considered because of many imponderables associated with the hydraulics of boulder-bed streams and also due to presence of a concave river bend near the study reach.

The stone rip-rap required at the launching apron is

$$D_n = \frac{\phi_c K_T K_h}{\Delta m K_s} \times \frac{0.035}{\theta_c} \times \frac{v^2}{2g}$$

$\phi_c = 1.25$  (exposed edge)

$v = 4.3$  m/s

$$\begin{aligned} D_n &= \frac{1.25 \times 2.5 \times 0.36}{0.99 \times 0.72} \times \frac{0.035}{0.035} \times \frac{(4.30)^2}{2 \times (9.81)} \\ &= 1.08 \text{ m} \end{aligned}$$

Quantity of rip-rap for launching apron

$$= \sqrt{5} \times 5.02 \times 0.6 \quad (\text{Thickness of rip-rap cover } 0.6 \text{ m})$$

$$= 6.735 \text{ m}^3/\text{r.m}$$

According to USBR

$$V = 4.915 d^{1/2}$$

$V =$  average velocity of flow (m/s)

$d =$  mean dia of stone (m)

$$\text{Required } d = \left( \frac{V}{4.915} \right)^2 = 0.75 \text{ m with a weight of about } 750 \text{ kg.}$$

According to Blench,

Thickness of apron =  $(1.5 \sim 2) \times 0.75$

= 1.15 m

$\approx 1.2$  m

Length of apron = 5.91m  $\approx$  6.0 m

Thickness of rip rap apron = 1.20 m

Since size of stone is so large with about 750 kg weight that it can not be conveniently placed at the working site manually (man size being 40 kg). Also, it can not be cost-effectively placed by mechanized means because of inclement site conditions and this will increase cost also. So the apron is not to be constructed with rip-rap stone having size 750 mm with 750 kg weight. For this reason it is not considered feasible to implement rip rap apron.

### 8.5.3 Design of Cover Layer with Gabion

(a) Thickness of gabion (stone-mattress) is given by Pilarczyk (1985)

$$D_n = \frac{\phi_c K_T K_h}{\Delta m K_s} \times \frac{0.035}{\theta_c} \times \frac{v^2}{2g}$$

Where  $\phi_c = 0.50$  (for continuous protection of gabion mattress)

$K_T = 2.50$  (for high turbulent)

$K_h = 0.36$  (as calculated)

$R = 4.3$  m/s

$\Delta m = \Delta (1-\eta)$

$\eta = 40$  (percent of voids inside gabion mattress)

$\Delta = (\gamma_s - \gamma) / \gamma = 1.65$

$\Delta m = 1.65 \times 0.6 = 0.99$  m

$\theta_c = 0.06$  (critical shear stress for gabion mattress)

$$D_n = \frac{0.50 \times 2.50 \times 0.36}{0.99 \times 0.72} \times \frac{0.035}{0.06} \times \frac{(4.3)^2}{2 \times 9.81} = 0.35 \text{ m}$$

$\approx 0.50$  m

(b) Escarameia and May (1993)-HR Wallingford.

$$D_{n50} = C \frac{U_b^2}{2g(S-1)}$$

$D_{n50}$  = Characteristic size of stone

$$= \text{size of equivalent cube} = \left( \frac{w_{50}}{\rho_s} \right)^{\frac{1}{3}}$$

$w_{50}$  = weight of particle

$\rho_s$  = density of stone

$C = 12.3TI - 1.65$ ,  $TI = \text{Turbulence Intensity} > 0.12$

$$= 12.3 \times 0.2 - 1.65$$

$$= 0.81$$

$U_b = (-1.48 \times TI + 1.04) \times U_d$ , where  $U_d = 4.3 \text{ m/s}$

$$= 3.199 \text{ m/s}$$

$$D_{n50} = 0.81 \frac{(3.199)^2}{2 \times 9.81 \times (2.65 - 1)}$$

$$= 0.26 \text{ m}$$

Consider larger of the two, provide 2m x 1m x 0.5m size gabion boxes in the slope.

#### 8.5.4 Design of Launching Apron with Gabion

(a) Thickness of gabion mattress by Pilarczyk

Maximum scour depth = 5.04 m

$\phi_c = 1.0$  (exposed edge)

$$D_n = \frac{1.0 \times 2.50 \times 0.36}{0.99 \times 0.72} \times \frac{0.035}{0.06} \times \frac{(4.3)^2}{2 \times 9.81} = 0.70 \text{ m}$$

(b) Escarameia and May (1993)-HR Wallingford.

$$D_{n50} = C \frac{U_b^2}{2g(S-1)}$$

$D_{n50}$  = Characteristic size of stone

$$= \text{size of equivalent cube} = \left( \frac{w_{50}}{\rho_s} \right)^{\frac{1}{3}}$$

$w_{50}$  = weight of particle

$\rho_s$  = density of stone

$C = 12.3TI - 1.65$ ,  $TI = \text{Turbulence Intensity} > 0.12$

$$=12.3 \times 0.2 - 1.65$$

$$=0.81$$

$$U_b = (-1.48 \times TI + 1.04) \times U_d, \text{ where } U_d = 4.3 \text{ m/s}$$

$$=3.199 \text{ m/s}$$

$$D_{n50} = 0.81 \frac{(3.199)^2}{2 \times 9.81 \times (2.65 - 1)}$$

$$= 0.26 \text{ m}$$

Quantity of gabion work for launching apron

$$= \sqrt{5} \times 5.04 \times 0.50 = 5.61 \text{ m}^3/\text{r.m}$$

Thickness of apron = 1.2 m

Length = 4.67 m  $\approx$  6.0 m

**Provide gabion mattress size = 2 m x 1.2m x 1.2m with 6.0 m length of apron (Three boxes along the length of apron)**

**For safety of the work the apron length have been provided 6.0 m to take into account all the uncertainties.**

**It is also recommended that there should be some stock pile of man size stone at a convenient place on the bank of river to use them during emergency.**

### 8.5.5 Design of Cover Layer with Concrete Block

The thickness of concrete block is given by Pilarczyk

$$D_n = \frac{\phi_c K_T K_h}{\Delta m K_s} \times \frac{0.035}{\theta_c} \times \frac{V^2}{2g}$$

Here,  $\phi_c = 0.50$  (for continuous protection of block)

$K_T = 2.5$  (for high turbulent and impingement)

$K_h = 0.36$  (same as calculated above)

$$\Delta m = \frac{(\gamma_s - \gamma)}{\gamma} \times (1 - n) = \frac{(2.65 - 1)}{1} \times (1 - 0.4) = 0.99$$

$K_s = 0.72$  (same as calculated above)

$$D_n = \frac{0.50 \times 2.50 \times 0.36}{0.99 \times 0.72} \times \frac{0.035}{0.075} \times \frac{(4.3)^2}{19.62}$$

$$= 0.277 \text{m}$$

Provide 0.6m x 0.6m x 0.3m, 1:3:6 cement concrete block in slope.

### 8.5.6 Design of Launching Apron with Concrete Block

(a) Thickness of concrete block is given by Pilarczyk

$$D_n = \frac{\phi_c K_T K_h}{\Delta_m K_s} \times \frac{0.035}{\theta_c} \times \frac{V^2}{2g}$$

Here,  $\phi_c = 1.0$  (for exposed edge)

$K_T = 2.5$  (for high turbulent and impingement)

$K_h = 0.36$  (same as calculated above)

$$\Delta_m = \frac{(\gamma_s - \gamma)}{\gamma} \times (1 - n) = \frac{(2.65 - 1)}{1} \times (1 - 0.4) = 0.99$$

$K_s = 0.72$  (same as calculated above)

$$D_n = \frac{1.0 \times 2.50 \times 0.36}{0.99 \times 0.72} \times \frac{0.035}{0.075} \times \frac{(4.3)^2}{19.62}$$

$$= 0.56 \text{m}$$

Provide 1.0m x 1.0m x 0.6m, 1:3:6 cement concrete block for a length of 6m in launching.



## 8.6. DESIGN OF FILTER UNDER COVER LAYER

### 8.6.1 Design of Granular Filter under the Cover Layer

Given information

Grain size of bank material

$$d_{10} = 0.18\text{mm}$$

$$d_{15} = 0.20\text{mm}$$

$$d_{50} = 1.2\text{mm}$$

$$d_{60} = 2.20\text{mm}$$

$$d_{85} = 12\text{mm}$$

$$d_{90} = 15\text{mm}$$

Size of rip-rap gradation

$$d_{15} = 450\text{mm}$$

$$d_{50} = 600\text{mm}$$

$$d_{85} = 700\text{mm}$$

$$d_{100} = 750\text{mm}$$

#### 1) Retention Criteria

$$\frac{d_{15}(\text{Riprap})}{d_{85}(\text{bank material})} = \frac{450}{12} = 37.5 \gg 5$$

So filter is required

$$\frac{d_{15}(\text{filter material})}{d_{85}(\text{bank material})} = 4.5$$

$$d_{15}(\text{filter material}) = 4.5 \times 0.2 = 0.9\text{mm}$$

#### 2) Uniformity Criteria

$$\frac{d_{50}(\text{Riprap})}{d_{15}(\text{bank material})} = \frac{600}{1.2} = 500 \gg 25$$

So from this consideration filter is required

$$\frac{d_{50}(\text{filter material})}{d_{15}(\text{bank material})} = 22$$

$$d_{50}(\text{filter material}) = 22 \times 1.2 = 26.4\text{mm}$$

#### 3) Permeability Criteria

$$\frac{d_{15}(\text{riprap})}{d_{15}(\text{bank material})} = \frac{450}{0.2} = 2250 \gg 40$$

So filter is required

$$\frac{d_{15}(\text{filter material})}{d_{15}(\text{bank material})} = \frac{0.9}{0.2} = 4.5 > 4.0$$

Hence o.k

Now for this layer of filter

$$d_{15} = 0.9 \text{ mm}$$

$$d_{50} = 26.4 \text{ mm}$$

$$d_{85} = 45 \text{ mm}$$

$$d_{100} = 50 \text{ mm}$$

Again we have to check all the criteria between this filter and riprap

1) Retention criteria

$$\frac{d_{15}(\text{riprap})}{d_{85}(\text{1st layer filter material})} = \frac{450}{45} = 10 \gg 5$$

Another filter layer is required

$$\frac{d_{15}(\text{2nd layer filter})}{d_{85}(\text{1st layer filter})} = \frac{31.5(\text{taken from below})}{45} = 0.7 < 5$$

Hence o.k

2) Uniformity Criteria

$$\frac{d_{50}(\text{riprap})}{d_{50}(\text{1st layer material})} = \frac{200}{26.5} = 7.5 < 25 \text{ Hence O.K}$$

3) Permeability Criteria

$$\frac{d_{15}(\text{2nd layer filter material})}{d_{15}(\text{1st layer filter material})} = 35$$

$$d_{15}(\text{2nd layer material}) = 35 \times 0.9 = 31.5 \text{ mm} \quad \text{So it is recommended to use it}$$

Now 2<sup>nd</sup> layer filter

$$d_{15} = 31.5 \text{ mm}$$

$$d_{50} = 200 \text{ mm}$$

$$d_{85} = 250 \text{ mm}$$

$$d_{100} = 300 \text{ mm}$$

We can provide thickness of filter as 500mm. First layer 100mm and 2<sup>nd</sup> layer 400mm

## 8.6.2 Design of Fabric Filter (Geotextile)

Given information

Grain size of bank material

Size of rip-rap gradation

$d_{10} = 0.18\text{mm}$

$d_{15} = 450\text{mm}$

$d_{15} = 0.20\text{mm}$

$d_{50} = 600\text{mm}$

$d_{50} = 1.2\text{mm}$

$d_{85} = 700\text{mm}$

$d_{60} = 2.20\text{mm}$

$d_{100} = 750\text{mm}$

$d_{85} = 12\text{mm}$

$d_{90} = 15\text{mm}$

Depending on the grain size distribution of bank material we provide geotextile of opening size 0.2mm .

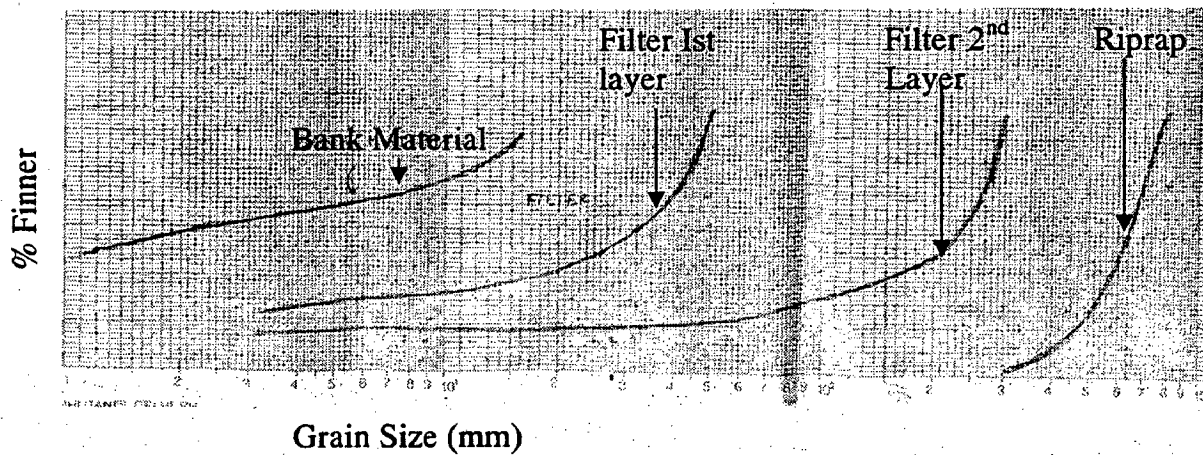
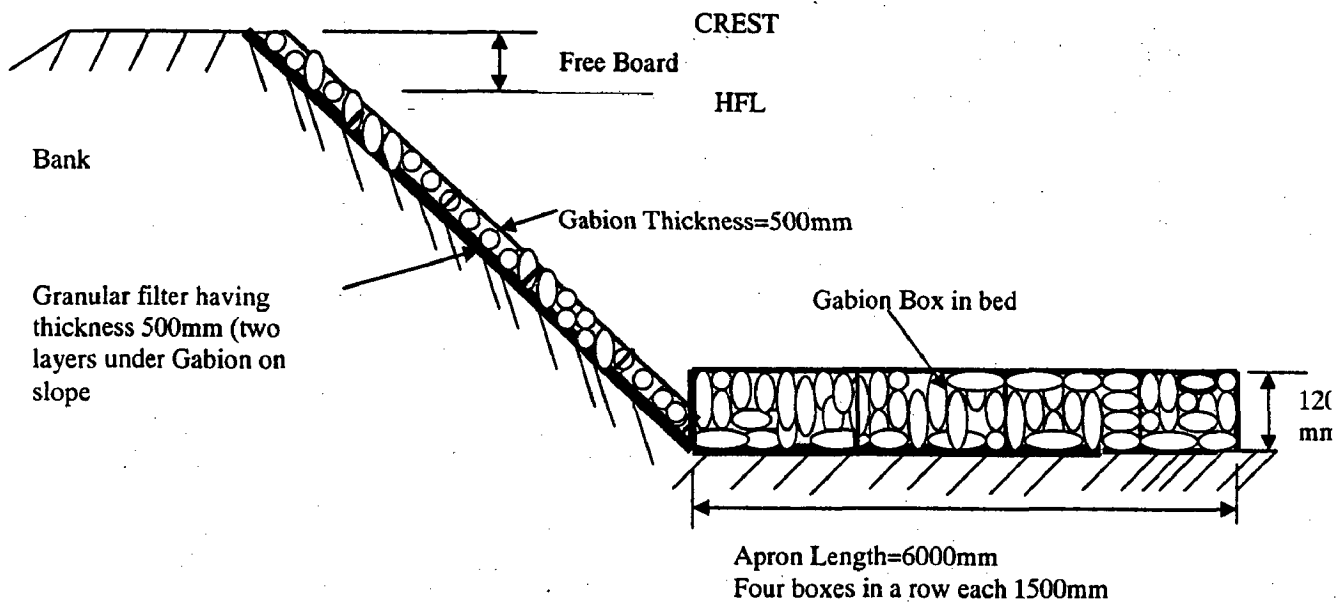
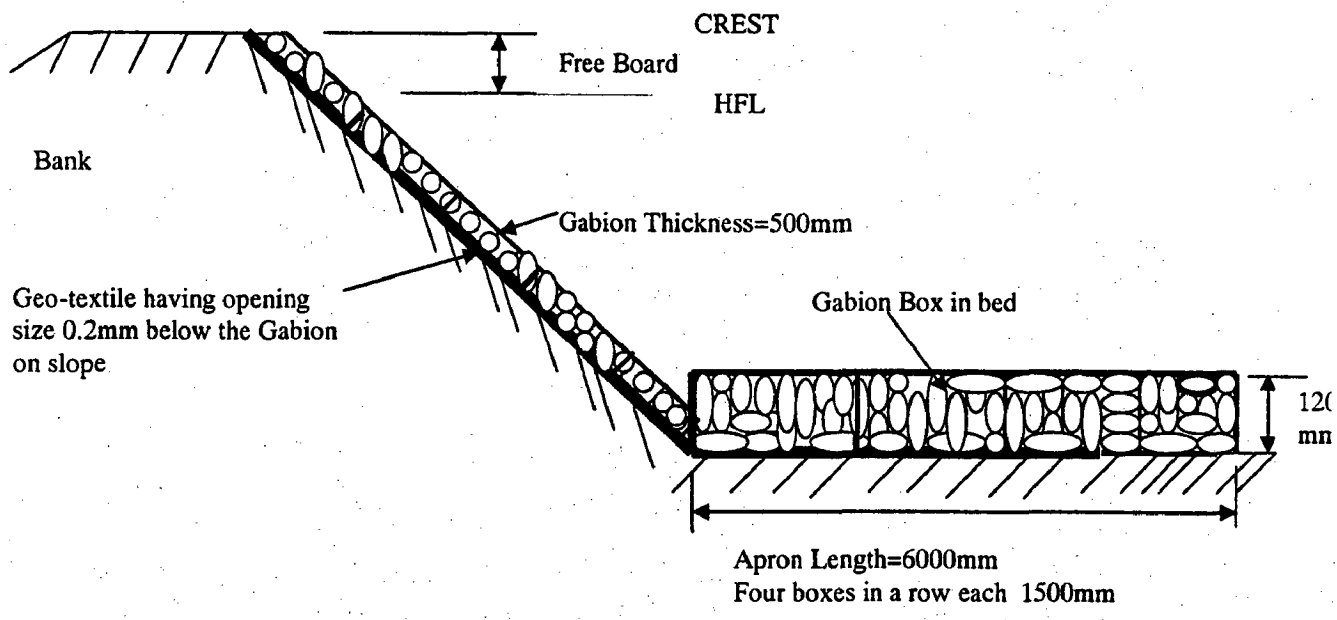


Fig-8.2 Grain Size Distribution of Filter material



**Fig- 8.3** Cross-Section of River Bank Protection Work With Gabion Boxes along with granular filter In Beas River near SASE,MANALI



**Fig-8.4** Cross-Section of River Bank Protection Work With Gabion Boxes along with Geotextile in Beas River near SASE,MANALI

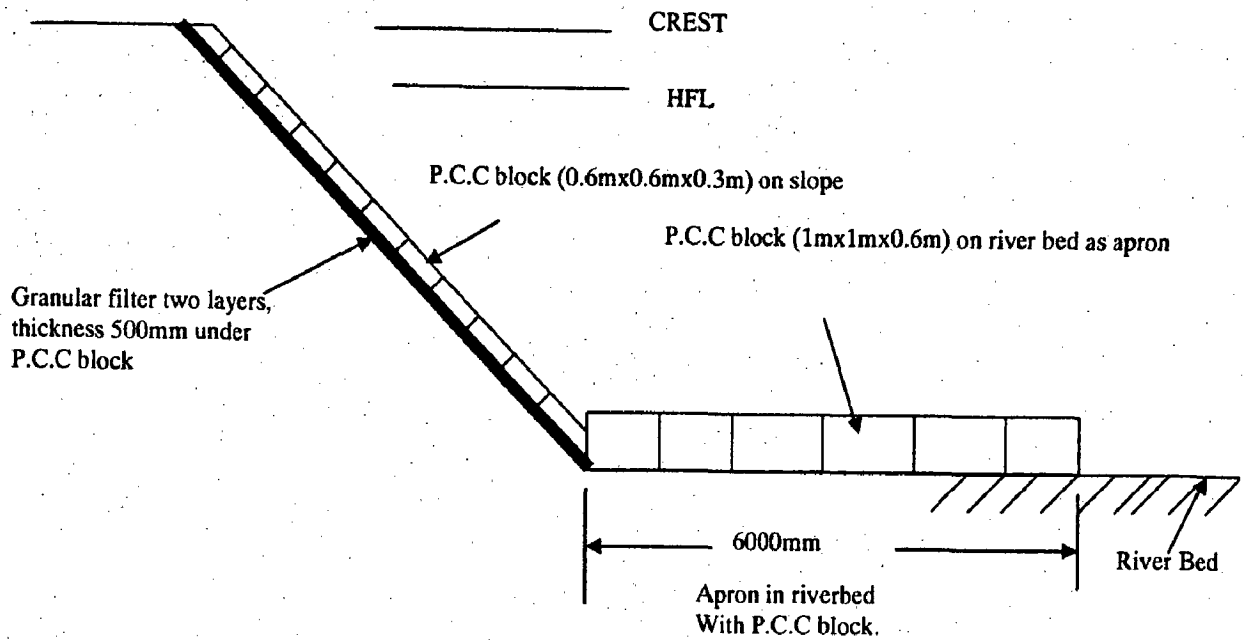


**Fig-8.5 Cross-Section of River bank Protection work with P.C.C block along with granular filter beneath it**

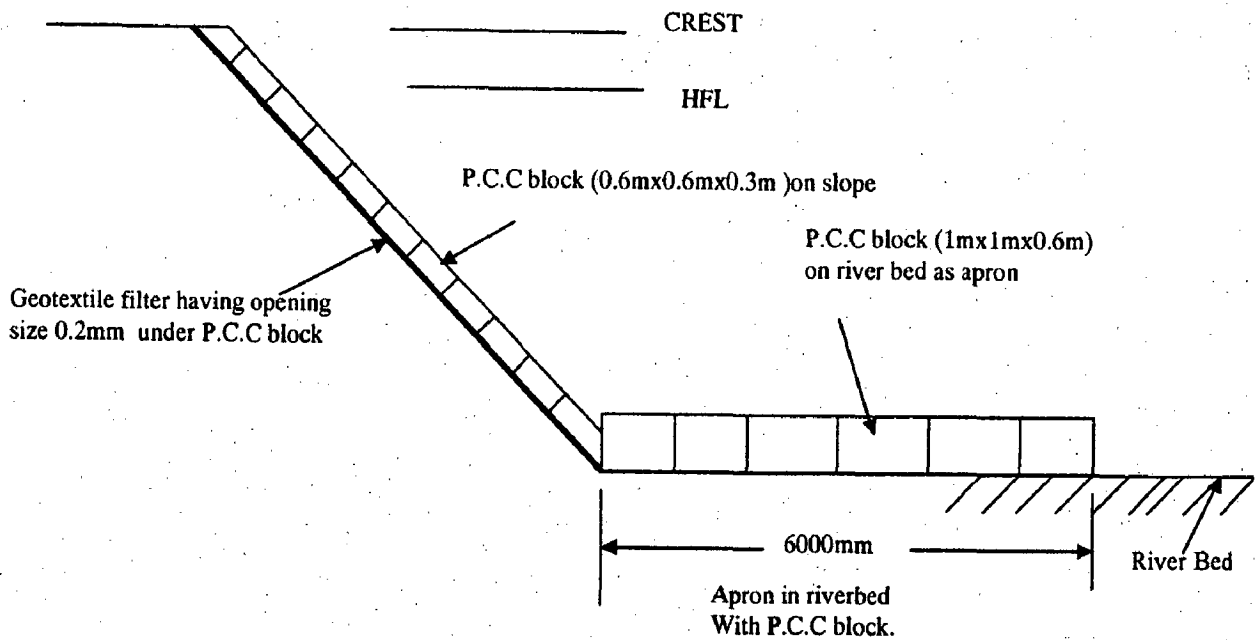


**Fig-8.6 Cross-Section of River bank Protection work with P.C.C block along with Geotextile Filter beneath it**

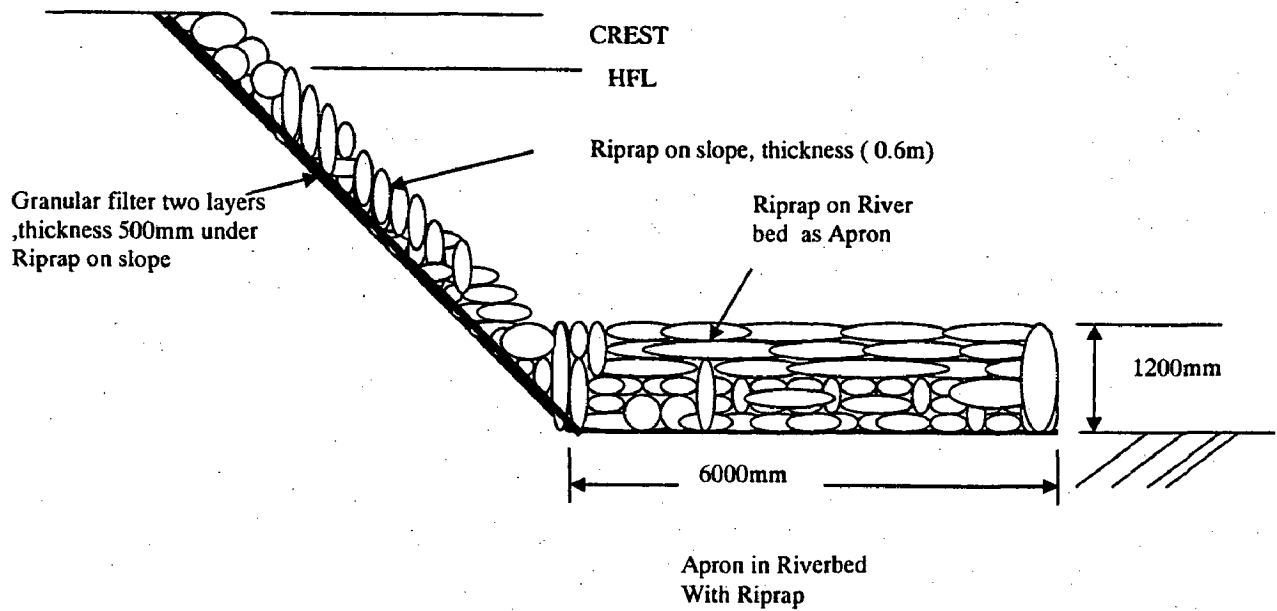


**Fig-8.7 Cross-Section of River bank Protection work with Riprap along with Granular Filter beneath it**

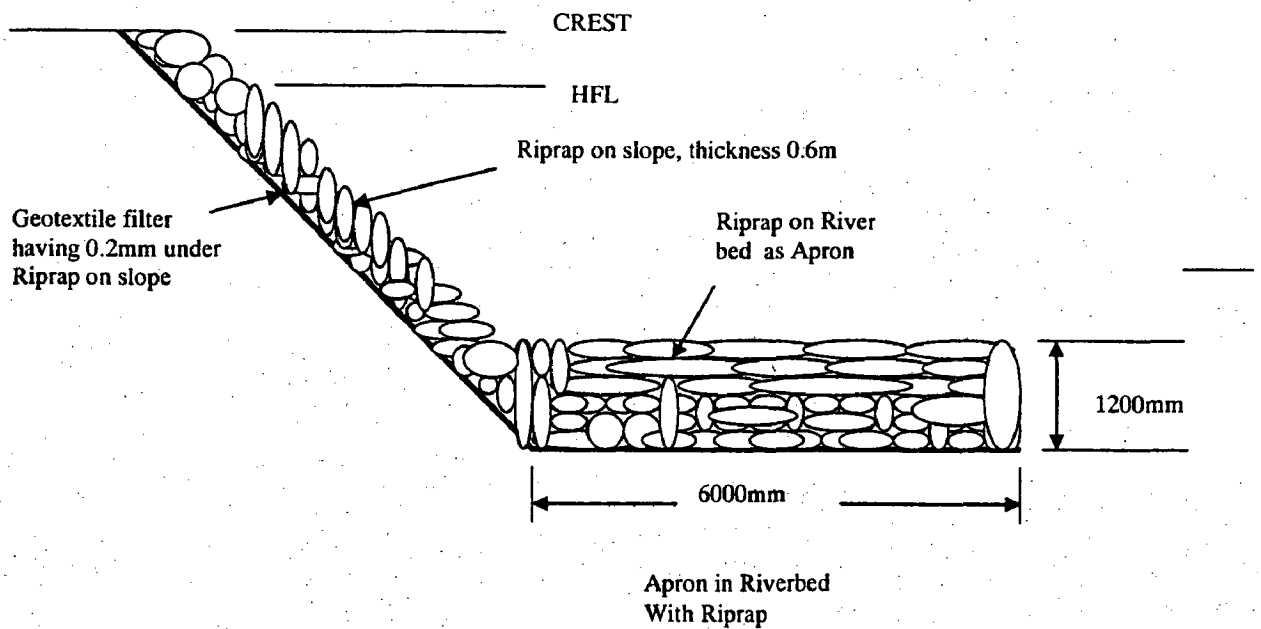


**Fig-8.8 Cross-Section of River bank Protection work with Riprap along with Geotextile beneath it**

**FIELD PERFORMANCE STUDY OF FLEXIBLE POLYMER ROPE  
GABION IN BOULDER BED RIVER.**

**9.1 GENERAL**

Gabions are made of polymer ropes, which are filled with stones. The idea of scour protection system is to hold small stones together. Function of this type of polymer rope gabion is similar to that of gabion made of wire mesh with some advantages. Typical size of polymer rope gabion is (2-3) m in length 1-2m in width and 1-1.5m in thickness, opening size is normally 150mm x 150mm. Polymer rope gabions with less than 0.5m thickness is known as gabion mattresses. In general gabions having less than 0.5m thickness or large length width ratio is known as Reno-mattresses.

The main drawbacks of GI wire type of protection system are durability and rigidity. In wire mesh gabion, corrosion is another major problem. In order to prevent corrosion, plastic coating and corrosion protective steels are used, in polymer rope gabion there is no problem of corrosion but durability is a question, which needs to be examined. Especially in gravel or boulder stage river bed, when flash flood comes, polymer rope should withstand the impact of large boulder coming from upstream and it should be sufficiently durable. This polymer ropes are definitely an improvement over wire mesh gabions, But unless the performance evaluation, of this material is studied in field, this cannot be considered for use in apron protection work in boulder bed river.

For good appearance, the exposed walls of the gabions should be carefully constructed like a dry stonewall. Where there is sufficient suitable stones construction of the fill in a similar way gives a very strong structure that will not settle. Normally it is sufficient to roughly fill the center with smaller stones, behind the constructed wall.

**9.2 PROBABLE TYPE OF DAMAGE**

- (a) For slope protection gabion may be slided downward

- (b) Due to excess uplift individual gabion box can be lifted out
- (c) A local slip circle can occur resulting failure of slopes
- (d) The subsoil can wash away through the gabions
- (e) Smaller stones can cut through the mesh
- (f) Salinity can adversely affect the rope
- (g) Rupture of mesh with impact of boulder
- (h) Vandalism may be harmful for the project

### **9.3 LOCATION OF FIELD EXPERIMENTS**

Beas river is located in Himachal Pradesh. It is a hilly river having bed slope 1 in 25 at observational site. Grain size distribution of bed material (Fig-9.1) indicates more than 50% of the material is having larger than 0.750mm. So it is evident that it is a boulder bed river. Selected site (map enclosed) is near DRDO Guest House where erosion in the riverbed is taking place. So this is a suitable place to carry out performance evaluation of flexible polymer ropes in gabions as apron protection work.

Since after computation, the length of apron is found to be 6m, width of the trial field has been taken as 6m. Thickness has been taken as 1.2m. Length of the trial field has been selected arbitrarily. As per design, each gabion size has been taken as 4m x 3m x 1.2m.

### **9.4 MATERIAL SPECIFICATION**

#### **(i) Gabion**

Each gabion box size was 4m x 3m x 1.2m. Polymer rope diameter was 8mm and mesh opening was 150mm x 150mm. Mesh strength was 80KN/meter width of gabion. Breaking strength was 900Kg/m.



**(ii) Geotextile**

Oven geotextile was used under the gabion box in order to retain the soil. Thickness of the same was less than 1mm and opening size was 0.15mm.

**9.5 OBJECTIVE OF THE STUDY**

- (i) To observe suitability of polymer rope gabion in river bed erosion control
- (ii) To observe its suitability especially during transportation, placing, anchoring, filling with stones and covering
- (iii) To observe its adherence capability with the uneven surface during erosion
- (iv) To observe damage type due to impact of larger boulder coming from upstream during high flood.
- (v) To find out its economic viability over GI wire gabion
- (vi) To observe its biodegradability
- (vii) To observe its durability

**9.6 INSTALLATION PROCEDURE**

- (i) Carry the geotextile and place it on the river bed
- (i) Anchor it in four corners
- (iii) Carry the gabion box and place it over the geotextile
- (iv) Open the box maintaining proper alignment
- (v) Fix four corners with big size boulders so that desired thickness can be maintained.
- (vi) Anchor four top corners so that it may not create any trouble during filling.
- (vii) Fill the box with stones. In the middle there should be smaller size of stones but should be at least 1.5 times the mesh size and along the periphery of the box there should be larger stones.
- (viii) After maintaining the proper thickness it should be covered and anchored with the lace attached with it.
- (ix) After completion in all respect top levels of boxes are taken considering one arbitrary B.M=100m

(x) Reduced levels of 7-points are taken. They are marked with fluorescent colour. Points are:

Point- A=97.75m

Point-B=97.7m

Point-C=97.67

Point-D=97.68m

Point-E=97.67m

Point-F=97.64m

Point-G=97.59m

When river bed is dry, this installation procedure can be performed easily. Under water it is quite troublesome especially in boulder stage river like the Beas where velocity is high. In the case of submersed site, on the river bank, crane can be used to place the filled boxes to the proper place on the river bed but in that case box size should be such that total weight does not exceed 80KN/meter width with factor of safety of at least 1.5

## **9.7 PRELIMINARY ASSESSMENT AND FINDINGS**

From the field observation it is evident that transportation, placement and filling with stones in polymer rope gabion is much easier than in conventional GI wire gabion. Polymer material is not biodegradable, non-corrosive and no adverse effect with salinity. Because of its excellent flexibility it can adhere to uneven river bed contour during erosion whereas GI wire gabions are not having that quality. It has excellent durability, resistance to alkaline and acidic environment. It has got high tensile strength, abrasion resistance and thermal stability. Polymer rope costs Rs. 110/sqm. The preliminary assessment of the polymer rope gabion made at site was quite satisfactory, as the rope gabion could withstand the river flow and also apparently sheltered the bank line from active flow of the Beas. However Final observation and findings would be done after passage of current monsoon.

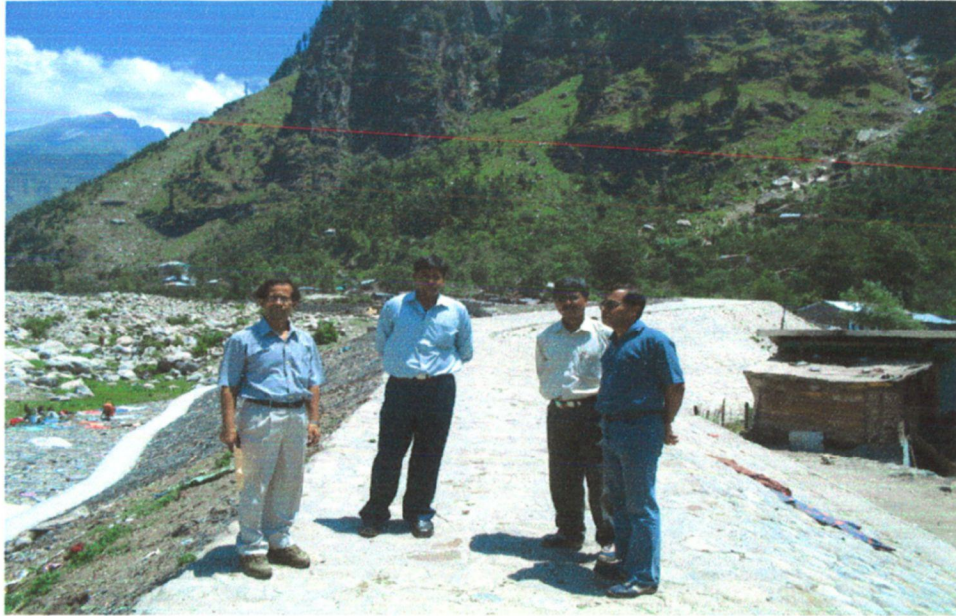


**Fig-9.1 Site Selection to Conduct Field Trial with Polymer Gabion**



**Fig-9.2 GI wire Gabion is affected by Corrosion**





**Fig-9.3 Due to Rigidity GI Wire Gabions do not Adhere to Undulation**



**Fig-9.4 Stones are Coming out due to Damage of Mesh**





**Fig-9.5 Polymer Rope Gabion Box Carried to the River Bed**



**Fig-9.6 Polymer Rope Gabion Box is Anchored**





**Fig-9.7 Polymer Rope Gabion is being Filled with Stones**



**Fig-9.8 Geotextile is being Placed on the River Bed**





**Fig-9.9 Top Surface is being leveled with Required Size of Stones**



**Fig-9.10 Gabion Box is Ready for Covering**





**Fig-9.11 After filling gabion Box is covered**



**Fig-9.12 After Covering, Gabion Box is Anchored with laces**





**Fig-9.13 Gabion Box filling, Covering and Anchoring Complete**



**Fig-9.14 After completion Top Levels are taken**

## DISCUSSIONS, CONCLUSIONS AND RECOMMENDATIONS

### 10.1 DISCUSSIONS ON SOIL NAILING

Fig-4.6 (a) For purely cohesionless soil nailed wall, factor of safety (FOS) increases with the increase of angle of internal friction and also increases with the increase of L/H ratio. This increase is not proportional. Rate of increase is more with the increase of angle of internal friction.

Fig-4.6 (b) For purely cohesive soil nailed wall, FOS increases with the increase of cohesion of soil and it is proportional to cohesion and it increases with L/H ratio. For one pair of L/H ratio, difference in FOS also increases with the increase of cohesion value.

Fig-4.7 (a) For a soil nailed wall (c- $\phi$  soil), FOS increases with the increase of nail diameter but not proportionately. Rate of increase also increases with the increased value of nail diameter and it also increases with L/H ratio.

Fig-4.7 (b) FOS is higher for an inclined nailed wall than for a vertical wall.

Fig-4.8 (a) For vertical wall, FOS increases with nail inclination but rate of increase is less beyond 15<sup>o</sup> nail inclination and FOS increases with L/H ratio.

Fig-4.8 (b) For an inclined wall, FOS increases up to 15<sup>o</sup> nail inclination but beyond that it decreases. It increases with the increase of L/H ratio.

Fig-4.9 (a) For nail inclination of 10 degree, FOS increases with wall inclination. Rate of increase increases up to 25 degree and beyond that increase is too high.

In this case  $27^{\circ}$  angle of internal friction has been considered. Graph indicates that at this level without nail, a wall can with stand.

Fig-4.9 (b) For horizontal nail, FOS increases with wall inclination and tendency is almost same

Fig-4.10 (a) In a nailed wall where nail is inclined FOS is more than that of where nail is horizontal and it coincides beyond  $25^{\circ}$  wall inclination.

Fig-4.10 (b) FOS is more for grouted nail than for driven nail.

Fig-4.11 (a) FOS increases with yield stress of nail. Rate of increase decreases with increase of yield stress.

Fig-4.11 (b) FOS decreases with increases of horizontal and vertical spacing of nail

Fig-4.12 (a) FOS increases with L/H ratio

Fig-4.12 (b) FOS increases up to  $L/H = 0.8$ , beyond that rate of increase decreases

## 10.2 DISCUSSIONS ON GEOSYNTHETICS

There may be many alternatives in bank protection work. But we have to select the most suitable alternative depending upon many factors such as importance of the project, budget provision etc.

Geosynthetics should be used as filter material in river erosion control. When filter is to be used under water, it would be better to use geosynthetics instead of granular filter.

In boulder stage river where velocity of flow is high, stones in gabion box in the field should be used for better performance and convenience.

In the present case, 100yrs return period flood has been considered for design purpose, as it should protect many infrastructures adjacent to Manali Town.

### 10.3 CONCLUSIONS AND RECOMMENDATIONS

- 1) Soil nailing technique is not suitable in soft soil
- 2) FOS increases with wall inclination
- 3) Nail inclination beyond 15 degree will not be cost effective.
- 4) From economical point of view, nail length should vary  $0.5H-0.8H$
- 5) Grouted nail is preferable since it gives more FOS
- 6) Soil nailing technique will not be suitable under water, so it will not be wise to use for river bank erosion control
- 7) Soil nailing technique may be successfully used to control erosion or sliding of river bank above HFL
- 8) For under water retention of soil geosynthetics is suitable.
- 9) When flow velocity is high, gabion box will perform well in controlling erosion..
- 9) Polymer rope diameter of 10mm and mesh size of 100mm may give much better result in erosion control of boulder stage river.
- 10) Polymer rope gabion is much better than GI wire gabion considering its excellent flexibility, adherence to uneven river bed.
- 11) Polymer rope gabion is suitable since it is noncorrosive, non-biodegradable.
- 12) Transportation, placement, installation of polymer rope gabion boxes are easier.

#### **10.4 SCOPE OF FURTHER STUDY**

In the present study of soil nailing component, nail and soil interface angle has been considered  $2/3$  of angle of internal friction. This value can be determined from pullout test in field condition with different cohesion value.

Simulation study by HEC-6 for flood discharge can be carried out incorporating sediment discharge

Preliminary assessment report has been presented for field experiment of flexible polymer rope in the present study. That should be continued up to the end of flood season to have better idea regarding performance of the same thing.

## REFERENCES

---

**Ahmad, M. (1953),** "Experiments on Design and Behavior of Scour Dikes". Proc. IAHR Conf. Minnesota: 145-159

**Bathurst, R.J and Simal, M. (1993),** "Two Computer Programs for The Design and Analysis of Geosynthetic-reinforced Soil Retaining Wall" Geotextiles and Geomembranes, Vol-12 ,pp 381-396

**Cafiso, F. and Umilta, G. (1996),**"Reinforcement Works of The Calcareous Rock under The Castle of Caccamo, Sicily," Proc. Of the International Symposium on Geotechnical Engineering for Preservation of Monuments and Historic Sites, NAPOLI/ITALY/3-4 October

**Chang. H.H.** "Fluvial Processes in River Engineering" A Wiley-Interscience Publications

**Colorado State University,** "Highways in the river environment: Hydraulic and Environmental Design Considerations" Prepared for the Federal Highway Administration, US Department of Transportation, May 1975

**Copeland, R. R. (1983).** Bank Protection Techniques using Spur Dikes. Hydraulics Laboratory, US Army Engineer waterways Experiment Station, Vicksburg, Mississippi, Washington, DC

**Davis,M.C.R., Jacobs, C.D and Bridle, R.J.1993),** " An Experimental Investigations of Soil Nailing ", Retaining Structures, pp 587-598,Thomas Telford, London.

**Drumm, E.C., Tant C.R., Mauldon, M. and Berry, R. M.** "Instrumentation and Monitoring of a Nailed Mine-Waste Slope".

**Dembicki, E., Niespodzinska. L.** "Geotextiles in Coastal Engineering Practice" Geotextiles and Geomembranes 10- 147-154.

**Escarameia, M. and May, R.W.P(1992),** " Channel Protection Downstream of structures," Report SR 313, April 1992,HR Wallingford

**Gassler and, Gudehus,**” Soil Nailing –Statistical Design”, Institute of Soil Mechanics and Rock Mechanics, University of Karlsruhe, W-Germany.

**Gill, M. A. (1972),** “ Erosion of Sand Beds around Spur Dikes” Proc. ASCE, J. of the Hydr. Div, Sept.

**Guilloux, A. Notte, G. and Gonin, H.,** “Experiences on a Retaining Structure by Nailing in Moraine Soils”. Bureau d’Etudes simecsol, Paris, France

**Ghoshal, A and Som. N; (1993),** “Geotextiles State of Usage and Economic Evaluation.” Geotextiles and Geomembranes 12 , 193-213.

**Gupta, R. P (2002)** “A Study on Soil Nailing with Respect to Open Excavation and Slopes” M-Tech. Dissertation, IIT, Roorkee.

**Garde. R.J. and RangaRaju. K.G.** “Mechanics of sediment Transportation and Alluvial Stream Problems”

**Hudson, R.Y. (1953)** “Wave Forces on Break Waters”. Transaction of ASCE 118:653

**Ingold, T. S (1984),** “ Geotextiles and Filters beneath Revetments “ International Conference on Flexible Armoured Revetments Incorporating Geotextiles:59-70. London: Thomas Telford.

**Jain S.C. and Fischer E.E.** “Scour Around Circular Bridge Piers at High Froude Numbers” Report FHWA-RD-79-104. Federal Highway Administration, US Department of Transportation, April 1979

**Juran,I Baudrand, G., Farrag, K. and Elias, V. (1988),**” Kinematic Limit Analysis Approach for The Design of Nailed Soil Retaining Structures”, International Geotechnical Symposium on Theory and Practice of earth reinforcement/ Fukuoka Japan /5-7 October,.

**Juran,I, Shaffiee,S. Schlosser,F. Humbert,P. and Guenot, A.,** “ Study of Soil-Bar Interaction in The Technique of Soil Nailing”.

**Jewell ,R. A. and Pedley, M. J. (1990a),** “Soil Nailing Design: The Role of Bending Stiffness”, Ground Engrg, March, PP. 30-36

**Juran, I. and Elias, V. (1991),** "Soil Nailing for Stabilization of Highway Slopes and Excavation," Federal Highway Administration Publication No. FHWA-RD-89-193.

**Juran, I. and Elias, V. (1992),** "Ground Anchor and Soil Nailing in Retaining Structures", Found. Engg, Handbook, Van Nostrand Company, Second Edition, pp 868-905.

**Komura, S. (1971).** "River Bed Variation at Long Constrictions" XIVth Congress of IAHR, Vol. 3, Subject C, Aug. 29-Sep. 3: 109-116.

**Laursen, E. M. (1962),** "Scour at Bridge Crossings," Trans. ASCE. 127(1) PP. 166-180

**Long, J. H., Sieczkowski, W.F., Chow, E. and Cording, E.J. (1990),** "Stability Analysis for Design of Soil-Nailed Walls," Proc. of a Conf. on Design and Performance of Earth Retaining Structures, ASCE Special Publication No-25, pp. 676-691.

**Mutreja K.N (1986).** "Applied Hydrology" Tata McGraw Hill Publishing Company Ltd.

**Mitchell and Villet (1987),** "Soil Nailing", Reinforced of Earth Slopes and Embankments, NCHRP Report No-290, Appendix, pp. 258-312.

**Maynard, S.T. (1993),** "Corps Riprap Design Guidelines for Channel Protection". International Riprap Workshop: 692-711

**Michiue, M., Suzuki, Hinokidani, O. (1984),** "Formation of Low-water Bed by Spur-dikes in Alluvial Channel," Proc. 4<sup>th</sup> APD- IAHR: 685-698

**Myles, B. and Bridle, R.J. (1997),** "Fired Soil Nails :The Machine" Ground Engg. Vol.24 July/Aug, pp42-43.

**Mannsbart G and Resl. S** "An Expert System for the Design of Geotextiles" Geotextiles and Geomembranes 12, 441-450.

**Murthy V.N.S.** "Geotechnical Engineering" Principles and Practices of Soil Mechanics and Foundation Engineering

**Neill. C. R. (1973),** "Guide to Bridge Hydraulics", Toronto and Buffalo: RTAC, University of Toronto Press



**Plumelle, C. and Schlosser, F. (1990),** "A French National Research Project on Soil Nailing: Clouterre," Performance of Reinforced Soil Structure, Proc. Of Int. Reinforced Soil Conference, Glasgow, pp, 219-223.

**Przedwojski, B., Blazejewski, R. and Pilarczyk, K. W. (1995),** "River Training Techniques"

**Pokharel, G. and Ochiai, T. (1997),** "Design and Construction of a New Soil Nailing Method " Ground Improvement Geosystems, Thomas Telford, London. Pp. 409-413.

**Pokharel, G.(2001),** "Stabilization of Slopes by Soil Nailing Method: Theory, Experiment and Practice", International Symposium on Geotechnical & Environmental Challenges in Mountainous Terrain. November 6-7.

**Patra C.R., Basudhar P.K. (2001),** " Nailed Soil Structure: An Overview", Indian Geotechnical Journal, Vol-31 (4).

**Pierre. Y. J. (2002)** "River Mechanics" Press Syndicate of the University of Cambridge

**Petersen. M. S. "River Engineering"** Prentice-Hall, Englewood Cliffs, New Jersey (USA)

**Parau. P.K.** "Hydraulic and Geotechnical Investigations of the Bank slip on the West Bank of the River Hooghly near Sankaril in West Bengal, India" Indian Geotechnical Journal, 20 (2).

**Rao. G.V. (1992),** "Geo-synthetics – an Overview" National Work Shop on Role of Geo-synthetics in Water Resources Projects, Proceedings, 20-24 January, New Delhi

**Rao. G.V.(1992)** "Testing of Geotextile" –National Work Shop on Role of Geo-synthetics in Water Resources Projects , Proceedings,20-24 January, New Delhi

**Rao. G.V, Pradhan. P.S.** "Erosion and its Control" - National Work Shop on Role of Geo-synthetics in Water Resources Projects , Proceedings,20-24 January, New Delhi

**Rao. G.V. (1995)** "Geo-synthetics-Property Evaluation. Engineering with geosynthetics" Compilation of Papers of Two Workshops held at Guwahati and Hyderabad, October.

**Raju, G.V.R., Wong, I.H. and Low, B.K** " Experimental Soil Nailed Wall", Geotechnical Testing Journal Vol.20,No-1, March 1997, PP 90-102.

**Raju, G.V.R.**, "Behavior of Nailed Soiled Retaining Structures" Ph.D thesis, Nanyang Technological University, Singapor.

**Rajagopal, K , Ramesh, G.V.(2001),** " Studies on The Behaviour of Soil Nailed Retaining Walls" International conference on Civil Engineering ,Bangalore, July.

**Shen, C.K, Herrmann, L.R.,(1981b),** " An in-situ Earth reinforcement Lateral Support System; A Report prepared for the National Science Foundation, Deptt. Of Civil Engg.

**Sivakumar, G.L., Srinivasa B.N., Murthy and Srinivas, A.** "Influence of Construction Practice on Performance of Soil Nailed Retaining Wall" The New Millennium Conference 14-16 Dec, Indore (M.P), India.

**Sprague. C.J., Kout Sourais, M.M. (1992)** "Fabric Forward Concrete Revetment System" Geotextiles and Geomembranes" 587-609.

**Sanyal. T and Chakraborty, K.** "Application of Bitumen -Coated Jute Geo-textile in Bank-Protection Works in the Hoogly Estuary" Geotextiles and Geomembranes 13, 127-132.

**Scott Brown, A., Eric Clyde S.,** "Design of Riprap Revetment " Report No-FHWA-IP-89-016, HEC-11, March 1989

**Theisen. M.S. (1992),** "The role of Geo-synthetics in Erosion and Sediment control: An overview " Geotextiles and Geomembranes 11, 535-550

**Timulshena, K.R.(1992),** "Design Analysis of River Training for Gravel Bed River- A Case Study" an M-Tech Dissertation , IITR

**U.S Army Corps of Engineers (1981),** " Final Report to Congress. The stream Bank Erosion Control Evaluation and Demonstration Act of 1974"

**Varshney, R. S.** " Theory and Design of irrigation structures, Volume II"

**Wong, H.N,** "A Partial Factor Approach for Reinforced Fill Slope Design in Hong Kong" Geotechnical Engg. Office, Civil Engg Deptt. Hong Kong Government, Hong Kong,

**Wallingford. HR. (1998),** "Revetment Systems against Wave Attack-A design manual" Thomas Telford Ltd.

**Wallingford. HR. (1998),** " River and Channel Revetment –A design manual' Thomas Telford ltd.

**<http://tc17.poly.edu/sn.htm>**

**<http://sbe.napier.ac.uk/project/rewall/help/soilnail:htm>**.

**<http://rembeo.com/soil-nailing.html>**

**[www.forester.net/ec\\_0109\\_soil.html](http://www.forester.net/ec_0109_soil.html)**.

## APPENDIX-A

### COMPUTER PROGRAMMING IN FORTRAN AND RESULTS (SOIL NAILED WALL)

! PROGRAMMING FOR CALCULATION OF FACTOR OF SAFETY FOS) of a  
nailed soil wall.

```
OPEN(1,FILE='POINT.DAT',STATUS='OLD')
```

```
OPEN(2,FILE='RESULT.DAT',STATUS='UNKNOWN')
```

```
! ALPHA = Arc angle in degree  
! Beta = Angle in degree of the line joining center of  
! failure circle with the point where failure arc meets with earth  
! GAMA= Unit weight of soil in KN/cum  
! 'H' = The height of wall in meter  
! ad=d= Diameter of nail in mm  
! AAD=D=diameter of grout hole in mm  
! SH = Horizontal spacing of two consecutive nails in m  
! SV= Vertical spacing of two consecutive nails in m  
! PHIE= Angle of repose of soil in degree  
! SIE= Inclination of wall with vertical.  
! FY= Yield stress of Steel in KN/sqm  
! FC= Partial factor of safety with respect to cohesion  
! FPHIE=Partial factor of safety with respect to angle of repose.  
! 'c'=Unit cohesion of soil in KN/sqm  
! THETA= Inclination of nail with the horizontal.  
! AL=L=Length of nail in m  
! q= Surcharge load in KN/sqm
```

```
READ(1,*)ALPHA,BETA,GAMA,H,ad,AAD,SH,SV,PHIE,SIE,FY,FC,FPHIE,C
```

```
1THETA,AL,q
```

! Calculation of radius of failure circle and length over which

! surcharge load acting

$$r = H / (\sin((3.14/180.) * (\alpha + \beta)) - \sin((3.14/180.) * \beta))$$

$$s = r * \sin((3.14/180.) * \alpha) / \sin((3.14/180.) * (\alpha + \beta))$$

$$1 - H / \tan((3.14/180.) * (\alpha + \beta)) - H * \tan((3.14/180.) * \beta)$$

! Determination of resisting moment due to cohesion(MC)

! MC=AMC

$$AMC = 3.14 * r^2 * \alpha * C / (180 * FC)$$

$$\phi_{HIEM} = \text{ATAN}(\tan(3.14 * \phi_{HI} / 180.) / \phi_{HI})$$

$$AK = (1 - (2 * \alpha / 180.)^2) / \cos(3.14 * \alpha / 180.)$$

$$W1 = 3.14 * r^2 * \alpha * \gamma / 360.$$

$$X = (120 * r) / (3.14 * \alpha) * (\sin(3.14 * \alpha / 180.) * \cos(3.14 * \beta / 180.)$$

$$1 + \cos(3.14 * \alpha / 180.) * \sin(3.14 * \beta / 180.) - \sin(3.14 * \beta / 180.))$$

! M1=AM1

$$AM1 = W1 * X$$

$$\text{WRITE}(2,2)r,s,AMC,\phi_{HIEM},AK,W1,X,AM1$$

2 FORMAT('r =F10.3//s =F10.3//AMC =F10.3//PHIEM='F10.3

$$1 //AK =F10.3//W1 =F10.3//X =F10.3//AM1 =F10.3)$$

$$W2 = \gamma * 0.5 * r * \sin(3.14 * \beta / 180.) * r * \cos(3.14 * \beta / 180.) - \gamma * 0.5 * r$$

$$1 * \sin(3.14 * \beta / 180.) * (r * \cos(3.14 * \beta / 180.) - (H / \tan(3.14 * \alpha / 180.$$

$$1 + 3.14 * \beta / 180.) + s + H * \tan(3.14 * \beta / 180.)))$$

! M2=AM2

$$AM2 = (1/6.) * \gamma * r * \sin(3.14 * \beta / 180.) * (H / \tan(3.14 * \beta / 180. + 3.14 * \alpha$$

$$1 * \alpha / 180.) + s + H * \tan(3.14 * \beta / 180.)) * (2 * r * \cos(3.14 * \beta / 180.)$$

$$1 * (H / \tan(3.14 * \beta / 180. + 3.14 * \alpha / 180.) + s + H * \tan(3.14 * \beta / 180.)))$$

```

W3=0.5*H*H/TAN(3.14*BETA/180.+3.14*ALPHA/180.)*GAMA
! M3=AM3
AM3=0.5*H*H/TAN(3.14*BETA/180.+3.14*ALPHA/180.)*GAMA*(r*COS(3.14*
1BETA/180.)-s-1./3.*H/TAN(3.14*BETA/180.+3.14*ALPHA/180.)-H*
1TAN(3.14*SIE/180.))
W4=0.5*H*H*TAN(3.14*SIE/180.)*GAMA
! M4=AM4
AM4=0.5*H*H*GAMA*TAN(3.14*SIE/180.)*(r*COS(3.14*BETA/180.)-s+(2.*
1H*TAN(3.14*SIE/180.))/3.)
W=W1-W2-W3-W4
X1=(AM1-AM2-AM3-AM4)/W
! Calculation of disturbing moment due to weight(W)
WX1=W*X1
Ala=r*3.14*ALPHA/(360.*sin(3.14*ALPHA/(2.*180.)))
THETA2=asin(X1/Ala)
! Determination of moment due to Intergranular forces(Moment due to reaction)(Mrea)
! Mrea=AMrea
AMrea=(W+q*s-(C*3.14*r**2.*ALPHA*sin(THETA2)))/(FC*180.))
1/cos(THETA2-PHIEM)
WRITE(2,3) W2,AM2,W3,AM3,W4,AM4,W,X1,WX1,Ala,THETA2,AMrea
3 FORMAT('W2 =F10.3//AM2 =F10.3//W3 =F10.3//AM3 ='
1 F10.3//W4 =F10.3//AM4 =F10.3//W =F10.3//X1 ='
1 F10.3//WX1=F10.3//Ala=F10.3//THETA2=F10.3//AMrea=F10.3)
THETA1=ATAN((SIN(3.14*BETA/180.)*(s+H*TAN(3.14*SIE/180.)))

```

```

1 /(r-s*COS(3.14*BETA/180.)-H*TAN(3.14*SIE/180.)
1 *COS(3.14*BETA/180.)))
oa=r*SIN(3.14*BETA/180.)/SIN(3.14*BETA/180.+THETA1)
WRITE(2,4)THETA1,oa
4  FORMAT(THETA1='F10.3'/'oa='F10.3)
TP=(FY*3.14*ad**2.)/(4000000.)
AMP=TP*(2./3.)*ad/(3.14*1000.)
WRITE(2,5)TP,AMP
5  FORMAT(TP  ='F10.3'/'AMP='F10.3)
!  Determination of coefficient of active earth pressure(Ka)
!  AK=Ka
AK= (1-sin(3.14*PHIE/180.))/(1+sin(3.14*PHIE/180.))
!  Calculation of disturbing moment for surcharge load
PX1=q*s*(r*cos(3.14*BETA/180.)-0.5*s)
WRITE(2,6)AK,PX1
6  FORMAT('AK='F10.3'/'PX1='F10.3)
N=H/SV
WRITE(2,7)N
7  FORMAT('N  ='I5)
sum=0
sum1=0
DO 10 I=1,N

womega=ATAN((oa*COS(THETA1+3.14*BETA/180.))/((I-SV*0.5)*SV+
1TAN(THETA1+3.14*BETA/180.)*oa*COS(THETA1+3.14*BETA/180.)))
og=oa*COS((3.14*BETA/180.)+THETA1)/SIN(womega)

```

$$\alpha_1 = \arcsin\left(\frac{og}{r} \cos(\omega + 3.14 \cdot \theta/180)\right) - 3.14 \cdot \beta/180 + 3.14 \cdot \theta/180$$

$$gm = og \cdot \cos(\omega + \alpha_1 + 3.14 \cdot \beta/180) / \sin(3.14 \cdot \beta/180 + \alpha_1 - 3.14 \cdot \theta/180)$$

c km = akm

$$akm = gm \cdot (H - (I - SV/2) \cdot SV) \cdot \sin(3.14 \cdot SIE/180)$$

c lei = alei

$$Ale_i = AL - akm$$

! li = Ali

$$Ali = r \cdot \sin(3.14 \cdot \beta/180 + \alpha_1 - 3.14 \cdot \theta/180)$$

! lci = Alci

$$Alci = r \cdot \cos(3.14 \cdot \beta/180 + \alpha_1 - 3.14 \cdot \theta/180)$$

$$\sigma_{av} = (I \cdot SV + akm \cdot \sin(3.14 \cdot \theta/180)) \cdot \gamma + q$$

$$\sigma_{max} = \sigma_{av} \cdot AK$$

$$T = (3.14 \cdot ad/1000) \cdot (\sigma_{av} \cdot Ale_i) \cdot \tan\left(\frac{2}{3} \cdot 3.14 \cdot \phi_{IE}/180\right)$$

$$\sigma_{ab} = \sigma_{av} \cdot (1 + AK)/2 \cdot \tan\left(3.14/4 + 3.14 \cdot \phi_{IE}/(2 \cdot 180)\right)$$

$$1 \cdot \exp\left(\frac{3.14}{2} + 3.14 \cdot \phi_{IE}/180\right) \cdot \tan\left(3.14 \cdot \phi_{IE}/180\right)$$

$$\sigma_{mani} = (\sigma_{max} \cdot \sin(3.14 \cdot \theta/180))^2 + \sigma_{av} \cdot$$

$$1 \cos(3.14 \cdot \theta/180))^2 / (1 + \tan\left(\frac{2}{3} \cdot 3.14 \cdot \phi_{IE}/180\right))^2$$

$$1 \tan\left(2 \cdot 3.14 \cdot \theta/180\right) + ((\sigma_{av} - \sigma_{max})/2) \cdot$$

$$1 \left(\sin\left(2 \cdot 3.14 \cdot \theta/180\right) \cdot \tan\left(2 \cdot 3.14 \cdot \theta/180\right)\right) / (1 +$$

$$1 \tan\left(\frac{2}{3} \cdot 3.14 \cdot \phi_{IE}/180\right) \cdot \tan\left(2 \cdot 3.14 \cdot \theta/180\right) - (C \cdot \tan\left(2 \cdot 3.14 \cdot$$



```

1THETA/180.)))/(1.+TAN(2./3.*3.14*PHIE/180.)*TAN(2.*3.14*
1THETA/180.))
Ti=(C+sigmani*TAN(2./3.*3.14*PHIE/180.))*3.14*ad/1000.*AleI/SH
Tixli=Ti*Ali
Alsi=SQRT((8.*AMP*1000.)/(sigmab*ad)*(ad/AAD)*(1.-T/TP)**2.)
Tci=(4*AMP)/(Alsi*SH)*(1.-(Ti/TP)**2.)
Tcixlci=Tci*Alci

WRITE(2,8) womega,og,alpha1,gm,akm,alei,AlI,Alci,sigmav,sigmax
1,T,sigmab,sigmani,Ti,Tixli,Alsi,Tci,Tcixlci
8  FORMAT('womega='F10.3,5X, 'og ='F10.3,5X,'alpha1='F10.3,5X,
1'gm='F10.3,5X,'akm='F10.3,5X,'alei='F10.3,
1 5X,'AlI='F10.3,5X,'Alci='F10.3,5X,'sigmav='F10.3,5X,
1'sigmax='F10.3,5X,'T='F10.3,5X,'sigmab='F10.3,5X,'sigmani='F10.3
1,5X,'Ti='F10.3,5X,'Tixli='F10.3,5X,'Alsi='F10.3,5X,'Tci='F10.3,
15X,'Tcixlci='F10.3)

sum=sum+Tixli
sum1=sum1+Tcixlci
10 ENDDO
WRITE(2,9)SUM,SUM1
9  FORMAT('sum='F10.3,5X,'sum1='F10.3)
! Calculation of Factor of safety(FOS)

FOS=(sum+sum1+AMC+AMrea)/(WX1+PX1)

WRITE(2,11)FOS
11  FORMAT('FOS='F10.3)
STOP
END

```

## APPENDIX-B

### RESULT FILE FOR COMPUTING FOS OF NAILED WALL (Example-1)

r = 8.468

s = 4.154

AMC = 700.552

PHIEM= .327

AK = 1.095

W1 = 595.469

X = 4.095

AM1 = 2438.227

W2 = 121.693

AM2 = 364.418

W3 = 117.677

AM3 = 267.182

W4 = 53.928

AM4 = 258.961

W = 302.171

X1 = 5.122

WX1= 1547.666

Ala= 8.815

THETA2= .620

AMrea= 85.710

THETA1= .333

oa= 3.587

TP = 196.250

AMP= 1.042  
AK= .376

PX1= 1154.289  
N = 9

womega= .918 og = 3.826 alpha1= .157 gm= 4.886 akm= 3.918  
alei= .882 Ali= 1.761 Alci= 8.283 sigmav= 66.760 sigmax= 25.083  
T= 1.501 sigmab= 211.625 sigmani= 56.021 Ti= 3.831 Tixli= 6.747  
Alsi= .623 Tci= 11.148 Tcixlci= 92.337

womega= .805 og = 4.218 alpha1= .229 gm= 4.634 akm= 3.770  
alei= 1.030 Ali= 2.352 Alci= 8.135 sigmav= 76.523 sigmax=  
28.752 T= 2.010 sigmab= 242.574 sigmani= 64.928 Ti= 4.864  
Tixli= 11.439 Alsi= .580 Tci= 11.963 Tcixlci= 97.324

womega= .712 og = 4.654 alpha1= .303 gm= 4.335 akm= 3.575  
alei= 1.225 Ali= 2.943 Alci= 7.940 sigmav= 86.149 sigmax=  
32.368 T= 2.690 sigmab= 273.087 sigmani= 73.709 Ti= 6.239  
Tixli= 18.362 Alsi= .545 Tci= 12.733 Tcixlci= 101.107

womega= .635 og = 5.123 alpha1= .378 gm= 3.986 akm= 3.330  
alei= 1.470 Ali= 3.534 Alci= 7.696 sigmav= 95.627 sigmax=  
35.929 T= 3.582 sigmab= 303.132 sigmani= 82.355 Ti= 8.026  
Tixli= 28.363 Alsi= .515 Tci= 13.468 Tcixlci= 103.650

womega= .572 og = 5.617 alpha1= .456 gm= 3.582 akm = 3.031  
alei= 1.769 Ali= 4.125 Alci= 7.396 sigmav= 104.942 sigmax=  
39.429 T= 4.734 sigmab= 332.660 sigmani= 90.853 Ti= 10.303  
Tixli= 42.496 Alsi= .488 Tci= 14.179 Tcixlci= 104.863

womega= .519 og = 6.131 alpha1= .538 gm= 3.116 akm= 2.669  
alei= 2.131 Ali= 4.716 Alci= 7.034 sigmav= 114.074 sigmax=  
42.860 T= 6.198 sigmab= 361.608 sigmani= 99.183 Ti= 13.165  
Tixli= 62.081 Alsi= .465 Tci= 14.871 Tcixlci= 104.597

womega= .474 og = 6.658 alpha1= .625 gm= 2.578 akm= 2.234  
alei= 2.566 Ali= 5.307 Alci= 6.599 sigmav= 122.992 sigmax=  
46.211 T= 8.045 sigmab= 389.879 sigmani= 107.319 Ti= 16.735  
Tixli= 88.804 Alsi= .443 Tci= 15.549 Tcixlci= 102.615

womega= .436 og = 7.197 alpha1= .718 gm= 1.951 akm= 1.712  
alei= 3.088 Ali= 5.897 Alci= 6.077 sigmav= 131.651 sigmax=  
49.465 T= 10.364 sigmab= 417.327 sigmani= 115.218 Ti= 21.177  
Tixli= 124.892 Alsi= .423 Tci= 16.216 Tcixlci= 98.548

womega= .403 og = 7.745 alpha1= .821 gm= 1.212 akm= 1.077  
alei= 3.723 Ali= 6.488 Alci= 5.442 sigmav= 139.977 sigmax=  
52.593 T= 13.286 sigmab= 443.719 sigmani= 122.813 Ti= 26.736  
Tixli= 173.472 Alsi= .404 Tci= 16.869 Tcixlci= 91.799

sum= 556.656 sum1= 896.841

FOS= .829

**APPENDIX-C**

**INPUT FILE FOR COMPUTATION OF FOS OF NAILED WALL**

56.,13.,17.,6.,25.,100.,0.6,0.6,27.,10.,400000.,1.5,1.5,15.,10.,4.8,45.

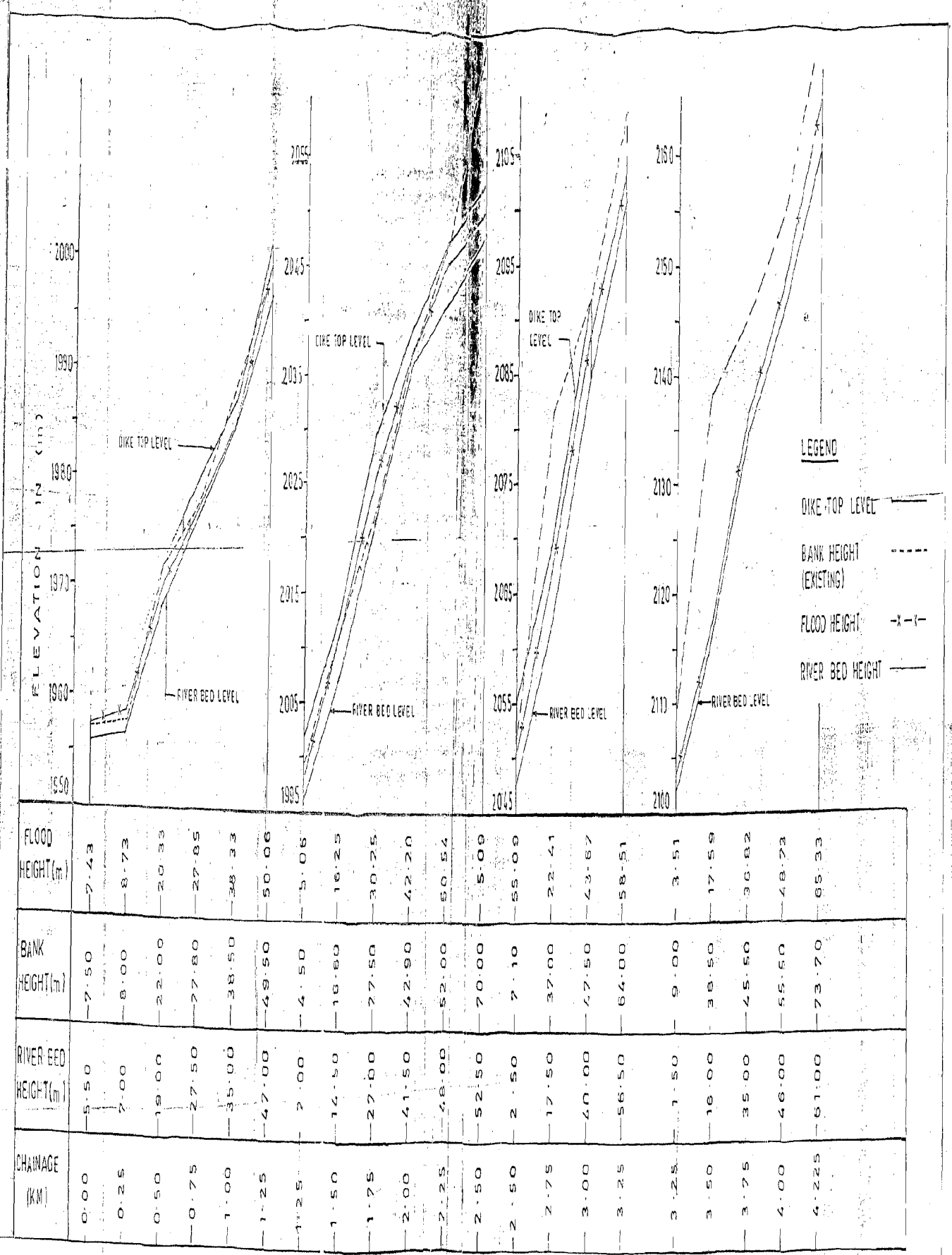
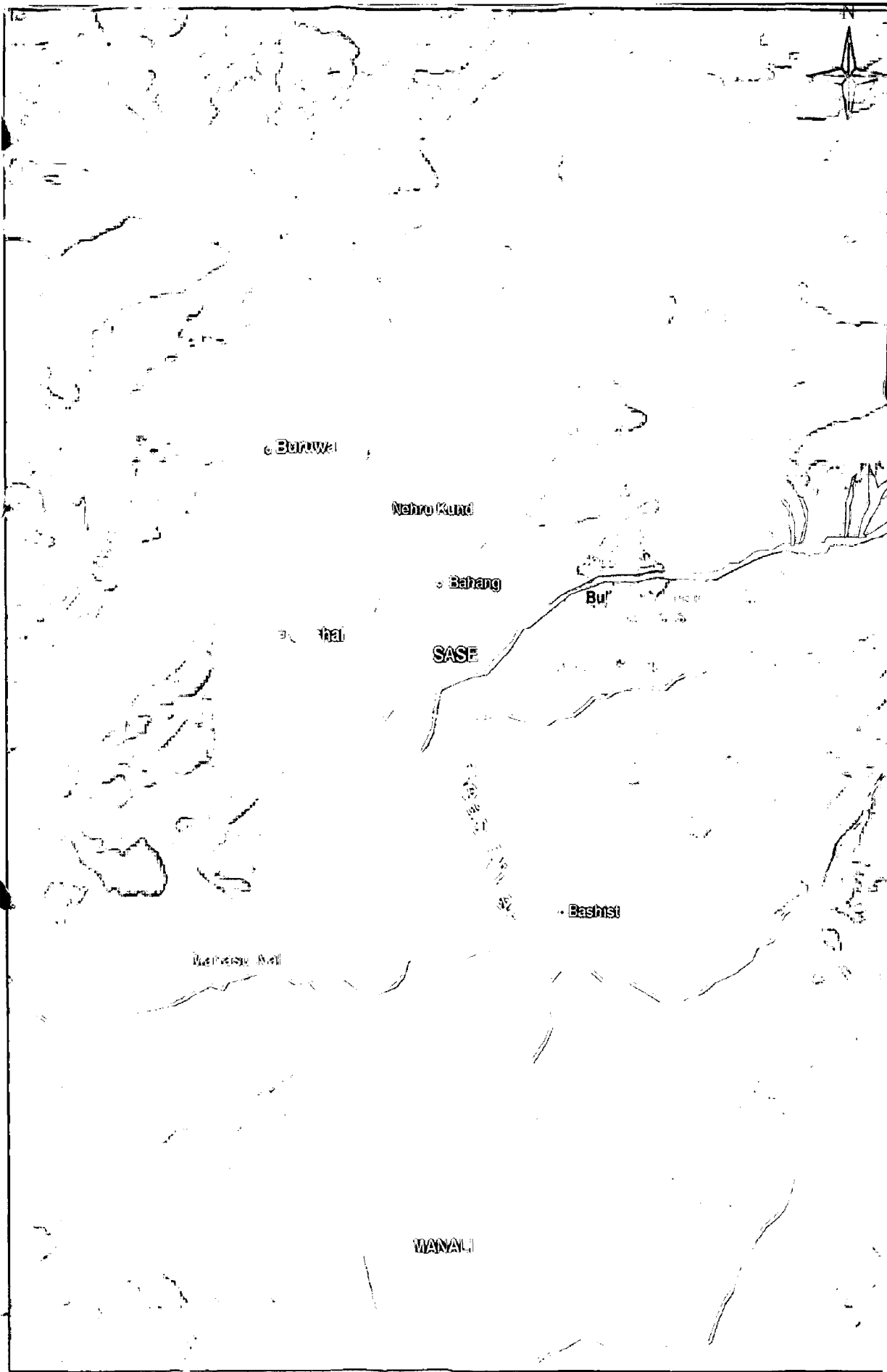


FIG. A1 (PROFILES OF BEAS RIVER AT BHANG)



0.4 0 0.4 0.8 1.2 Miles

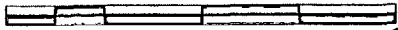


Fig-A2

Satellite Image of IRS-1D LISS-III of SASE & MANALI Area, Date-13.2.2004